AN ABSTRACT OF THE THESIS OF

Ali H. Hassan for the degree of Doctor of Philosophy in Chemical Engineering presented on April 4, 1997.

Title: Phase Behavior of Multicomponent Mixtures of Complex Molecules in Supercritical Fluids

Abstract approved: _____ Redacted for Privacy _____

Keith L. Levien

Supercritical fluid (SCF) technology is an attractive approach for impregnation of solid wood and wood composites with biocides for protection against fungal attack. Pure or modified carbon dioxide can be used to dissolve and deposit biocides within the wood structure. The phases formed by such mixtures at subcritical as well as supercritical conditions must be known for reliable scale-up of SCF impregnation of wood.

Experimental equipment was designed and used for the measurement of critical temperatures and pressures of multicomponent systems. The critical loci of binary (CO_2/Propiconazole) and ternary (CO_2/acetone/TCMTB (2-(thiocyanomethylthio) benzothiazole) or CO_2/methanol/tebuconazole) mixtures were determined experimentally for biocide and cosolvent concentrations up to 2 and 5 wt%, respectively. The effect of cosolvent and biocide levels on critical temperature and pressure of binary and ternary mixtures were determined. Compositions of the coexisting phases in two and three fluid phase equilibria were measured using a stoichiometric technique from measured volumes. The CO_2/acetone/TCMTB system was studied at three (T, P) sets using TCMTB at two levels of purity. For the phase equilibria studies, overall biocide concentrations ranged up to 45 wt% and cosolvent concentrations up to 30 wt%.

Mathematical models were used to predict high-pressure phase equilibria of multicomponent systems. Models were first examined for liquid-liquid equilibria (LLE) of three binary systems (n-butane/water, propylene/water, n-butyl alcohol/water), vapor-liquid equilibria (VLE) of one binary system (CO_2/methanol), and vapor-liquid-liquid equilibria (VLLE) of four ternary systems (CO_2/isopropanol/water, CO_2/water/C_4E_1 (2-butoxyethanol), CO_2/water/C_8E_3 (n-octyl tri(oxyethylene) mono ether), CO_2/acetone/TCMTB). Two different equations of state (Peng-Robinson and Redlich-Kwong) and three different mixing rules (van der Waals, Panagiotopoulos and Reid (1987), Kwak and Mansoori (1986)) were used. The critical temperature of one component for each of the three complex ternary systems was not known. The unknown critical temperature was either estimated using a group contribution method based on normal boiling point or fitted to the experimental phase composition data. Agreement between experimental and calculated phase compositions was better at lower pressures when the system was farther from the critical region. The CO_2/acetone/TCMTB system was the most difficult to model, but the fitting improved when the Peng-Robinson equation of state with Panagiotopoulos and Reid's mixing rules (instead of van der Waals mixing rules) were used.

PHASE BEHAVIOR OF MULTICOMPONENT MIXTURES OF COMPLEX MOLECULES IN SUPERCRITICAL FLUIDS

by

Ali Hassan

A THESIS

submitted to

Oregon State University

in partial fulfillment of
the requirements for the
degree of

Doctor of Philosophy

Completed April 4, 1997
Commencement June 1997

Doctor of Philosophy thesis of Ali Hassan presented on April 4, 1997

APPROVED:

Redacted for Privacy

Major Professor, representing Chemical Engineering

Redacted for Privacy

Chair of Department of Chemical Engineering

Redacted for Privacy

Dean of Graduate School

I understand that my thesis will become part of the permanent collection of Oregon State University libraries. My signature below authorizes release of my thesis to any reader upon request.

Redacted for Privacy

Ali Hassan, Author

Acknowledgments

The successful completion of this work was made possible through the assistance of many people. I am most deeply indebted to my parents, Amir and Ehteram, without whose support and encouragement I would have not been able to have this and other accomplishments of my life. I am grateful to have such caring parents who would sacrifice anything for me and help me with the best of their abilities throughout my life. I am sure I can never thank them enough, but to show a small part of my appreciation, I would like to dedicate this little dissertation to them.

My special thanks go to my older brother, Changiz, for his valuable assistance, guidance and advice throughout my studies. I am also greatly thankful to my wife Khadijeh, my younger brother, Kurosh, my sisters, Khorsheed, Khavar and Mahtab and their families for their support and encouragement. Without the support of my family and relatives, the completion of my studies would have been impossible. For this I remain grateful to all of them throughout my life. Also the warm and joyful moments I shared with them will always be remembered and appreciated.

I would like to express my gratitude to my major professor, Dr. Keith Levien, for his technical advice and support during the course of my studies. Special thanks are also extended to Dr. Milo Koretsky and Dr. Glenn Evans for their help in developing the thermodynamic model used in this study. I would also like to thank Dr. Jeffrey Morrell and Dr. Michael Milota for having served on my committee and their useful advice. Contributions from the members of my Ph.D. committee are greatly appreciated.

I would like to thank a very good friend, Endalkachew Sahle, for his technical help and advice during the first two years of my Ph.D. program. I am also grateful to him for his encouragement and help with my presentations and publications, his friendship and the unforgettable moments I shared with him. My thanks also go to Nick Wannenmacher who was always available and helped me in many aspects of my Ph.D. program.

I have been very fortunate to meet Dr. Levenspiel and to have his course on thermodynamics, learning about his ideas of a "simple thermo" book prior to publishing the book titled "Understanding Engineering Thermo". Having the opportunity to solve almost all of the problems of his book was a pleasant experience and is greatly valuable to me. I am honored to have been the recipient of his book for academic excellence. In addition, I have always enjoyed his nice discussions and his picnics at the coast. I would like to thank him and his wife, Mary Jo, for their kindness and wonderful friendship.

I have truly enjoyed the friendship of Dr. Goran Jovanovic and his family and appreciate his encouragement during difficult times. I would also like to thank all of my other friends for the precious and enjoyable moments I shared with them. The memories I have from each of my friends will always be remembered.

Siroos Karimpoor (Ali H. Hassan)

TABLE OF CONTENTS

LIST OF FIGURES

LIST OF TABLES

LIST OF APPENDICES

NOMENCLATURE

A, B	variables in equations of state; Antoine constants
$A°, B°, C°$	constants in vapor pressure equation
a, b	parameters in the equation of state
C	molar concentration, mole/cm^3; number of components in a mixture; Antoine constant
d	total derivative symbol
f	fugacity, Pa
F	number of degrees of freedom
k_{ij}	binary interaction parameter
M	number of independent chemical reactions; molecular weight
N	number of moles, mole
n	number of components in a mixture; total number of moles
P	pressure, Pa; number of phases
Q	constant in vapor pressure equation
R	universal gas constant $= 8.314$ Pa m^3/mole-K
T	temperature, K
V	volume, cm^3
x	mole fraction
y	vapor-phase mole fraction
Z	compressibility factor

Greek letters

α	phases G, L1, or L2; parameter in equation of state, fugacity coefficient and vapor pressure equation; activity coefficient parameter
β	activity coefficient parameter; parameter in normal boiling point equation
θ	parameter in acentric factor equation $= T_b/T_c$
κ	parameter in equation of state
γ	activity coefficient
μ	chemical potential, J/mole
Φ	fugacity coefficient
ε	convergence limit in the computer algorithm
Δ	group contribution increment
δ	binary interaction parameter
ψ	parameter in vapor pressure equation
∂	partial derivative symbol
ω	acentric factor

Subscripts

b	normal boiling point property
c	critical property
I	component identifier
j	component and phase identifier
k	component, phase and experiment identifier
r	reduced property; reference phase
sat	property along vapor-liquid coexistence line

Superscripts

I, II	phase
cal	calculated parameter
exp	experimentally determined parameter
G	gas phase
IG	ideal gas property
IGM	property of ideal gas mixture
L	liquid phase
$L1$	lower liquid phase
$L2$	upper liquid phase
obj	objective
sat	property along vapor-liquid coexistence line
V	vapor phase
vap	property change on vaporization

Symbols

– (underscore as in $\underline{V}$)	property per mole
– (overbar)	partial molar property

CAUTION

Some of the chemicals used for this study are toxic and
can cause health hazard. For anyone who wants to reproduce
or continue this work, care must be taken to handle those chemicals
as recommended by the respective Material Safety Data Sheets.

This thesis is dedicated to my parents, Amir and Ehteram

PHASE BEHAVIOR OF MULTICOMPONENT MIXTURES OF COMPLEX MOLECULES IN SUPERCRITICAL FLUIDS

CHAPTER 1

INTRODUCTION

Supercritical fluid technology is a rapidly growing technology that has attracted engineers from diverse fields. The basic reason for utilizing supercritical fluids (SCFs) is that the properties of such fluids can be varied from gas-like to liquid-like values by simply adjusting the temperature and pressure. Because of these characteristics, supercritical fluids find use in applications of extraction, purification, separation, impregnation and surface deposition, chemical reactions, nucleation and particle size regulation, polymer processing, pharmaceutical manufacture, food processing, and environmental remediation. But partially due to a lack of high-quality fundamental data, only a relatively small number of commercial-scale plants are now in operation. Therefore the measurement and modeling of the phase behavior of solute species in a SCF medium is essential for reliable scale-up of commercial processes.

One important potential application of SCFs is in wood preservation. Utility poles exposed in environments conducive to biodeterioration must be protected against fungal attack in order to extend their useful life. In conventional treatments of wood, preservatives are dissolved in a liquid (solvent) and the solution is then forced into the wood structure by pressure (up to 200 psia/1.38 MPa). The solvent is used to improve flow and penetration of the chemical into the wood structure, but because of the low diffusivity and the high viscosity of the solution and the high surface tension in small

pores of wood, liquid preservatives can penetrate only a short distance into some wood species. Therefore only the surface and the outer layer of such wood become protected. Cracks or checks in the wood permit fungi to attack the unprotected interior of the wood with the result that the average life of poles treated by these conventional methods is only 30 to 40 years. During that lifetime toxic biocide can be leached from the surface of wood by rain and such weathering has the potential to contaminate ground water. The use of such conventional solvents is expensive because of environmental regulations on contaminated solvents which are generated.

The basic treatability problems associated with the conventional treatment of wood can be overcome by using SCF technology. This research is in support of developing a SCF impregnation technology. In this technology, biocides are first dissolved in a SCF and then passed through the wood structure. Faster diffusion, lower viscosities, and the absence of surface tension in SCFs enhance mass transfer and lead to deeper penetration. As shown in Figure 1.1, complete penetration and more uniform distribution with less toxic biocides at lower levels can be achieved with a treatment process designed to efficiently recycle biocide. Therefore, this approach has the potential to both prolong the useful life of poles and reduce undesirable effects on the environment.

Instead of a liquid solvent, supercritical carbon dioxide can be used in the new technology with the advantages of its low cost, availability, and nonflammable and nontoxic properties. In addition, solvent modification can be done by manipulating temperature and pressure or by adding a cosolvent at lower levels than that used in the conventional treatment of wood. Since a smaller amount of solvent is used in the new

Conventional Treatment Process   SCF Impregnation of Wood
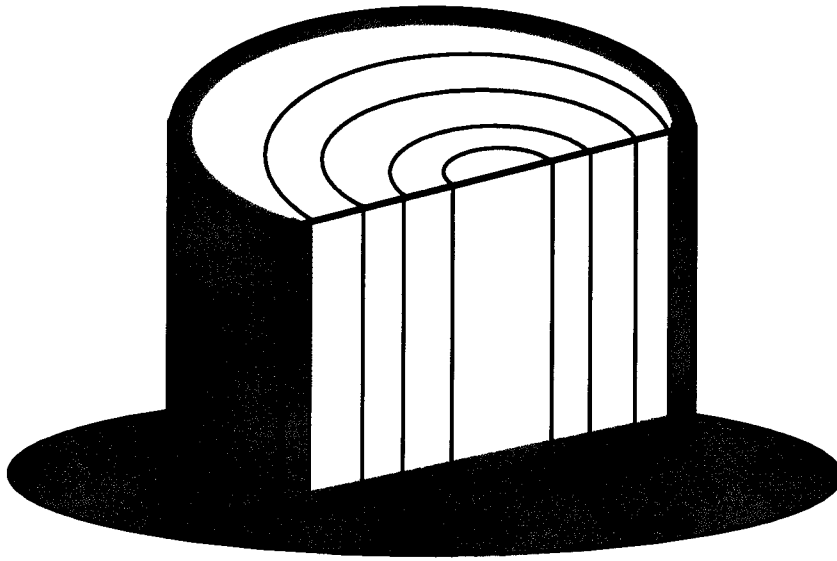
Penetration is only few centimeters

Toxic biocide can be leached from
wood by rain and weathering

Environmental regulations on solvent
handling
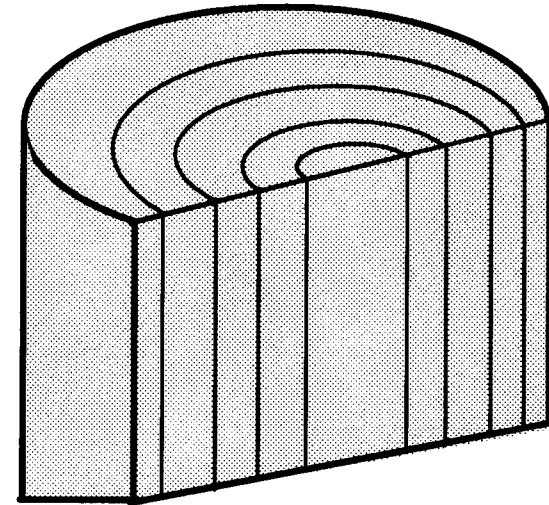
Prolong useful life of a pole by
    ● Deeper penetration
    ● More uniform distribution

Less impact to environment
    ● Less toxic biocide at lower levels
    ● Solvent modification by T, P, and
      cosolvent

Figure 1.1   A comparison between the results of a conventional treatment process and the SCF impregnation of wood.

technology, solvent handling would be less expensive in the SCF technology than that in the conventional treatment process.

Like other new technologies, SCF technology has its specific problems and difficulties. One of these problems is solute deposition within the apparatus, resulting in a shut down of the equipment. Phase equilibria studies may yield some insights on this problem. To develop SCF impregnation processes for wood and find appropriate operating conditions and cosolvents, initial trial experiments are necessary for each biocide. But because treatment process experiments and treated wood analyses are very time consuming, fundamental information about the phase behavior of the mixtures present in the process would be very useful. Solubilities of nine solutes in CO_2 or CO_2/cosolvent mixtures at SC conditions were reported (Sahle, 1994) but there is no data on critical point and phase behavior of CO_2, cosolvent, and biocide mixtures.

In order to obtain deep penetration and a high retention of preservatives in the wood structure, the fluid flowing over the wood samples should be in a supercritical state. It is important to know if the process conditions are above the critical point of the mixture, and if a single phase (SCF) is flowing over the wood samples. If either temperature or pressure is below the critical value for the mixture, the impregnation process would most likely be unsuccessful. Information about the conditions that ensure the existence of a single SCF phase must be developed. Such information can be obtained by determining the critical point of the mixture used in the wood treatment process. When critical properties of the mixture are known, process parameters can be set to values above those conditions to optimize treatment.

If the fluid in the treatment vessel is not a SCF, it is important to know how many phases are present, their densities, and what the compositions of each phase are. Subcritical phase equilibria studies provide information about the fluid(s) existing in different sections of the treatment process under equilibrium conditions. This information should help us understand the problems and difficulties of the process. Phase equilibria studies will also help us design the process more precisely.

This thesis was primarily a study of the phase behavior of multicomponent mixtures in the subcritical region and at conditions where mixtures form a single phase. First, an experimental method is developed to measure the critical point of mixtures as well as compositions of coexisting phases at subcritical conditions. Effects of cosolvent and biocide on critical properties of CO_2/cosolvent/biocide mixtures are determined. The stoichiometric method is used to measure the compositions of coexisting phases at equilibrium under the limitation that the number of phases must be equal to or greater than the number of components. A mathematical model and solution program is developed for liquid-liquid phase equilibria using the van Laar activity coefficient model and a method for vapor-liquid phase equilibria using the van Laar activity coefficient model and a Peng-Robinson or Redlich-Kwong equation of state. A method is also developed for vapor-liquid-liquid equilibria using the Peng-Robinson or Redlich-Kwong equation of state.

A literature survey of phase equilibria for systems near the critical region is given in Chapter 2. The objectives and significance of this research are presented in Chapter 3. Experimental methods are discussed in Chapter 4. Chapter 5 deals with critical point measurements and Chapter 6 with subcritical phase studies. Mathematical models are

presented in Chapter 7. Conclusions and recommendations for future work are discussed in Chapter 8.

CHAPTER 2

BACKGROUND AND LITERATURE SURVEY

2.1 Properties and Applications of Supercritical Fluids

The critical point for a pure substance or a mixture defines the temperature and pressure at which the vapor and liquid phases existing in equilibrium have identical properties and become indistinguishable. Measurements of critical properties and the phase behavior of mixtures are important because of the industrial significance of processes utilizing SCFs and the fundamental interest in the intermolecular energies of fluids (Brunner, 1985). A supercritical fluid is formed when a pure liquid or vapor is heated and pressurized beyond its critical point. Such fluids offer liquid-like or gas-like properties which make them unique as solvents. Supercritical fluids have higher diffusivities than normal liquids, which result in better mass transfer through a porous matrix (Tsekhanskaya, 1971; Saad and Gulari, 1984). Supercritical fluids have higher densities than normal gases, which can facilitate higher solubilities of solutes than in gases. Supercritical fluids also have low viscosities (similar to gases) which allow high flow rates for small pressure drops. Typical diffusivities, densities, and viscosities of a gas, a SCF, and a liquid are compared in Table 2.1. Near the critical point, density of the fluid changes very significantly with a small change in pressure at a constant temperature or with a small change in temperature at a constant pressure. Therefore properties of the fluid can be varied from gas-like to liquid-like by simply making small changes in temperature or pressure. These novel properties of SCFs are often beneficial in processes and are the basis for SCF technology.

Table 2.1   **A comparison of properties of a typical gas, SCF, and liquid**

Property	Gas	SCF	Liquid
Diffusion Coefficient (cm^2/s)	10^{-1}	$10^{-5} - 10^{-3}$	10^{-5}
Density (Kg/m^3)	1	300-900	1000
Viscosity (Ns/m^2)	10^{-5}	$10^{-5}-10^{-4}$	10^{-3}

One application of SCFs is the extraction and recovery of polar organic compounds from aqueous solutions (Panagiotopoulos and Reid, 1987). Supercritical fluids are used in industrial operations for the separation of components of natural materials such as caffeine from coffee beans. Table 2.2 lists some of the commercial-scale supercritical CO_2 extraction (SCE) processes (Anonymous, 1995). However, the limited data and lack of adequate mathematical models can make process design and scaling up of new technologies difficult (Hutchenson and Foster, 1995).

Table 2.2   **Commercial-scale supercritical CO_2 extraction processes (Anonymous, 1995)**

Process	Plant Location
Coffee Decaffeination	Bremen, Germany (two plants) Poszzillo, Italy Houston, Texas
Tea Decaffeination	Munchmuenster, Germany
Fatty Acids from Spent Barley	Dusseldorf, Germany
Nicotine Extraction	Hopewell, Virginia
Rose-Residual Oil SCE	Oklahoma City
CO_2 Refining of Extracted Pyrethrum	United Kingdom
Hops Extraction and Spices	Munchmuenster, Germany Wolnzach, Germany Reigat, United Kingdom Melbourne, Australia Sydney, Nebraska Yakima, Washington (two plants)
Flavors Extraction	Grasse, France
Flavors/Aromas	Rehlingen, Germany
Corn Oil	Japan
Color Extraction-Red Pepper	Japan (six plants)

2.2 Critical Point Measurements

Mixture critical properties are used in petroleum and natural gas engineering, and for the design of chemical reactors and high pressure extraction and separation equipment (Ohgaki and Katayama, 1975). In addition, thermodynamic properties of compounds can be predicted using a knowledge of the critical properties in equations of state, such as van der Waals' equation of state.

The existence of a critical point was first observed by de la Tour (1822). However, quantitative measurements of the critical point were done by Andrews (1869) for the first time. Kuenen (1892) obtained the first reliable experimental investigation of the critical point and showed that the observation could not be reproduced unless the sample was well stirred. Extensive work on the critical region of a mixture was done during 1876-1914 by van der Waals and his associates at the universities of Amsterdam and Leiden. Kay (1968) developed phase diagrams of a series of binary systems, from relatively simple to more complex forms, by the determination of the critical locus curves. Brunner (1985) measured the critical curves of 10 binary mixtures (a gas + methanol).

Recently Gurdial et al. (1993) used a constant volume static device to measure the critical point of binary polar and non-polar organic compound-CO_2 systems. A known amount of solvent was first added to the cell after which liquid CO_2 was added to approximately the 2/3 fill level of the cell. The cell was placed in a water bath and the temperature raised slowly until the gas-liquid critical point was reached. The final total mass of CO_2 present in the cell was determined by venting the gas through a wet-test

meter. Unfortunately, the authors could only measure the critical point and not the phase equilibria of mixtures.

2.3 Phase Composition Measurements

Phase equilibrium properties form the basis for a large number of separations used by process industries and determine the behavior of a wide range of physical systems (Panagiotopoulos, 1987). Appropriate operating conditions for supercritical fluid extraction can be estimated using phase boundaries of mixtures. The economic assessment of new processes utilizing supercritical fluids requires the knowledge of PVT properties of mixtures used in the process near the critical region.

In order to design a reliable experimental apparatus, a literature review on the methods used by previous investigators was necessary. Problems and limitations associated with previous methods must be fully understood and eliminated. A summary of the systems and techniques studied by different investigators is provided in Table 2.3. Experimental devices commonly reported in the literature for phase equilibrium studies can be classified as flow (dynamic) (Jennings et al., 1991; Suleiman et al., 1993) or static (Ohgaki and Katayama, 1975; Suzuki and Sue, 1990; Panagiotopoulos and Reid, 1987; Brunner et al., 1987; DiAndreth et al., 1987; Fall and Luks, 1984). Some of the methods were limited to binary mixtures (Jennings et al., 1991; Suleiman et al., 1993; Ohgaki and Katayama, 1975; Suzuki and Sue, 1990; Brunner et al., 1987; Fall and Luks, 1984). Some were limited to molecules which had low solubility or were insoluble in the SCF or the gas phase (Suleiman et al. 1993).

Constant volume and variable volume cells are the two types of static vessels used in the literature. A constant volume cell is more commonly used because it is easier to operate (Ohgaki and Katayama, 1975; Brunner et al., 1987). The only limitation of a constant volume cell is that it is difficult to obtain measurements at different pressures while holding temperature and total composition constant. A variable volume cell (by movable piston) (DiAndreth et al., 1987), enables measurements to be made over a wide range of pressures while holding both temperature and overall composition constant. The major problem in use of the variable volume cells is elimination of seal leaks.

Table 2.3   Examples of methods used for phase equilibria studies

Method	Authors	Device	Solvent(s)	Solute(s)
direct	Ohgaki and Katayama, 1975	static, constant volume	CO_2	ethyl ether, methyl acetate
direct	Suzuki and Sue, 1990	static, constant volume	CO_2, CH_4, C_2H_8	MeOH, EtOH, 1-propanol
direct	Panagiotopoulos and Reid, 1987	static, constant volume	CO_2	acetone, EtOH, acetone + water
direct	Suleiman et al., 1993	flow	CO_2	heavy paraffins
direct & indirect	Brunner et al., 1987	static, constant volume	H_2, N_2, CO, CH_4, CO_2	MeOH
indirect	Jennings et al., 1991	flow	CO_2	EtOH, butanol
indirect	DiAndreth et al., 1987	static, constant volume	CO_2	trans-decalin, 2-propanol+H_2O
indirect	Fall and Luks, 1984	static, constant volume	CO_2	heavy hydrocarbons

Different methods of mixing were used for each type of static device. Methods discussed in the literature for obtaining mixing in the cell include: magnetic stirrer, electromagnetic reciprocating stirrer and mechanical convection oven.

Analysis of the compositions of phases in equilibrium can be done by direct or indirect methods. In direct methods, compositions are measured by sampling each phase and analyzing the samples usually by gas chromatography (GC) or another chromatographic method with a suitable detector. Ohgaki and Katayama (1975) and Brunner et al. (1987) used a sampling method to study phase equilibrium of binary mixtures. Suzuki and Sue (1990) also used a sampling method for a binary system of liquid solutes in gases with the advantage of recirculating the coexisting phases. Panagiotopoulos and Reid (1987) used a similar method to study phase equilibria in ternary mixtures using recirculation and sampling of all phases. Because of the pressure drop during sampling, partial condensation, re-evaporation, and adsorption can introduce significant errors. There is also the possibility of preferentially sampling the more volatile components when operating at elevated pressures. In addition, it is difficult to sample phases that are nearly critical because the sampling procedure itself can cause large disturbances to equilibrium conditions.

The most common indirect method of determining equilibrium compositions is the stoichiometric technique (DiAndreth et al., 1987; Fall and Luks, 1984) which uses only visual measurements of phase volumes. Some investigators assumed the gas phase to be pure and thus, limited their method to nonvolatile liquids (Fall and Luks, 1984). Other indirect methods measure amounts of liquids using cold traps or by the advances

(volumetric displacement) of a pump and the amounts of gases using equations of state or wet-test meters. The stoichiometric technique is described below.

From the Gibbs phase rule, the number of degrees of freedom for the thermodynamic states of the phases at equilibrium can be determined from:

$$F = C - M - P + 2$$
<div align="right">2.1</div>

Where F is the number of degrees of freedom; C, the number of components; M, the number of independent chemical reactions; and P, the number of phases present in the system. In this work, no chemical reactions occur, therefore equation (2.1) can be simplified to:

$$F = C - P + 2$$
<div align="right">2.2</div>

A mixture with the number of equilibrium phases equal to the number of components thus has two degrees of freedom. If temperature and pressure are fixed in an experiment, the compositions of the coexisting phases remain independent of the overall composition. Thus relative volumes of the phases will change depending on the overall amounts of each component.

Knobler and Scott (1980) have described an indirect stoichiometric method for determining the compositions of equilibrium phases provided the system potentials (e.g., temperature, pressure, and number of phases) are fixed. The analysis requires that the overall mixture composition (i.e., the total number of moles of each component) and the measured volumes for each of the coexisting phases be known. The limitation with this method is that the number of phases coexisting in the equilibrium cell must be equal to or

greater than the number of components. For example, for a three component system forming three equilibrium phases at constant temperature and pressure, a mole balance for each component, i, can be written as:

$$C_i^{L1} V_k^{L1} + C_i^{L2} V_k^{L2} + C_i^G V_k^G = n_{i,k} \qquad\qquad 2.3$$

C_i^α is an unknown molar concentration of component i in the α phase, V_k^α is the measured volume of α phase in experiment k, and $n_{i,k}$ is the total number of moles of component i in experiment k. This mole balance is a linear relationship of three measured independent variables (the phase volumes) and one known dependent variable ($n_{i,k}$). The molar concentrations are the coefficients of this linear expression and can be determined from a linear least-squares fit of experimental data (linearly independent sets of phase volumes and $n_{i,k}$) (DiAndreth et al. 1987). For three component systems, at least three experiments at the same temperature and pressure but with different amounts of one or more components of the mixture are necessary. As more experimental sets of data are used, the accuracy of the parameter estimation should improve. The stoichiometric method does not require sampling and problems associated with the sampling method are avoided.

2.4 Models for Phase Equilibria

Experimental studies on the phase behavior of multicomponent systems are essential for the technical and economic assessment of high pressure processes, but are very time-consuming. The number of required experimental studies can be considerably

reduced if the predicted phase compositions can be correlated by reliable mathematical models. However a mathematical model usually has parameters which are evaluated based on experimental data which can also be used to evaluate the model's ability to describe physical reality (Traub and Stephan, 1990).

In order to develop a mathematical model for phase equilibria of high pressure systems, a literature review of the models used by previous investigators was performed. Restrictions, limitations, and simplifications discussed in the literature are reviewed here.

An ideal model would be a theoretically-based model which uses a limited set of measured physical properties to predict phase equilibria at other conditions. Existing models, however, contain many regressed parameters, are semiempirical at best, and may succeed in fitting the data with adequate accuracy only in portions of the phase diagram. Many theoretically-based models are forced to better fit data by the introduction of additional adjustable parameters (Ekart et al., 1991).

The purpose of reviewing existing models was to search for a fundamental model that could be used to gain an understanding of the supercritical wood treatment process. Process development of this new technology requires a model that explains high pressure phase equilibria of complex molecules. Since limited experimental data are available in this area, the model should have as few parameters as possible. This section of the thesis discusses different models, their simplicity, range of applicability and number of parameters as well as the compounds or systems used to test the models.

Brennecke and Eckert (1989) reviewed some models for phase equilibria in the supercritical region and classified the models into two major approaches:

(1) SCF as dense gas = equation of state (EOS) approach. The most common method treats the SCF phase as a dense gas and uses an EOS to calculate the fugacity coefficient of a compound in a fluid phase. In this EOS approach, the results are often very sensitive to the composition dependence of the interaction energies and size factors, making mixing rules extremely important (Ekart et al., 1991).

(2) SCF as extended liquid = activity coefficient approach. Mackay and Paulaitis (1979) used activity coefficient and fugacity of the pure reference liquid (hypothetical if the component is not a liquid at the system conditions) to calculate the fugacity coefficient in a fluid phase.

Sandler (1989, p.382) discussed the validity of the two major approaches and noted that the EOS approach for the gas and the liquid phases gives a good prediction of phase equilibrium for mixtures of hydrocarbons, inorganic gases, and a few other substances over a wide range of temperatures and pressures, including near the critical region. According to Sandler, the activity coefficient approach gives a good prediction of phase equilibrium for liquid mixtures of all species outside the critical region of the mixture. When both approaches (an equation of state for the vapor phase and an activity coefficient model for the liquid phase) are combined in one equilibrium model, the properties (i.e. density) of the two phases cannot become identical and thus the predicted vapor-liquid behavior near the critical region is incorrect. Twenty four papers on the use of an EOS and one paper on the extended liquid approach are summarized in Table 2.4 and discussed below. In addition to these two approaches, there are also a large number of models that have been developed for computer simulations. Four papers which discuss computer simulation approaches to modeling SCFs are also reviewed later in this section.

2.4.1 Types of Equations of State

EOSs can be classified into five types; (1) virial-EOS, (2) cubic-EOS, (3) perturbation-EOS, (4) lattice-gas-EOS, and (5) association models. Many investigators (King and Robertson, 1962, Najour and King, 1970; Rössling and Franck,1983) have used virial-EOS to model SCF-phase behavior. However, fourth or higher order virial coefficients are required to model the dense fluid region at densities near the critical. Since such high-order coefficients are not easy to estimate, the virial-EOS approach is limited.

Table 2.4 **A summary of EOSs and the extended liquid approach to modeling phase equilibria at high pressures**

EOS	Authors	# of Parameters	Parameter Estimation	Mixing Rules	Reference (System)
Virial	King & Robertson, 1962	1 (B_{12})	fit to concentration vs. density data	–	naphthalene in He, H_2, Ar, Ne, CH_4, and C_2H_4. T: 20-75 °C, P: 1-110 atm
Virial	Najour & King, 1970	1 (B_{12})	fit to optical absorbance-gas density data	–	anthracene in methane, ethylene, ethane, and CO_2. T: 63-185 °C, P: 1-100 atm
Soave's modification of Redlich-Kwong (SRK)	Soave, 1972	3 (T_c, P_c, ω)	T_c & P_c estimated and ω from vapor pressure data	$a_m=(\sum_i x_i a^{1/2}_i)^2$ $b_m=\sum_i x_i b_i$	methane/n-butane at 100 °F, methane/n-decane at 400 °F, H_2/propane at 100 °F, CO_2/propane at 40 °F. P: ~3 to ~8000 psia
modified RK-EOS	Katayama et al., 1975	2 EOS parameters & 3 activity coefficient parameters	fit to phase composition data	– (vapor phase assumed pure)	acetone/CO_2, methanol/CO_2 T: 25, 40 °C, P: ~2 to ~73 atm
modified RK-EOS	Ohgaki & Katayama, 1975	2 EOS parameters & 3 activity coefficient parameters	fit to phase composition data	– (vapor phase assumed pure)	ethyl ether/CO_2, methyl acetate/CO_2 T: 25, 40 °C P: ~6 to ~89 atm
Patel-Teja	Patel and Teja, 1982	Tc, Pc, 2 additional parameters, & 1 interaction parameter	2 parameters: fit to minimize saturated liquid densities. interaction parameter: fit to phase composition data	$a_m=\sum_i\sum_j x_i x_j a_{ij}$ $b_m=\sum_i x_i b_i$ $c_m=\sum_i x_i c_i$	38 pure fluids including polar substances, 32 binary systems containing the light hydrocarbons, CO_2, & H_2S, 20 binary systems containing the heavy hydrocarbons, H_2O, & alcohols. T: 150-423 K, P: up to ~60 bar
RK, PR, & vdW	Kwak and Mansoori, 1986	2 EOS parameters (a, b) & 1-3 interaction parameters	EOS parameters: estimated from critical and physical parameters. interaction parameters: fit to solubility data	based on statistical mechanical theory of vdW mixing rules	2,3-dimethylnaphthalene/CO_2 T: 308, 318, 328 K P: up to 300 bar
Panagioto-poulos & Reid's modification of PR-EOS	Panagioto-poulos & Reid, 1987	2 EOS parameters (a, b) & 2 interaction parameters for a	interaction parameters fit to phase composition data	vdW with 2 interaction parameters for a_{ij}	CO_2/acetone, CO_2/ethanol, CO_2/acetone/water T: 313, 333 K P: 20-150 bar

Table 2.4   (Continued)

EOS	Authors	# of Parameters	Parameter Estimation	Mixing Rules	Reference (System)
Peng-Robinson (PR)	DiAndreth & Paulaitis, 1989	2 EOS parameters (a, b) & 1 binary interaction parameter (δ_{ij})	a: fit to vapor pressure data , b: estimated from T_c, P_c. δ_{ij}: fit to phase composition data	vdW	isopropanol/water/CO_2 T: 40, 50, 60 °C P: 8.4, 9.4, 12.2 MPa
Traub & Stephan's modification of SRK	Traub & Stephan, 1990	4 EOS parameters (a, b, n, m) & 3 interaction parameters per binary	a, b: estimated from T_c & P_c. n, m: fit to pure component vapor pressure. interaction parameters: fit to phase composition data for binary systems.	Huron-Vidal	CO_2/n-butane at 37.8 °C CO_2/acetone at 40 °C and CO_2/water/acetone at 40 °C, P: 40 & 100 bar
PR & SRK	Huang & Sandler, 1993	2 EOS parameters plus 2 (for PR) or 3 (for SRK) parameters used in mixing rules	EOS parameters: estimated from critical properties & vapor pressure data. parameters in the mixing rules: from activity coefficient models	MHV2 & W-S	methanol/water, ethanol/water, C_2H_6CO/H_2O, C_2H_6CO/CH_3OH, C_5H_{12}/C_2H_5OH, CH_3OH/C_6H_6, CH_3OH/C_2H_5OH, C_5H_{12}/CH_3OH, C_5H_{12}/C_2H_6CO, T: 373-523 K, P: 1.5-85 bar
SRK	Nitta et al., 1993	8 (T_c, P_c, ω, k_{ij}, c_{ij}, ΔH_{sub}, $\Delta C_{p,sub}$, V^s_m)	Tc, Pc, ω : fit to sublimation pressure data, k_{ij}, c_{ij}: fit to minimize relative error in solubility, ΔH_{sub}, $\Delta C_{p,sub}$, V^s_m: fit to melting pressure	vdW	naphthalene/ethylene, naphthalene/CO_2, naphthalene/fluoroform, naphthalene/chlorotrifluoro-methane
PR, Patel-Teja, & Singh's Modification of PR-EOS	Singh et al., 1993	Singh's modification of PR EOS: 3 adjustable parameters. Ternary systems have 3 interaction parameters (k_{12}, k_{13}, k_{23})	adjustable param.: fit to minimize the error in solubility data. k_{12} & k_{13}: fit to binary VLE data, k_{23}: optimized	vdW	binary: cholesterol in ethane at T: 313.1, 323.1, 333.1 K, & P: 7-19 MPa ternary: cholesterol in ethane and propane or CO_2 at T: 308.1-338.1 K, P: 8.5-22 MPa

Table 2.4   (Continued)

EOS	Authors	# of Parameters	Parameter Estimation	Mixing Rules	Reference (System)
RK, hard-sphere RK (HSRK), vdW, HSvdW	Carnahan & Starling, 1972	2 EOS parameters (a, b)	estimated from critical properties	$a_m = (\sum_i x_i a^{1/2}_i)^2$ $b_m = \sum_i x_i b_i$	methane, ethane, propane, n-butane, isobutane, H_2S, N_2, ethylene, acetylene, methyl chloride, cyclohexane, pentane, octane, N_2/methane, propane/methane, pentane/cyclohexane, & pentane/octane
Perturbed hard-chain theory (PHCT)	Beret & Prausnitz, 1975	3	from PVT and vapor pressure data	–	3 polymers & 22 fluids: light and heavy hydrocarbons, N_2, CO_2, H_2, CO, H_2S, SO_2, H_2O T: up to ~975 K, P: up to 321 bar
Carnahan-Starling vdW (CSvdW)	Johnston & Eckert, 1981	2 EOS parameters (a, b) & 1 parameter in the mixing rule	EOS parameters: fit to solubility data, parameter in the mixing rule: optimized for each choice of b until the optimal value of b was found	vdW	naphthalene, anthracene, & phenanthrene in SC ethylene. T: 25-85 °C, P: up to 400 atm
Augmented vdW (AvdW)	Johnston et al., 1982	2 EOS parameters (a, b) & binary energy parameters ($\epsilon_{11}, \epsilon_{12}$)	ϵ_{12}: fit to optimize b	vdW	nonpolar hydrocarbon solids in ethylene, ethane, & CO_2. T: 20-70 °C Reduced density: 1-1.5
HSvdW	Wong et al., 1985	2 EOS parameters for each component (a_{11}, a_{22}, b_1, b_2) & 1 interaction parameter (k_{12})	a_{11}, a_{22}: estimated from critical properties, b_1: fit to PVT data, b_2: vdW volume, k_{12}: fit to minimize the error in phase composition data	vdW	naphthalene, anthracene, phenanthrene, pyrene, hexamethylbenzene, fluorene, 2,3-dimethylnaphthalene, & 2,6-dimethylnaphthalene in CO_2 & in ethylene. T: 25-85 °C, density: 0.009-0.025 mole/cc
HSvdW	Dobbs & Johnston, 1987	2 EOS parameters (a, b) & binary attraction parameters (for ternary systems: (a_{12}, a_{22}, a_{23}))	a_{12}, a_{23}: fit to solubility data, a_{22}: from critical properties	vdW	solid/CO_2, solid/CO_2/cosolvent, solid/solid/CO_2, solid/solid/CO_2/cosolvent T: 35,45, 55 °C P: 100-350 bar

Table 2.4   (Continued)

EOS	Authors	# of Parameters	Parameter Estimation	Mixing Rules	Reference (System)
Lattice-gas	Vezzetti, 1984	1	fit to solubility data	–	CO_2 (solid)/air, CH_4 (solid)/Ne, C_2H_4 (solid)/Ne T_r: 1.08-3.07, P_r: up to 10
Lattice-gas	Kumar et al., 1987	2 pure component parameters & 1 interaction parameter	pure component parameters: fit to P-V data, interaction parameter: fit to VLE data	Kumar, Suter and Reid mixing rules	polymer/SCF, acetone/CO_2, ethanol/H_2O, H_2S/n-heptane, benzoic acid/CO_2, acridine/CO_2, acetone/benzene T: 303-363 K, P: up to 40 MPa
Association	Chapman et al., 1990	3 molecular parameters & 2 association parameters	molecular parameters: fit to saturated liquid density, association parameters: fit to phase equilibria data	not required	methanol, acetic acid, n-octane, n-butane, propane, & monomers in methanol and in acetic acid T: up to ~600 K, density: up to ~0.03 mole/cc
Association	Huang & Radosz, 1990	3 molecular parameters & 2 association parameters	fit to vapor pressure and liquid density data	–	chain, aromatic, and chlorinated hydrocarbons, ethers, alkanols, carboxylic acids, esters, ketones, amines, and polymers, T: up to 773 K
Patel-Teja & Association	Jennings et al., 1993	5 (for Patel-Teja-EOS), 5 (for association-EOS), & 1 interaction parameter	Patel-Teja parameters: from critical & physical properties and properties recommended by Patel & Teja. association parameters: from Huang & Radosz, 1990. interaction parameter: fit to phase composition data	vdW & volume fraction	CO_2/1-alkanol T: 314-337 K P: 4.63-11.98 MPa
Extended Liquid Treatment	Mackay and Paulaitis, 1979	2 (γ, k_{12})	fit to solubility data	Chueh & Prausnitz	naphthalene in SC CO_2 and in SC ethylene. T: 12-55 °C, P: up to 300 atm

2.4.1.1 Cubic Equations of State

Cubic equations of state are the most widely used methods for analyzing

supercritical fluid equilibria data. The remarkable success of cubic EOSs in correlating

SCF phase behavior and also their simplicity make them very popular. Since cubic EOSs

can be rapidly "solved" analytically for compressibility factor as a function of pressure,

temperature and molar volume, computation time is significantly reduced when trial and

error calculations of phase compositions are necessary. Multicomponent systems are

easily treated using cubic EOSs, but because of the approximate and somewhat empirical

basis of the equations, the quality of the models depend on the mixing rules (Ekart et al.,

1991).

The earliest cubic EOS, that of van der Waals (vdW), can predict almost all types

of phase behavior qualitatively, but it may not be very good quantitatively. Equations

such as the Redlich-Kwong (RK) (1949), the Soave modification (1972) of the Redlich-

Kwong (SRK), and the Peng-Robinson (PR) (1976) have been widely used to model

phase equilibria. There are two parameters in PR and RK-EOS and three parameters in

SRK-EOS. Additional parameters may be needed for mixtures depending on the mixing

rules used. The parameters in these equations are usually calculated from critical

properties, although a better approach may be to optimize the parameters to fit pure

component vapor pressure or liquid molar volume data.

Soave (1972) applied his model to nonpolar compounds using the same equation

for both vapor and liquid phases and a mixing rule which did not have any fitting

parameters. His equation fitted the experimental data of binary systems of nonpolar

substances well. In the case of polar compounds, he needed to include one or more fitting parameters in the mixing rules.

Patel and Teja (1982) presented a cubic-EOS which required four parameters to characterize each particular fluid. Their mixing rules consisted of three mixture constants (a_m, b_m and c_m) as defined in Table 2.4. The authors claimed that their EOS was capable of accurate and consistent predictions of the thermodynamic properties of binary mixtures and was as good as the SRK and PR-EOS for vapor-liquid equilibria calculations for mixtures of light hydrocarbons. They also claimed that their equation was superior to the SRK and PR-EOS for systems containing heavy hydrocarbons and polar substances.

Panagiotopoulos and Reid (1987) used a modified PR-EOS with vdW mixing rules (having two interaction parameters) to model the experimental data in simple binary (CO_2/acetone, CO_2/ethanol) and ternary (CO_2/acetone/water) systems at high pressures. The agreement between experimental and predicted phase compositions was within the experimental uncertainty of the data.

DiAndreth and Paulaitis (1989) used the PR-EOS with vdW mixing rules and predicted all the regions of multiple equilibrium phases that were observed in the experiments for the simple ternary mixtures of isopropanol, water, and CO_2 near the critical point of CO_2. The authors used the same equation for both vapor and liquid phases.

Several authors (Traub and Stephan, 1990; Huang and Sandler, 1993; Nitta et al., 1993; Singh et al., 1993) used PR, SRK, or a modification of these cubic equations of state with many additional parameters (as indicated in Table 2.4) for binary and ternary

systems. They showed some improvements in the agreement between experimental and predicted phase compositions by introducing the additional parameters.

A few authors (Katayama et al., 1975; Ohgaki and Katayama, 1975) used an EOS for the vapor phase and an activity coefficient model for the liquid phase in simple binary systems, but did not compare experimental results to the results obtained by their model.

2.4.1.2 Mixing Rules in Cubic Equations of State

As indicated in Table 2.4, vdW mixing rules have been used by many authors. Kwak and Mansoori (1986) claimed that vdW mixing rules have been used erroneously in EOSs other than the vdW-EOS without attention to the algebraic form of the equations. They introduced a new concept for the development of mixing rules for cubic EOSs consistent with the statistical-mechanical theory of the vdW mixing rules. They applied their concept to the RK and PR EOS, and tested the resulting mixing rules through prediction of the solubility of 2,3-dimethyl naphthalene in SC-CO_2. The new mixing rules predicted supercritical solubilities more accurately than the original mixing rules of the RK and PR EOS. Kwak and Mansoori's mixing rules use the same number of fitting parameters for the RK-EOS as the original vdW mixing rules. However, the Kwak and Mansoori's mixing rules have three fitting parameters for the PR-EOS per binary, compared to only one fitting parameter per binary in the original vdW mixing rules.

As mentioned earlier the parameters in the cubic-EOSs are either calculated from critical properties or fitted to pure component vapor pressure or liquid molar volume data. When experimental data on critical properties, vapor pressures, or liquid molar volumes are not available, the critical properties must be estimated. The critical temperature and

pressure of organic compounds may be estimated from Lydersen's correlation (Lyman et al. 1982) which is a group contribution method. This correlation requires that the normal boiling temperature of the compound be known. The normal boiling temperature is usually available for materials which have been synthesized and studied. If a measurement is not available, an approximate value of the normal boiling temperature must be estimated. For example Miller's correlation (1984) may be used for this purpose, where the critical volume of organic compounds is usually estimated by the group contribution method of Vetere (1984). The acentric factor is often necessary in many correlation equations and can be calculated from vapor-pressure data. If vapor pressure data are not available, the acentric factor may be estimated from a correlation proposed by Lee and Kesler (1975).

2.4.1.3 *Other Equations of State*

The other three types of equations of state are perturbation-EOS, lattice-gas-EOS and association models. Perturbation-EOS (Carnahan and Starling, 1972; Johnston and Eckert, 1981; Wong et al., 1985; Dobbs and Johnston, 1987; Johnston et al., 1982; Beret and Prausnitz, 1975) have been applied to pure fluids as well as binary and ternary mixtures and have only been successful outside the critical region. Lattice-gas-EOS (Vezzetti, 1984; Kumar et al., 1987) have also shown satisfactory results but only outside the critical region for binary mixtures. Association models (Chapman et al., 1990; Huang and Radosz, 1990; Jennings et al., 1993) have been applied to pure compounds as well as binary mixtures. These models have been successful for pure compounds but have not

been as successful as Patel-Teja-EOS for binary mixtures of CO_2 and 1-alkanol

(Chapman et al., 1990).

2.4.2 Extended Liquid Approach

The extended liquid approach is another modeling strategy used for supercritical

phase equilibria. Rather than requiring the fugacity coefficient of the components in the

mixture as in the EOS approach, this method requires the activity coefficient and the

fugacity of the pure liquid. Sandler (1989, pp. 322-345) discusses two types of activity

coefficient models; the correlative and the predictive models. The correlative models

have one or more adjustable parameters that are adjusted to fit some experimental data.

The predictive models have no adjustable parameters and the activity coefficients are

estimated using physical properties and group contribution methods. The simplest

correlative equations are the one-constant Margules equations, which are satisfactory only

for liquid mixtures containing constituents of similar size, shape, and chemical nature.

One-constant Margules equations are obtained by taking the excess Gibbs free energy to

be a symmetric function of the mole fraction and the activity coefficients of the species in

a mixture. In the two-constant Margules equations, the excess Gibbs free energy is not

symmetric in the mole fraction and thus the two-constant Margules equations perform

better than the one-constant Margules equations.

The van Laar theory for activity coefficients is based on the assumptions that:

(1) A binary mixture is composed of two species of similar size and energies of

  interaction, which implies that the molecules of each species will be uniformly

  distributed throughout the mixture and the intermolecular spacing will be similar

to that in the pure fluids. Thus at a given temperature and pressure, the volume and entropy change on mixing are assumed to be zero.

(2)   The van der Waals EOS applies to both the pure fluids and the binary mixture.

Regular solution theory is a predictive activity coefficient model which arises from the van Laar theory and uses experimental internal energy change on vaporization (usually at 25 °C) instead of using an equation of state to predict the internal energy change on vaporization as in the van Laar theory. Regular solution theory is good only for nonpolar substances.

The UNIQUAC (universal quasichemical) model is a correlative activity coefficient model that is based on statistical mechanical theory which allows local compositions to result from both the size and energy differences between the molecules in the mixture. The underlying idea is that a molecule can be considered to be a collection of functional groups which would be approximately the same in any molecule in which that group occurs.

UNIFAC (UNIquac functional-group activity coefficient) model is a predictive activity coefficient model and arises from the UNIQUAC model. UNIQUAC and UNIFAC models have a (1) *combinatorial term* that depends on the volume and surface area of each molecule and a (2) *residual term* that is a result of the energies of interaction between the molecules. In UNIQUAC, the combinatorial term is evaluated using group contributions to compute the size parameters, whereas the residual term has two adjustable parameters for each binary system that are adjusted to fit the experimental data to be correlated. In the UNIFAC model, both the combinatorial and residual terms are calculated using group contribution methods. Of the predictive methods, UNIFAC is the

most accurate and regular solution theory is the least accurate. Among the correlative activity coefficient models, UNIQUAC is the best model. The limitation with the UNIQUAC and UNIFAC models is that parameters for only a limited number of groups have been determined.

Mackay and Paulaitis (1979) used the extended liquid treatment in determining the solubility of solid naphthalene in $SC-CO_2$ and in SC-ethylene. They assumed that the solid was infinitely dilute in the SCF and also treated the activity coefficient as a fitting parameter. One additional parameter was required in the formulation for the binary system. By adjusting these two parameters, they described their results as "agreeable" with previous methods for predicting solubilities in SCFs.

Computer simulations (such as Monte Carlo techniques) are the most theoretical methods for predicting phase equilibria but are only applicable to simple systems (single component or binary mixtures at low pressures). A few computer simulation approaches are summarized in Table 2.5. The Monte Carlo technique has been used by several authors (Shing, 1991; Panagiotopoulos, 1987; Panagiotopoulos, 1989; Shing and Chung, 1987) and gives a reasonable approximate representation of the properties of spherically symmetric, nonpolar real fluids. Quantitative agreement with experimental solubility or equilibrium data was not possible for binary or ternary mixtures. A drawback of the Monte Carlo technique is that it requires a very large number of simulations for the calculation of equilibria between fluid phases (liquid-gas, liquid-liquid, or fluid-fluid). Calculations required to describe the vapor-liquid phase equilibria for binary systems are lengthy, and some prior knowledge of the approximate location of the phase equilibrium region is required.

Johnston et al. (1987) used a computer simulation method called the local composition concept to correlate phase equilibria of both nonpolar and polar systems. They reported an average absolute deviation of 15 to 19% for the solubility of acridine in carbon dioxide.

Table 2.5   A summary of the computer simulations approach to predicting phase equilibria

Computer Simulations	Authors	# of Parameters	Parameter Estimation	Mixing Rules	Reference (System)
Monte Carlo (MC)	Panagiotopoulos, 1987	none	–	–	Lennard-Jones fluids T_r: 0.75-1.3
MC	Panagiotopoulos, 1989	3 pure component parameters & 3 interaction parameters	pure component parameters: from critical properties & VLE data, interaction parameters: fit to phase composition data	not reported	CO_2/acetone/water T: room temperature
Potential Distribution Theorem & Kirkwood Chemical Potential Equation	Shing and Chung, 1987	4 potential theorem parameters	physical properties & literature sources	–	CO_2/naphthalene T: 320-342 K, P: 74.4-992 atm
Local Composition Concept	Johnston et al., 1987	1 interaction parameter	fit to solubility data	vdW	acridine/CO_2 T: 35, 55 °C, P: up to 380 bar

2.5 Wood Preservation and Supercritical Fluids

Supercritical fluids have been used in wood processing studies for both extraction (Ritter and Campbell, 1991; Calimli and Olcay, 1983) and impregnation (Ward et al., 1990; Sahle, 1994). The focus of this section is on finding an alternative method for the wood impregnation (treating) process so that less toxic biocides could be used, deeper penetration of biocides could be achieved, and the use of organic solvents could be eliminated or reduced. As mentioned in Chapter 1, SCF technology has the potential to overcome the problems and limitations of conventional wood treatment technology. In SCF wood treatment technology, the biocide is dissolved in supercritical CO_2 (sometimes a mixture of CO_2 and a cosolvent) and then contacted with the wood. The supercritical solution moves through the cell structure of the wood to the interior of the wood. When conditions are changed appropriately, the biocide can be precipitated within the wood, while the CO_2 or CO_2/cosolvent gas flows out of the wood structure. Several biocides have been deposited deeply within the wood through this method and were found to be more uniformly distributed than when conventional treatment processes were used (Morrell et al., 1993). Since the wood can be completely impregnated with biocide, it should resist fungal attack even if checks develop. Therefore it is possible to have longer lasting wooden structures with less impact to the environment. However, like in other new technologies, some problems are associated with the SCF wood treatment technology. To discuss these frequently encountered problems and understand the importance of this study in solving those problems, the pilot plant impregnation system (Figure 2.1) used by Sahle (1994) is explained here.
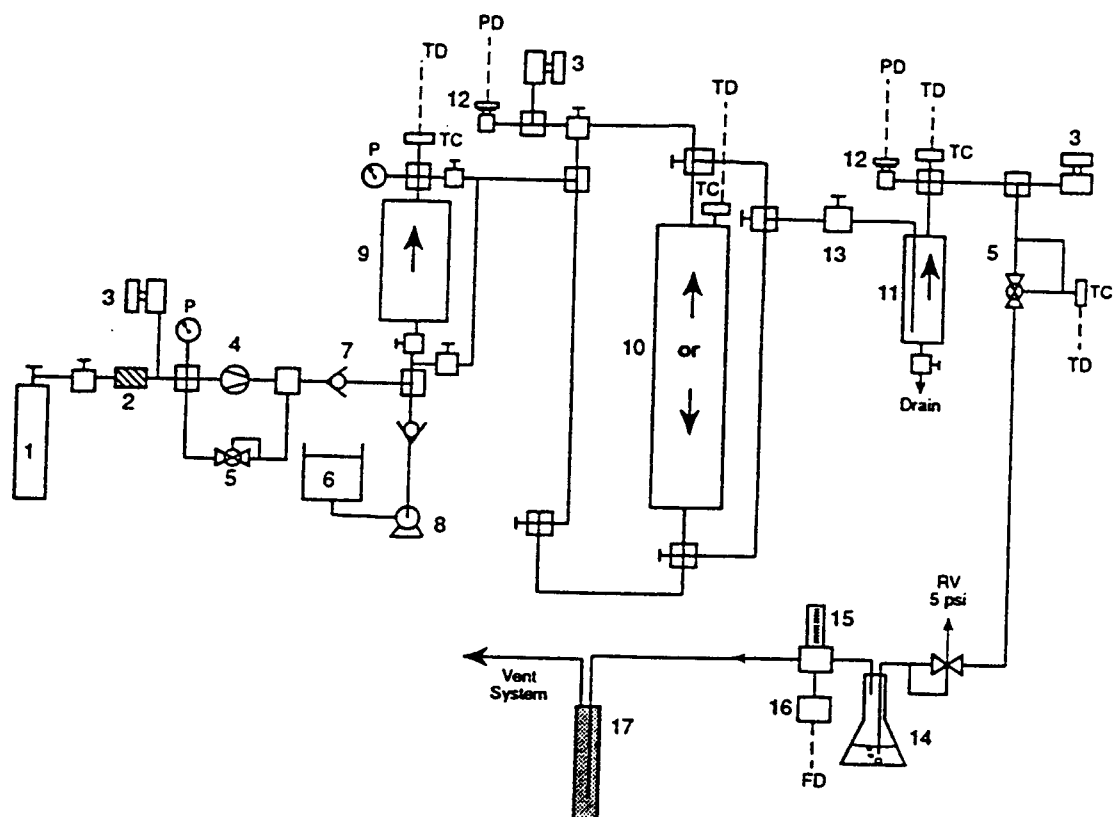
1.	Liquid CO_2 cylinder	9.	Saturator
2.	Relief Valve	10.	Treatment vessel
3.	Filter	11.	Separator
4.	Compressor	12.	Pressure transducer
5.	Back pressure regulator	13.	Metering valve
6.	Cosolvent tank	14.	Cold trap
7.	Check valve	15.	Digital flow meter
8.	Mini pump	16.	Digital totalizer
		17.	Entrainment trap

P - Pressure gauge
PD - Pressure transmitter to personal computer
TD - Temperature transmitter to personal computer
FD - Flow transmitter to personal computer

Figure 2.1   Schematic of the pilot plant impregnation system (Sahle, 1994).

The system had three main sections; saturation, impregnation or treatment, and separation. A SCF which consisted of CO_2, a cosolvent, and a solute flowed from saturator to the treatment vessel where wood samples were kept. The fluid was allowed to flow over the wood samples for a specified period of time (15-90 minutes), after which the pressure was released and the solute deposited in the wood structure while the CO_2/cosolvent mixture flowed through the separator and a cold trap.

To form the SCF and introduce it to the treatment vessel, three techniques were used:

1. CO_2 and cosolvent were mixed and flowed through a packed bed of biocide. Solute was in contact with the CO_2/cosolvent mixture at critical conditions for a sufficient time to dissolve the biocide. SCF then flowed past the wood samples which were kept in the treatment vessel.

2. Solute was dissolved in a cosolvent and that solution was mixed with CO_2 at supercritical conditions in a mixing vessel and then the SCF flowed over the wood samples in the treatment vessel.

3. Solute was loaded on some porous solid materials and the porous material was packed around the wood samples in the treatment vessel. CO_2 and cosolvent were mixed and flowed through the treatment vessel dissolving the solute and taking it into the wood structure. This technique eliminated the saturation vessel but a recirculation system was necessary to produce a uniform solution within the treatment vessel.

With all three techniques, viscous liquids and multiphase behavior were frequently observed in different sections of the treatment process, causing clogging problems and shut downs of the process. Moreover solid material often precipitated at the bottom of the three vessels (saturator, impregnator, and separator) impeding fluid flow. Cleaning the tubes is a very time consuming task and shut downs of a full-scale process must be avoided. Fundamental information about the phase behavior of the mixtures used in the process could be used to avoid operating conditions which allow the formation of a viscous liquid phase. In some cases, the treatment process might be modified in order to avoid multiphase behavior and clogging problems. For instance, when a fresh CO_2 stream is mixed with a premixed cosolvent/biocide stream at subcritical conditions, tubing can become clogged due to the presence of a multiphase system with one of the phases being a viscous liquid. A simple solution to this problem might be to mix the two streams at higher temperatures and pressures.

Like any other SCF technology, wood preservation technology requires that the fluid be in a single supercritical phase. By measuring the critical properties (temperature and pressure) of mixtures, minimum conditions that ensure the existence of only a single SC phase can be determined. Operating conditions can then be set to values above the critical properties of the mixture. If one of the operating conditions (T or P) is below the critical value of the mixture, the fluid would be subcritical. Depending on the operating conditions, this might result in a single gaseous phase, a single liquid phase, or most likely a combination of a gas and a liquid or a gas and several liquid phases. The number and amounts of each phase and the compositions depend on operating conditions as well as on the interactions between the fluid components. If there is only a subcritical gaseous

phase, biocide solubility would likely be low, and retention of the biocide in the wood would be much lower than for the case of a single SC phase, due to the lower solubility of biocides in gases compared to SCFs.

If there is only a liquid phase in the treatment vessel, the diffusivity of solute in that phase in the wood structure would be low. Again the process would no longer be a SC process; it would be a liquid treatment process similar to the conventional processes, but at higher pressures. In this case the penetration of the biocide into the wood is expected to be much shallower than for the case of a single SC phase.

If there are two or more phases (a gas and one or more liquid phases) in the treatment vessel, the result would be a combination of the two cases described above. Again the process would no longer be a SC process. The gas phase would contain very small amounts of the biocide (due to low solubility of the biocides in gases) and the liquid phase(s) would not penetrate deeply into the wood structure (due to high viscosity and surface tension on small pores and low diffusivity of liquids).

Not all three sections (saturation, impregnation or treatment, and separation) of the SC wood treatment process will be in the SC phase. For instance, initial mixing of compounds and the separation section of these processes are at subcritical conditions where multiphase behavior is expected to occur. Different phase(s) might be present in different sections of the treatment process as the conditions change from one section to another. The phenomena which occur in each segment of the process must be understood quantitatively for assessing the design and economic feasibility of this technology. At steady state, the number of phases and their compositions can be determined from the temperature and pressure in any section of the treatment equipment.

This thesis focuses on the phenomena which occur in the saturation and separation sections of the SCF wood treatment technology. In the saturation section, operating conditions that would ensure a single SCF phase must be determined. For this purpose, the critical point of binary and ternary mixtures of CO_2 and biocides with and without cosolvents were studied. For this process to be scaled up, the chemicals collected at the separation section must be recovered and recycled. The lower the pressure at the separation section, the easier the separation of chemicals. Lower pressures during separation increase the cost of recompression for SCF reuse. In other words, it would be expensive and impractical to recycle components by dropping the pressure to atmospheric pressure and then returning to SC conditions. Multiphase behavior is expected to occur at the operating conditions of the saturator. If the phases are to be recycled, it is important to know the chemical composition of each phase. For this reason, multicomponent phase behavior of CO_2, cosolvent, and biocide mixtures was studied.

CHAPTER 3

OBJECTIVES AND SIGNIFICANCE OF RESEARCH

The ultimate goal of this research is to contribute to the development of processes that utilize supercritical fluids. Fundamental knowledge of critical properties and subcritical phase behavior of mixtures is important in any SCF technology. Studies of SC impregnation of wood have shown some promise and have several advantages over the conventional treatment process. Wood treatment process experiments and wood sample analyses are very time consuming, however, a fundamental approach to studying the process may greatly speed our understanding of the variables that most affect the impregnation process. Phase equilibrium is one of the key fundamental phenomena involved in the impregnation process. Moreover for a full-scale process to be feasible, operating conditions must be known, problems of clogging must be eliminated, and fundamental information on phase behavior of mixtures involved is necessary for design and economic assessment of the process. The objectives and significance of this research are summarized below:

Objective 1: Develop a fundamental method for phase study of multicomponent mixtures at elevated pressures. Experimental apparatus was designed and built and the reliability of the method was tested. The method was used to study the complex behavior of binary and ternary systems of CO_2, cosolvent, and simple or complex molecules. Many limitations and problems of other methods such as leakage and errors of sampling

methods were eliminated. This equipment allowed measurements of critical properties as well as phase behavior studies of complex systems.

Objective 2: Determine the critical point of the CO_2, cosolvent, and biocide system(s) of interest (in the wood treatment process). The applicability of the SCF technology is in the critical region where only a single SC phase is present. Knowledge of mixture critical properties can be used to set operating conditions that ensure the existence of a single SC phase in the process. Failure to select proper operating conditions for wood treatment processes using SCF technology will result in inadequate deposition of biocide in the wood structure. In other words, good retention and distribution of biocide in the wood structure may not be achieved if critical properties of the mixture used in the process are not employed. Critical temperatures and pressures of binary and ternary mixtures of CO_2, cosolvent, and a biocide were determined at different levels of biocide and cosolvent. The three potential biocides for treatment of wood using SCF technology were 2-(thiocyanomethylthio) benzothiazole (TCMTB), propiconazole, and tebuconazole. There were no thermodynamic phase behavior data for these biocides in the literature, therefore the critical points of these biocides were studied here for the first time. The effect of biocide content for binary systems and the effects of biocide and cosolvent levels for ternary mixtures on critical temperature and pressure of the mixture were studied.

Objective 3: Determine equilibrium phase compositions of the CO_2, cosolvent, biocide system(s) of interest near the critical region. Knowledge of phase compositions can be used to eliminate clogging problems, design recovery systems and economically assess

the SC wood treatment process. Results of the phase study can also be applied to the phenomena which occur in each section of treatment process at equilibrium and would be useful in designing each section of the process. Phase compositions were determined for vapor-liquid equilibria of binary mixtures and vapor-liquid-liquid equilibria of ternary mixtures. Phase equilibria measurements of the biocide system(s) were studied here for the first time.

Objective 4: Develop and test a model for phase equilibria in the CO_2, cosolvent, biocide system(s) of interest. A theoretical knowledge of the phenomena that occur in the SC wood treatment process can be used to develop and improve the process and decrease the number of many experimental trials required. A thermodynamic phase equilibria model was developed and the accuracy and reliability of the model were assessed by studying binary and ternary systems of simple and complex molecules. Models were examined for LLE and VLE of binary and VLLE of ternary systems. Capabilities of two different equations of state and three different mixing rules in predicting phase compositions in binary and ternary systems were investigated and compared to the experimental values. In the case of compounds whose critical properties were not known, these properties were either estimated using a group contribution method or fitted to the experimental phase composition data.

CHAPTER 4

DEVELOPMENT OF A HIGH-PRESSURE EXPERIMENTAL METHOD

4.1 Introduction

Difficulties encountered in design and scaling up of new SCF technologies often occur because of limited fundamental data on the phase behavior of mixtures involved in the process (Hutchenson and Foster, 1995). In order to obtain high-quality fundamental data, a reliable experimental apparatus was designed. The apparatus was capable of measuring both the critical point and some of the equilibrium phase behavior of multicomponent mixtures. The accuracy and reliability of the critical point and phase equilibria measurements obtained using the apparatus were assessed. This chapter discusses the experimental equipment and the procedures for critical point and phase composition measurements.

4.2 Discussion of the Method Used for Wood Preservation Biocides

The experimental equipment used in this study was designed to eliminate many of the problems and limitations associated with the previous methods. The advantages to this method are discussed after the description of the method.

A static method was used to study phase equilibrium of binary and ternary mixtures near the critical point of CO_2. Analyses of the phases were done using a stoichiometric technique. A schematic of the apparatus used is shown in Figure 4.1. A high pressure optical cell (Jerguson model 12-T-40) was used to observe the phase behavior of mixtures. The cell had two tempered Borosilicate windows which allowed

observation of about 70% of the volume of the cell. The windows were 117.5 mm (4 5/8") wide and located along the centerline of the 210 mm (8 1/4") long view cell. The cell body was made of carbon steel and fluid contact parts were made of 316 stainless steel. The cell had a volume of 40 cm^3, weighed 15 kg and had a maximum operating pressure of 33 MPa at 90 °C. Because of the large mass of the cell, cell cooling by conduction was a very slow process and only three experiments could be performed per day. A J-type thermocouple (Omega model JMTSS-062-U-12) was fitted to the cell, and the cell was heated using a heating tape (Omega model FWH171-060). The thermocouple and the heater were connected to a temperature controller (Omega CN9000A) which controlled and displayed the temperature inside the cell. The precision of the temperature measurement was 0.1 °C and temperature fluctuations in the cell after mixing at equilibrium were less than 0.1 °C. The temperature controller was calibrated using two external mercury thermometers before and after each set of experiments. A precision pressure transducer/indicator (Heise Gauge model 901A) was used to determine the pressure inside the cell within ± 0.007 MPa (1 psia). Observed pressure fluctuations at equilibrium in the cell were less than 0.007 MPa. Throughout each experiment, the volume inside the optical cell was kept constant by closing the feed valve near the view cell.

A manual high pressure generator (HPG) (HiP model 87-6-5, screw pump) and a syringe pump (ISCO model 260D) were used to feed CO_2 to the cell. All wetted parts of the HPG were of 316 stainless steel or 17-4PH stainless steel. Pressure in the cell could be controlled more precisely by the HPG than by the syringe pump. On the other hand, the syringe pump was faster than the HPG in compressing CO_2. It usually took more than
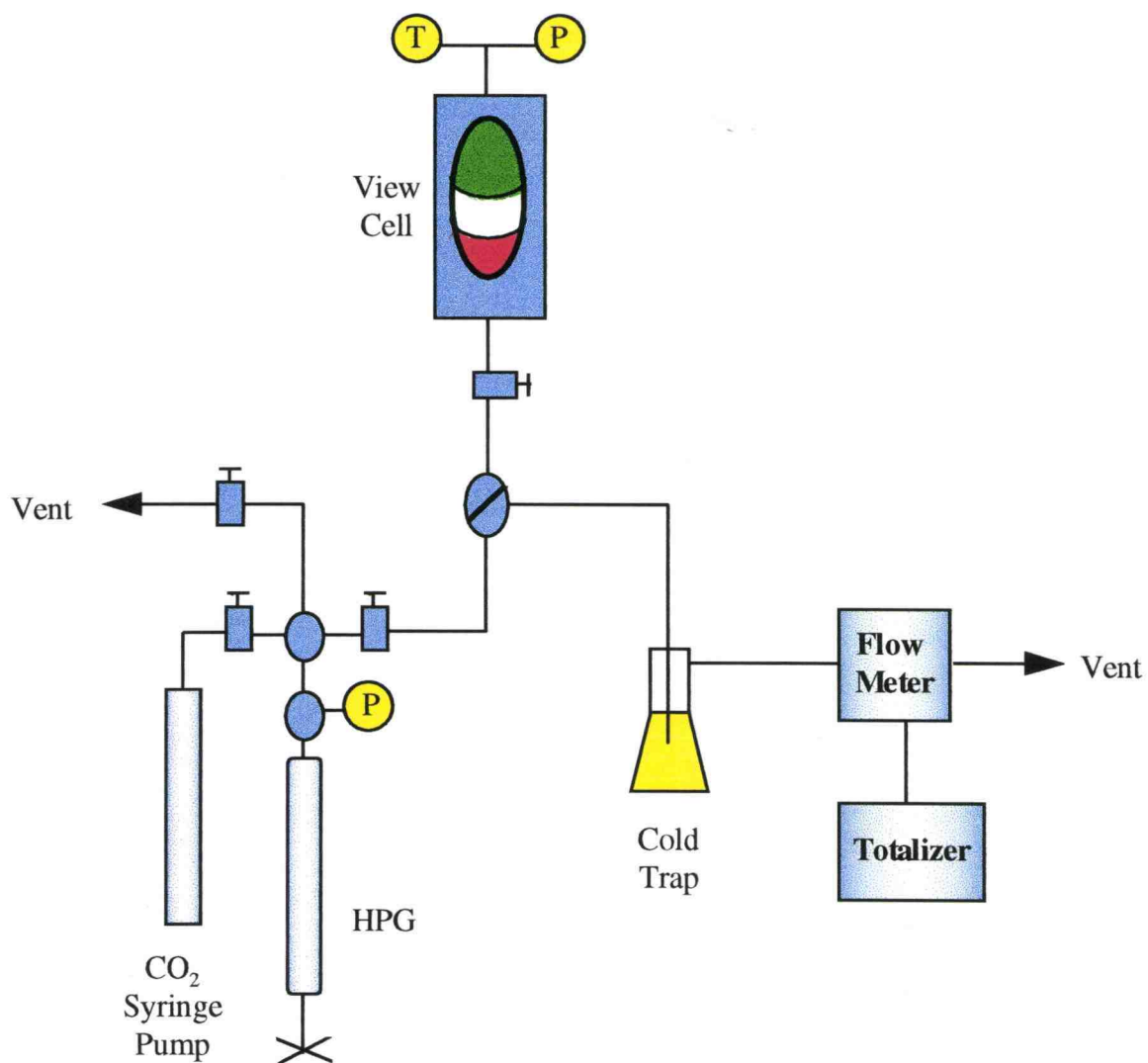
Figure 4.1   Schematic diagram of experimental apparatus used to study phase behavior of mixtures at high pressures.

20 minutes to obtain pressures near the critical pressure of CO_2 (7.38 MPa) using the HPG, while the same job took less than five minutes using the syringe pump. Therefore, the syringe pump was used to feed the initial loading of the CO_2, while the HPG was used to slowly add any further CO_2 to keep all phase boundaries visible. A cathetometer (Eberbach model 5100) was used to observe phase behavior and measure phase volumes at equilibrium. The meniscus height was calibrated to fluid volume by adding known amounts of water into the cell with a pipet and measuring the meniscus height with the cathetometer. Because of the differences in curvature of the meniscus when using water or supercritical fluids, an average level was used rather than the lowest point of the interface. Errors in measuring the cell volume were expected to be less than 0.05 cm^3. A cold trap containing dry ice and acetone was used to separate CO_2 from other components of the mixture. A turbine flow meter (McMillian Co. model 310-3) was used to indicate the instantaneous flow rate of CO_2 while a flow totalizer (Kessler-Ellis Products co., model INT96TBL1A) was connected to the flow meter and used to determine the cumulative volume of CO_2 exhausted.

The advantages to this equipment included:

- Sampling was not required in this method, therefore problems and errors of sampling methods were avoided.

- Mixing of the cell contents was done by rotation of the system, therefore leaking problems associated with magnetic pumps and stirrers were avoided.

- Problems encountered with variable volume cells were avoided.

- A flow meter and a flow totalizer were used to directly measure the CO_2 volume used.

- This method was capable of measuring both critical properties and composition of coexisting phases for multicomponent systems.
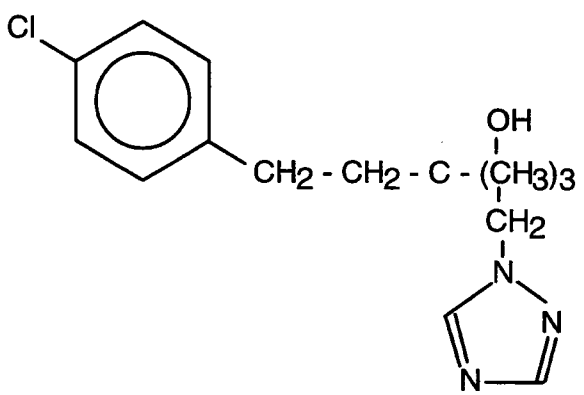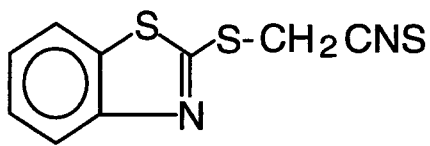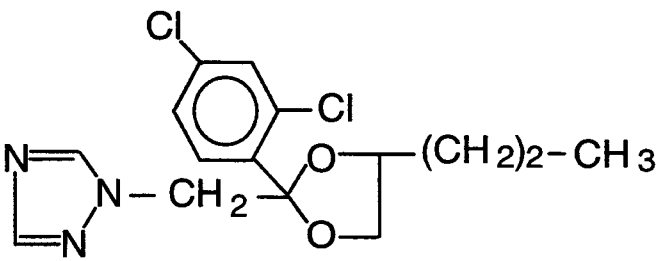
Since many of the problems and limitations associated with other methods were eliminated, the results were expected to be accurate and reliable.

4.3 Purity and Source of Materials

Carbon dioxide was obtained from Industrial Welding Supply (Albany, Oregon) at a purity of 99.9 wt%. Methanol and acetone were purchased from Mallinckrodt Chemicals (Paris, Kentucky) with purities of 99.9 wt% and 99.7 wt%, respectively. 2-(thiocyanomethylthio) benzothiazole (TCMTB) was supplied by Buckman Laboratories, Inc. (Memphis, Tennessee) at two purity levels of 99.6 wt% and 96.9 wt%, propiconazole by Janssen Pharmaceutica N. V. (Beerse, Belgium) at 88 wt% purity, and tebuconazole by Bayer Corporation (Pittsburgh, Pennsylvania) at 95 wt% purity. All of the chemicals were used without further purification. Table 4.1 contains the molecular structures of these biocides.

Table 4.1   **Structures of biocides used for phase equilibria studies**

Biocide	Molecular Mass	Molecular Structure
Tebuconazole	308	
TCMTB	238	
Propiconazole	342	

CHAPTER 5

CRITICAL POINT MEASUREMENTS

5.1 Introduction

In processes that utilize SCFs, it is important to know when process conditions are above the critical point of the mixture. For example, it is essential to know if in fact a single phase (SCF) is flowing over the wood samples. The critical temperature (T_c) and pressure (P_c) of a mixture determines conditions that would ensure the existence of only a single SC phase. Temperatures and pressures used in the treatment process can then be set to values above those conditions in order to achieve complete penetration and a high retention of the biocide in the wood. This chapter explains the procedures and presents the results of critical point measurements for binary and ternary mixtures of CO_2, cosolvent, and biocides.

5.2 Procedures for Critical Point Measurements

For measurements of T_c and P_c of mixtures, the thermocouple at the top of the optical cell described in Chapter 4 was first removed and the lines and the cell were flushed with CO_2 to remove air. Desired amounts of biocide, cosolvent, or a cosolvent/biocide mixture were then added through the top of the cell using a graduated pipet. The thermocouple was then reinstalled and CO_2 was added. First, the gas would fill the cell and then the liquid/gas meniscus would rise in the cell as the pressure was increased through addition of CO_2. The cell was then heated, and as the temperature increased, the meniscus level was maintained near the middle of the window by further

addition of CO_2. On reaching the critical point, the meniscus disappeared. At this point, rotating the cell to mix its contents created an opaque fluid and fluid motion was easily observed as opalescence. Observations were made repeatedly while increasing and decreasing the temperature around the critical temperature, to ensure accuracy of the final values of temperature and pressure. All data reported here are for decreasing temperature, since the absolute rate of change was smaller during cooling. After the critical point of the mixture was observed, the fluid was expanded through a cold trap to separate the components. The CO_2 was then sent to the flow meter and flow totalizer. Using the known initial amount and composition of the liquid and the total amount of the CO_2, the composition at the critical point of the mixture was calculated.

5.3 Results of Critical Point Measurements

The accuracy and reliability of the critical point measurement technique were assessed through measurements of a binary system of methanol in CO_2. Experimental data from this technique are presented in Table 5.1. Figure 5.1 presents the critical pressure data for CO_2/methanol mixtures obtained in this study along with the data of Gurdial et al. (1993). Figure 5.2 similarly presents data for critical temperatures. In both cases the critical property was found to increase with increasing methanol content for up to 8 mole% of methanol. For this range the two sets of data agree within about 3%, except for P_c at the upper limit of methanol concentration. In this work, the purities of CO_2 and methanol were slightly higher than used by Gurdial et al. (99.9 wt% versus 99.8 respectively). Brunner (1985) also presented data for T_c and P_c of CO_2/methanol mixtures, but without composition data for the two phases. Figure 5.3 is a plot of P_c

versus T_c data from this work, Gurdial et al. (1993) and Brunner (1985). From the plot the results of this work can be seen to be closer to those of Brunner (CO_2 at 99.95 wt%, methanol at 99.9 wt%) than to Gurdial et al., possibly because of the purities of the CO_2 and methanol used.

Table 5.1   **Critical points of binary mixtures of CO_2 and methanol**

Methanol Mole%	T_c (°C)	P_c (psia/MPa)
0.00	31.2	1071/7.38
1.93	35.5	1105/7.62
2.07	35.5	1108/7.64
2.24	36.3	1121/7.73
2.47	36.0	1114/7.68
2.51	36.2	1116/7.69
2.68	35.6	1119/7.72
3.22	38.1	1147/7.91
3.45	38.7	1147/7.91
3.45	39.5	1162/8.01
3.49	39.3	1163/8.02
3.51	38.3	1141/7.87
3.63	38.2	1146/7.90
5.11	42.8	1228/8.47
5.20	42.4	1221/8.42
5.23	42.5	1226/8.45
5.37	42.8	1229/8.47
5.42	42.5	1224/8.44
7.11	45.7	1280/8.83
7.17	46.1	1287/8.87
7.61	46.6	1290/8.89
7.70	46.3	1288/8.88
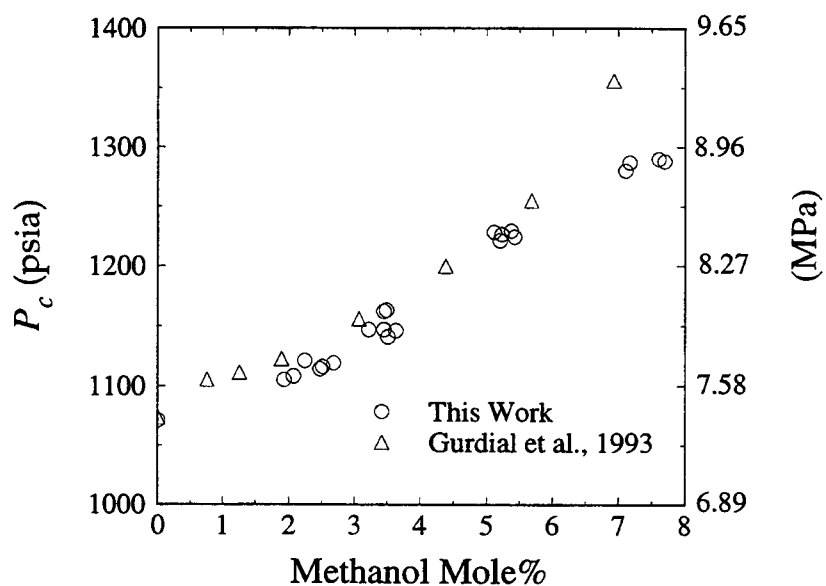
Figure 5.1 Critical pressures of binary mixtures of CO_2 and methanol.
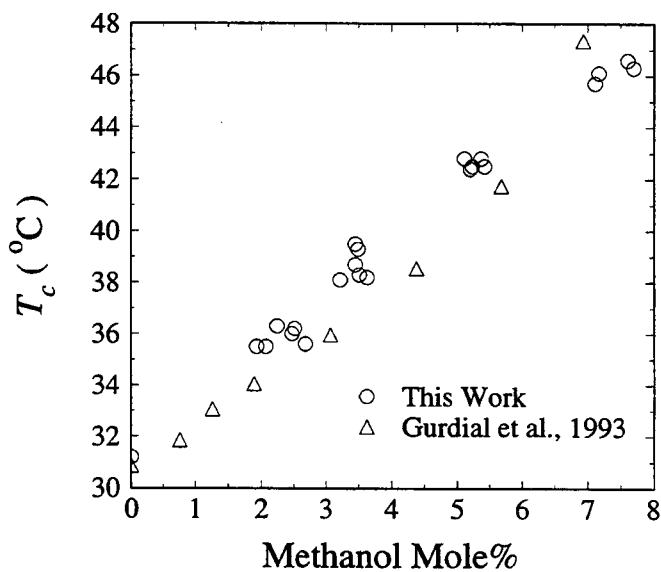
Figure 5.2 Critical temperatures of binary mixtures of CO_2 and methanol.
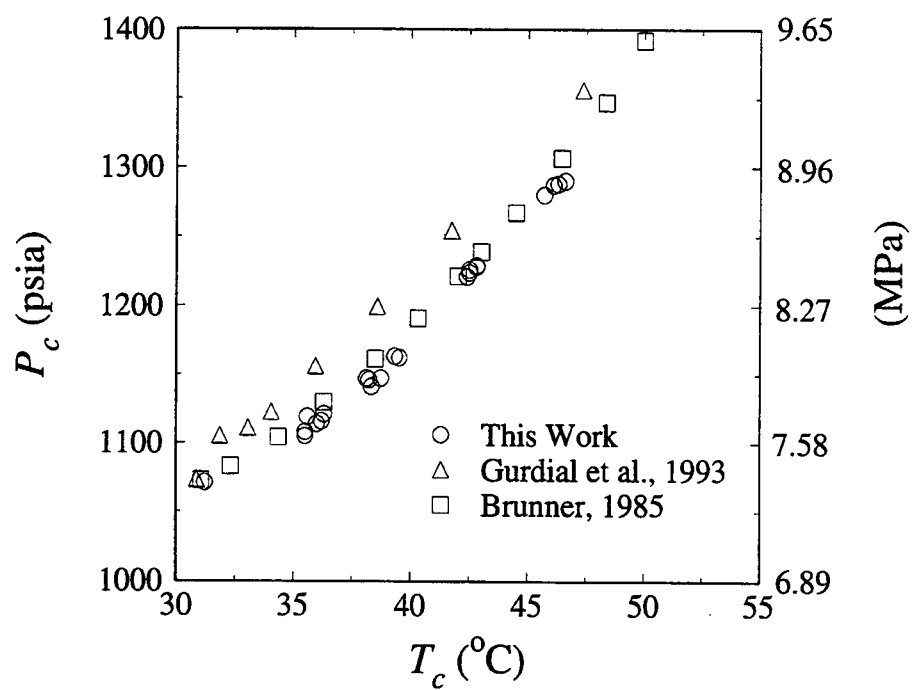
Figure 5.3   Comparisons of critical pressures and temperatures of binary mixtures of CO_2 and methanol from selected studies.

The critical point of binary mixtures of CO_2/propiconazole for less than 1 wt% of propiconazole was also studied (Table 5.2). Two phases existed below the critical point of the mixture in this range of compositions; a liquid phase which contained most of the propiconazole but was rich in CO_2, and a gas phase also rich in CO_2. The critical point of the mixture was the point at which the density of the two phases became identical and the phases became indistinguishable. As the amount of propiconazole was increased, the critical pressure and temperature of the mixture also increased, as shown in Figures 5.4 and 5.5 respectively.

For mixtures containing more than 1 wt% propiconazole, not all of the propiconazole dissolved in the two CO_2-rich phases and therefore a small amount of a third fluid phase was observed. In that case two phases were rich in CO_2 (a liquid and a gas phase), while the third phase was rich in propiconazole. The viscus propiconazole-rich phase was at the bottom of the cell with a volume less than 1% of the total volume of the cell, the liquid CO_2-rich phase was in the middle of the cell with about 45 to 55% of the total volume, and the gas CO_2-rich phase was at the top with about 45 to 55% of the total volume. The critical point in this case was the point at which the middle liquid and the gas phase became identical in the presence of the viscous liquid phase. Therefore a small amount of a viscous liquid was present at the merging point of the two phases. The remaining liquid dissolved further in the SCF as the temperature and pressure increased above the merging point. When the weight percent of propiconazole was increased, more of the viscous liquid was present at the merging point and higher temperature and pressures (above the critical point) were required to dissolve all of the liquid. Behavior of binary mixtures in the critical region and at the critical point of the mixture is very

complicated especially if the two components are very different in structure and properties. Since CO_2 and propiconazole are very different in structure and properties, their behavior would be expected to be complicated. Only the two phase critical behavior of CO_2/propiconazole mixture was quantitatively studied in this work.

Table 5.2   Critical points of binary mixtures of CO_2 and propiconazole

Propiconazole Wt%	T_c (°C)	P_c (psia/MPa)
0.51	31.8	1082/7.46
0.53	32.1	1083/7.47
0.54	32.4	1085/7.48
0.57	32.1	1083/7.47
0.63	32.7	1090/7.52
0.78	32.9	1090/7.52
0.78	32.9	1087/7.49
0.81	32.8	1091/7.52
0.87	33.1	1092/7.53
0.96	34.8	1108/7.64
1.00	35.2	1112/7.67
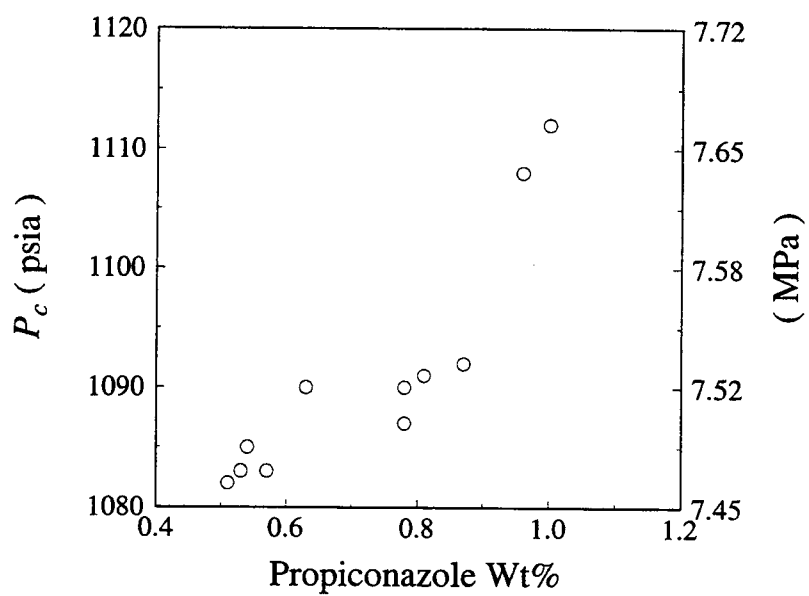
Figure 5.4   Critical pressures of binary mixtures of CO_2 and propiconazole.
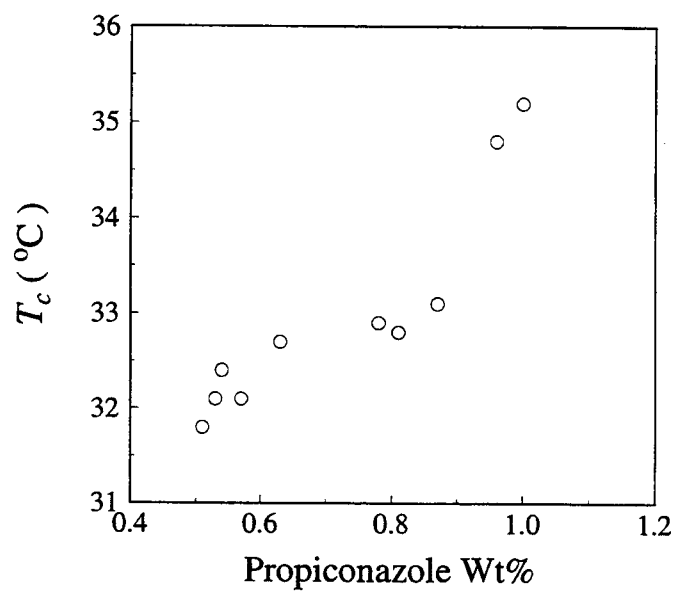
Figure 5.5   Critical temperatures of binary mixtures of CO_2 and propiconazole.

Ternary systems exhibit a critical surface in the four dimensional T-P-x_1-x_2 space which makes the phase behavior even more complicated than for binary mixtures when the components are dissimilar. The critical parameters of ternary mixtures of CO_2/acetone/TCMTB were studied for the two phase region, where acetone content was less than 4 wt% and TCMTB content was less than 2 wt% (Table 5.3). The method of Lyman et al. (1982) was used to estimate the critical temperature and pressure of TCMTB. The estimated critical temperature of TCMTB (405.48 °C) is higher than that of CO_2 or acetone, while its critical pressure (2.89 MPa) is lower than that of CO_2 or acetone.

The effect of acetone content on P_c of CO_2/acetone/TCMTB mixtures is shown in Figure 5.6 for three levels of TCMTB (0, 0.24 and 0.95 wt%). For each TCMTB level, the points represent a critical curve on the critical surface of the ternary mixture. As the composition of acetone was increased in this range, the critical pressure of the mixture also increased. Critical pressure of the mixture decreased by less than 0.03 MPa (5 psia) when TCMTB content was increased from 0.24 to 0.95 wt%.

Figure 5.7 presents T_c of CO_2/acetone/TCMTB mixtures at several levels of acetone for a TCMTB level of 0, 0.24 or 0.95 wt%. For a constant composition of TCMTB, higher acetone composition yielded a higher critical temperature. Critical temperature of the mixture decreased by less than 1.0 °C when TCMTB content was increased from 0.24 to 0.95 wt%.

Table 5.3   **Critical points of ternary mixtures of CO_2, acetone, and TCMTB**

Acetone wt%	TCMTB wt%	CO_2 wt%	T_c (°C)	P_c (psia/MPa)
0.00	0.00	100.00	31.2	1071/7.38
0.67	0.05	99.28	34.0	1099/7.58
1.35	0.16	98.49	35.0	1115/7.69
1.38	0.22	98.40	35.7	1111/7.66
1.67	0.16	98.17	36.5	1128/7.78
2.16	0.16	97.68	37.4	1143/7.88
3.24	0.95	95.81	38.7	1150/7.93
3.27	0.24	96.49	38.9	1154/7.96
3.35	0.24	96.41	39.3	1159/7.99
3.35	0.46	96.19	38.6	1152/7.94
3.45	0.95	95.60	38.9	1155/7.96
3.47	0.89	95.64	39.4	1163/8.02
3.55	0.24	96.21	39.6	1163/8.02
3.55	0.97	95.48	39.0	1160/8.00
3.63	1.18	95.19	39.8	1160/8.00
3.64	0.47	95.89	39.7	1164/8.03
3.71	0.95	95.34	39.4	1167/8.05
3.85	0.99	95.16	40.5	1173/8.09
4.06	1.18	94.76	40.7	1178/8.12
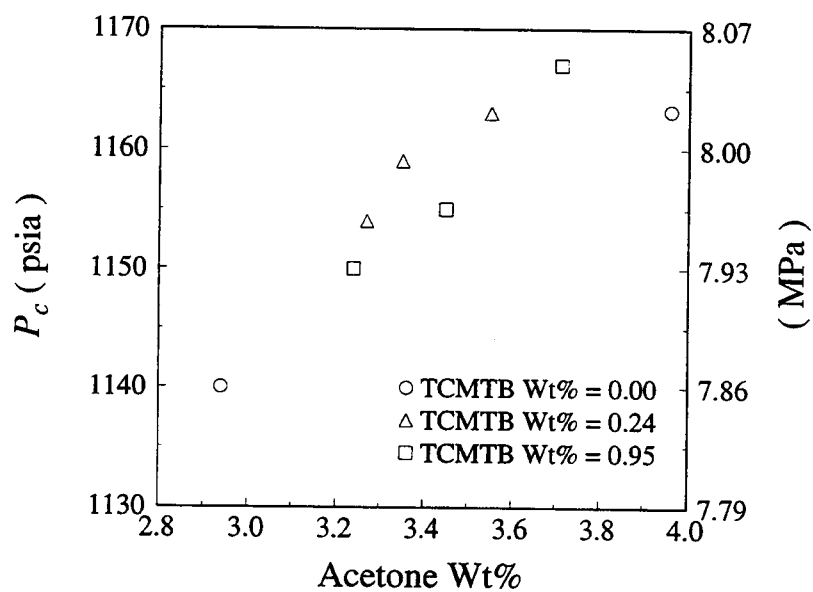
Figure 5.6   Critical pressures of ternary mixtures of CO_2, acetone, and TCMTB.
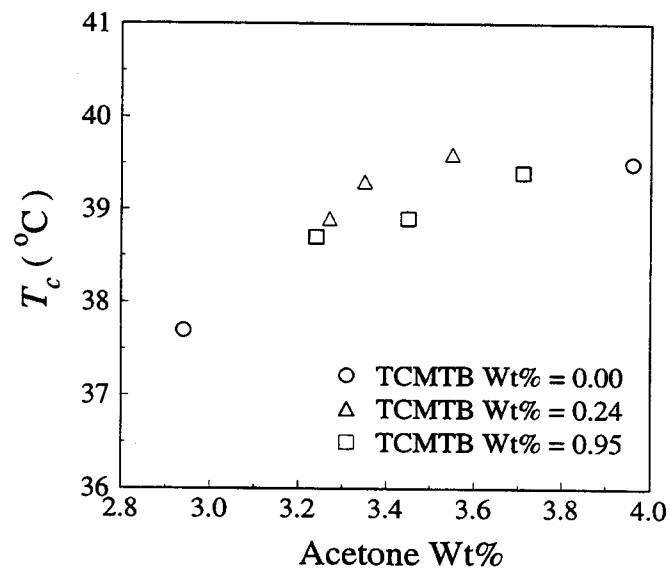
Figure 5.7   Critical temperatures of ternary mixtures of CO_2, acetone, and TCMTB.

Critical behavior was also investigated for ternary mixtures of CO_2/methanol/ tebuconazole in the two fluid phase region. In this study, transitions from two to a single fluid phase were studied in the region where methanol was less than 5 wt% and tebuconazole was less than 2 wt% (Table 5.4). In this region, all of the tebuconazole and methanol dissolved in the two CO_2-rich phases. The liquid phase contained most of the tebuconazole and the methanol. At a constant tebuconazole content, the critical temperature and pressure both increased as methanol content increased. The method of Lyman et al. (1982) was used to estimate the critical temperature and pressure of tebuconazole. The estimated critical temperature of tebuconazole (606.46 °C) is higher than that of CO_2 or methanol, while its critical pressure (1.83 MPa) is lower than that of CO_2 or methanol. A third fluid phase was observed at the bottom of the cell when the amount of tebuconazole exceeded 2 wt%.

The effect of methanol content on critical pressures in CO_2/methanol and CO_2/methanol/tebuconazole mixtures is shown in Figure 5.8. The total tebuconazole content was held constant in the ternary mixture at 0.44 wt%. The critical pressure of the mixture increased as the amount of methanol was increased and was slightly higher (about 0.07 MPa / 10 psia) in the presence of 0.44 wt% tebuconazole.

Figure 5.9 presents critical temperature data for the CO_2/methanol mixture versus methanol content both with and without tebuconazole. The critical temperature of the mixture increased as the methanol composition was increased, regardless of tebuconazole presence. The relative difference between absolute T_c in the presence of 0.44 wt% tebuconazole and that in the absence of tebuconazole was less than 1 %.

Table 5.4   Critical point of ternary mixtures of CO_2, methanol, and tebuconazole

Methanol wt%	Tebuconazole wt%	CO_2 wt%	T_c (°C)	P_c (psia/MPa)
0.75	0.44	98.81	33.9	1098/7.57
0.76	0.44	98.80	33.6	1092/7.53
0.78	0.44	98.78	33.4	1093/7.54
0.79	0.44	98.77	33.6	1096/7.56
0.86	0.35	98.79	35.5	1113/7.67
1.69	0.44	97.87	35.4	1118/7.71
1.71	0.44	97.85	35.7	1130/7.79
1.76	0.44	97.80	35.5	1129/7.78
2.73	0.90	96.37	40.1	1188/8.19
3.41	1.73	94.86	39.9	1185/8.17
3.43	0.90	95.67	40.8	1203/8.29
3.50	0.44	96.06	41.6	1216/8.38
3.51	0.90	95.59	41.0	1209/8.34
3.60	0.90	95.50	42.5	1238/8.54
3.62	0.18	96.20	42.6	1233/8.50
3.70	0.44	95.86	42.4	1224/8.44
3.87	0.95	95.18	42.0	1219/8.40
3.95	0.48	95.57	42.2	1226/8.45
4.02	0.52	95.46	41.1	1214/8.37
4.03	0.99	94.98	40.9	1208/8.33
4.07	0.49	95.44	41.9	1227/8.46
4.39	0.53	95.08	41.3	1214/8.37
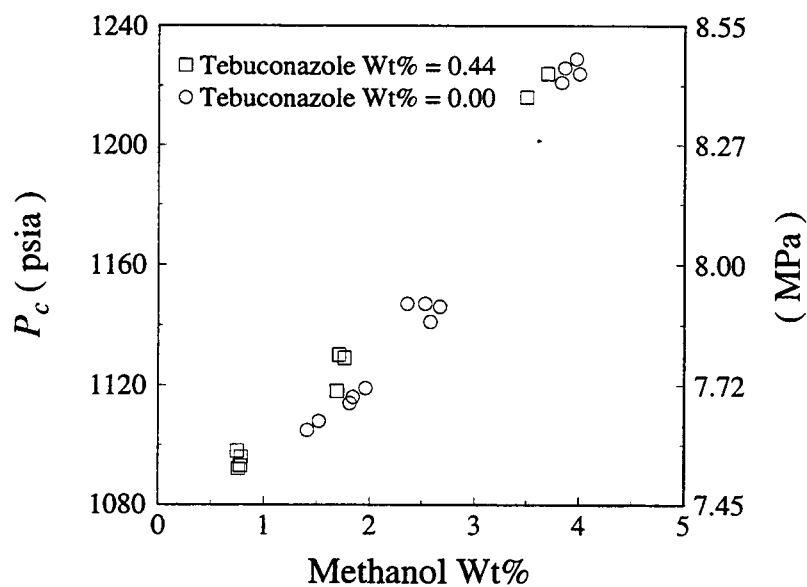
Figure 5.8   Critical pressures of ternary mixtures of CO_2, methanol, and tebuconazole.
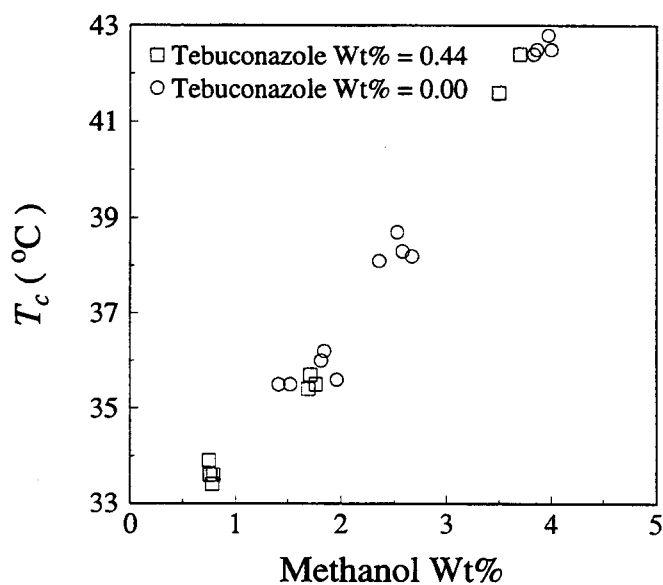
Figure 5.9   Critical temperatures of ternary mixtures of CO_2, methanol, and tebuconazole.

CHAPTER 6

PHASE COMPOSITION MEASUREMENTS

6.1 Introduction

Information on the phase behavior of mixtures in the near critical region is necessary for the design, economic assessment, and scale up of new processes utilizing supercritical fluids. Knowledge of phase boundaries can be used to estimate appropriate operating conditions for supercritical fluid processes. In addition, phase equilibria studies could explain and help to eliminate many problems in processes utilizing SCFs.

Fundamental information on phase behavior of the mixtures present in the process is essential for improving the SC wood treatment process and designing recycling system for SCF components. This chapter describes the procedures and results of phase equilibria studies for a binary system of CO_2/methanol and a ternary system of CO_2/acetone/TCMTB.

6.2 Procedures for Phase Composition Measurements

For phase equilibria at near critical conditions, the top thermocouple in the cell described in Chapter 4 was removed and the lines and cell were flushed with CO_2 to remove air. Known amounts of methanol, TCMTB, acetone, or an acetone/TCMTB solution were added. The thermocouple was reinstalled and the heater was turned on. CO_2 was fed to the cell to increase pressure to the desired value at which two or three phases were observed. Because a stoichiometric method was used for composition measurements, it was necessary that the number of phases be greater than or equal to the

number of components of the mixture. After CO_2 was added to the cell, the line to the

cell was disconnected and the cell was rotated and was shaken to ensure good mixing.

Equilibrium was established when the pressure, temperature and the meniscus level(s)

were stable. Equilibrium was usually observed after one hour, but measurements were

made only after at least three hours. The meniscus level was then measured using a

cathetometer and the volume of each phase was determined. The cell contents were then

expanded through the cold trap to capture the liquid solution and measure the CO_2 with

the flow meter and totalizer. The same procedure was repeated several times at a

constant temperature and pressure, but with different initial amounts of the components.

Each time the meniscus levels were different and the corresponding volumes of the

phases were recorded. Compositions of the phases were calculated from the phase

volumes and the total amount of each component, as discussed in Chapter 2. After each

experiment, the cell was rinsed and cleaned.

6.3 Results of Phase Composition Measurements

Many investigators have reported phase behavior of mixtures of simple cosolvents

and CO_2 at subcritical conditions. To check the accuracy and reliability of the

stoichiometric method, phase compositions of binary systems of CO_2/methanol were

measured at 25 °C. Phase volumes and overall mixture compositions for CO_2/methanol

mixture at 25 °C and four pressures are presented in Table 6.1. At least two experiments

at the same temperature and pressure but with different amounts of one or both

components of the mixture were necessary, but the accuracy of phase compositions

should improve as more experimental sets of data are used. Three or four different

experiments were performed at pressures of 6.16, 5.65 and 5.06 MPa. Additional

experiments at these pressures were necessary to obtain more agreeable phase

compositions with those reported in the literature. Compositions as well as densities of

the gas and liquid phase were determined from the volume measurements using the

stoichiometric method and the results are tabulated in Tables 6.2 and 6.3 respectively. A

sample calculation of the stoichiometric method is available in Appendix A. As

expected, the top phase (V) was always lighter than the bottom phase (L). Since phase

measurements were done at different overall phase compositions, there was no trend in

density as a function of pressure.

Figure 6.1 presents results obtained by this method and data from two previous

reports (Katayama et al., 1975; and Brunner et al., 1987). For the pressures studied here

(above 5 MPa), the gas phase mole fraction of CO_2 was always at or above 0.99, as found

by the other authors. This indicates that methanol is only slightly soluble in the gaseous

CO_2. From this study, conditions for two-phase (vapor-liquid) equilibrium as well as the

conditions at which only one phase (vapor or liquid) is present, were determined.

Table 6.1   Measured phase volumes and overall mixture compositions for CO_2/methanol mixtures at 25 °C

P (psia/MPa)	V^V (cm^3)	V^L (cm^3)	n_{CO2} (mole)	$n_{methanol}$ (mole)
904.0/6.23	23.0158	16.4842	0.4654	0.0099
	27.6652	11.8348	0.3975	0.0074
893.0/6.16	22.6378	16.8622	0.3671	0.0198
	28.5346	10.9654	0.3048	0.0124
	22.3732	17.1268	0.4045	0.0148
	25.1137	14.3863	0.3708	0.0099
820.0/5.65	24.9058	14.5942	0.2875	0.1238
	23.9230	15.5770	0.2857	0.1361
	21.0880	18.4120	0.3124	0.1485
	18.0073	21.4927	0.3851	0.1856
734.0/5.06	23.0725	16.4275	0.2421	0.1980
	17.9695	21.5305	0.3000	0.2723
	15.6826	23.8174	0.3102	0.2846

Table 6.2   Compositions for the vapor-liquid equilibrium of CO_2 and methanol at 25 °C

Pressure (psia/MPa)	x_{CO2}	y_{CO2}
904.0/6.23	0.9723	0.9948
893.0/6.16	0.9501	0.9938
820.0/5.65	0.6543	0.9898
734.0/5.06	0.4910	0.9943

Table 6.3   Densities for the vapor and liquid phase of CO_2/methanol mixtures at 25 °C

Pressure (psia/MPa)	ρ^L (g/cm³)	ρ^V (g/cm³)
904.0/6.23	0.9109	0.2511
893.0/6.16	0.7962	0.1850
820.0/5.65	0.9745	0.0754
734.0/5.06	0.9087	0.0973
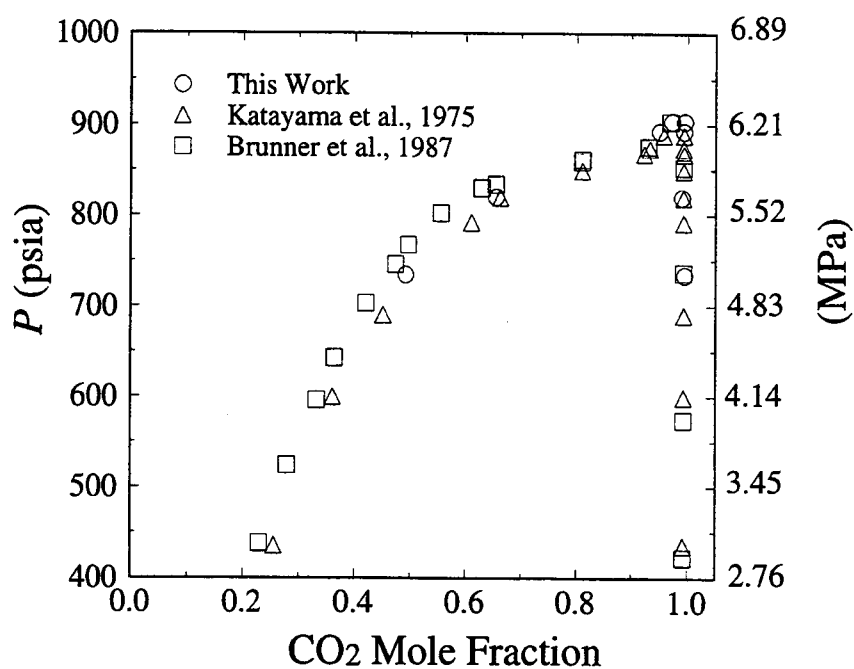
Figure 6.1   Comparisons of vapor-liquid equilibria for CO_2 and methanol mixtures at 25 °C from selected studies.

Data analysis was possible on the experimental phase compositions obtained at pressures for which three or four experiments were done. At each pressure, the relative deviation in the equilibrium phase compositions was calculated from phase compositions obtained using the total number of experiments and those obtained using one experiment less. This relative deviation can be used to determine the number of additional experiments necessary to achieve an acceptable precision in the equilibrium phase compositions obtained by the stoichiometric method. For the CO_2/methanol system at 25 °C and 6.16 MPa (893 psia), the relative deviation ranged from 0.18 to 2.4 % for the CO_2 mole fraction and from 3.4 to 46.5 % for the methanol mole fraction in the liquid phase. At the same pressure, the relative deviation in the CO_2 mole fraction ranged from 1.7 to 4.8 % while the relative deviation ranged from 256.3 to 692.4 % for the methanol mole fraction in the vapor phase. The large relative deviation in the methanol mole fraction is probably due to the small value of the methanol mole fraction in the two phases (0.0499 and 0.0062 in the liquid and vapor phase respectively using all four experimental data) which makes this component more sensitive to small variations. The methanol mole fraction in the vapor phase was always at or below 0.01 when the system temperature was 25 °C (Figure 6.1).

Phase compositions obtained from three experiments (out of the four experiments shown in Table 6.1 at 25 °C and 6.16 MPa) were not feasible (negative phase compositions) when the second or third data in the Table was omitted from the stoichiometric technique. This was also due to the small methanol mole fraction present, especially in the vapor phase. The unfeasible mole fractions obtained from these three

experiments suggest a limitation to the stoichiometric method since this linear regression technique does not limit mole fractions to values between zero and one.

Similar results to that at 25 °C and 6.16 MPa (893 psia) were obtained for the relative deviation in equilibrium phase compositions at 25 °C and 5.65 MPa (820 psia) or 25 °C and 5.06 MPa (734 psia). The relative deviation in the CO_2 mole fraction at 5.65 MPa (820 psia) ranged from 2.7 to 4.3 % in the liquid phase and from 5.1 to 16.9 % in the vapor phase while the relative deviation in the methanol mole fraction ranged from 5.0 to 8.2 % in the liquid phase and from 419.9 to 1,394 % in the vapor phase. Omitting the second or third data tabulated in Table 6.1 at 5.65 MPa (820 psia) from the stoichiometric technique, resulted in unfeasible phase compositions (negative phase compositions) due to the limitation of this technique for small mole fractions (methanol mole fraction in the vapor phase was 0.0102). Only three experimental sets of data were available for the CO_2/methanol system at the lowest pressure (5.06 MPa). The relative deviation in the equilibrium phase compositions between two experimental sets of data and all the three sets of data, showed that as with higher pressures, the relative deviation in the methanol mole fraction was largest in the vapor phase, ranging from 835.7 to 7,017.4 %. The relative deviation in the methanol mole fraction in the liquid phase ranged from 0.3 to 3.2 % while that in the CO_2 mole fraction ranged from 5.1 to 43.1 % in the vapor phase and from 0.3 to 3.4 % in the liquid phase. Unfeasible phase compositions (negative phase compositions) were found when the last data at 5.06 MPa (734 psia) (Table 6.1) was omitted.

Since the results of this work corresponded to published data, the stoichiometric method was used to further study the phase behavior of biocide mixtures at near critical

conditions. Compositions of the phases in vapor-liquid-liquid equilibrium were determined for CO_2/acetone/TCMTB mixtures at 35 °C and 5.28 MPa (766 psia) with the 99.6 wt% pure TCMTB and at 25 °C and 4.32 MPa (626 psia) and 4.05 MPa (588 psia) with the 96.9 wt% pure TCMTB. Phase volumes and overall mixture compositions for these systems are presented in Tables 6.4, 6.5 and 6.6.

Table 6.4   **Measured phase volumes and overall mixture compositions for CO_2/acetone/TCMTB mixtures at 35 °C and 5.28 MPa using 99.6 wt% purity TCMTB**

V^V (cm³)	V^{L2} (cm³)	V^{L1} (cm³)	n_{CO2} (mole)	$n_{acetone}$ (mole)	n_{TCMTB} (mole)
10.1638	19.2213	10.1149	0.3284	0.1211	0.0427
17.5348	11.6235	10.3417	0.2832	0.0964	0.0417
17.7238	10.8675	10.9087	0.2859	0.0945	0.0426
13.6603	14.3829	11.4568	0.3154	0.1065	0.0444
13.8493	13.5135	12.1372	0.3189	0.1043	0.0456
9.4456	20.9412	9.1132	0.3261	0.1258	0.0411

Table 6.5   Measured phase volumes and overall mixture compositions for CO_2/acetone/TCMTB mixtures at 25 °C and 4.32 MPa using 96.9 wt% purity TCMTB

V^V (cm³)	V^{L2} (cm³)	V^{L1} (cm³)	n_{CO2} (mole)	$n_{acetone}$ (mole)	n_{TCMTB} (mole)
11.0544	16.4688	11.0768	0.2186	0.1297	0.0495
12.0320	16.9764	9.5916	0.2149	0.1192	0.0449
12.2764	17.8412	8.4824	0.2137	0.1105	0.0416
11.5056	18.0668	9.0276	0.2164	0.1136	0.0435

Table 6.6   Measured phase volumes and overall mixture compositions for CO_2/acetone/TCMTB mixtures at 25 °C and 4.05 MPa using 96.9 wt% purity TCMTB

V^V (cm³)	V^{L2} (cm³)	V^{L1} (cm³)	n_{CO2} (mole)	$n_{acetone}$ (mole)	n_{TCMTB} (mole).
12.9908	16.8072	8.8020	0.1811	0.1287	0.0423
12.6712	14.8896	11.0392	0.1963	0.1311	0.0468
13.1976	15.6416	9.7608	0.1904	0.1289	0.0439
13.7616	15.6792	9.1592	0.1901	0.1270	0.0422
11.7688	16.5816	10.2496	0.1828	0.1329	0.0462

Mole fractions for the corresponding phases (top=V, middle=L2 and bottom=L1)

were calculated using a MATLAB computer program (Appendix C) using results from 4,

5 or 6 different experiments performed at the same temperature and pressure, but with

different overall compositions (Tables 6.7-6.9).

Table 6.7 Vapor-liquid-liquid equilibrium compositions for
CO_2/acetone/TCMTB mixtures at 35 °C and 5.28 MPa from 6
experiments

Phase	x_{CO2}	$x_{acetone}$	x_{TCMTB}
V	0.5204	0.3439	0.1357
L2	0.6125	0.3365	0.0510
L1	0.7645	0.1113	0.1242

Table 6.8 Vapor-liquid-liquid equilibrium compositions for
CO_2/acetone/TCMTB mixtures at 25 °C and 4.32 MPa from 4
experiments

Phase	x_{CO2}	$x_{acetone}$	x_{TCMTB}
V	0.5670	0.4019	0.0311
L2	0.8620	0.0596	0.0785
L1	0.3607	0.4596	0.1797

Table 6.9   Vapor-liquid-liquid equilibrium compositions for
CO$_2$/acetone/TCMTB mixtures at 25 °C and 4.05 MPa from 5
experiments

Phase	x_{CO2}	$x_{acetone}$	x_{TCMTB}
V	0.8458	0.1517	0.0025
L2	0.0393	0.7694	0.1912
L1	0.5165	0.3019	0.1816

Tables 6.8 and 6.9 show the three phase equilibrium compositions for

CO$_2$/acetone/TCMTB mixture with the same TCMTB purity (96.9%) and at the same

temperature. The only difference between the conditions at which these phase

equilibrium compositions were determined, was the pressure. The data reported in Table

6.8 were obtained at only 0.27 MPa higher than that of Table 6.9, however, at 4.32 MPa

the middle phase (L2) was rich in CO$_2$ while this phase was lean in CO$_2$ at 4.05 MPa.

Meanwhile the middle phase was lean in acetone at 4.32 MPa while it was rich in acetone

at 4.05 MPa. Moreover, the mole fraction of TCMTB in the middle phase increased by a

factor of 2.4 when the pressure was decreased from 4.32 MPa to 4.05 MPa (6.67 %

decrease in the pressure). To explain the changes in phase compositions and also to

ensure that the top phase was the lightest and the bottom phase the heaviest, densities of

the corresponding phases were calculated (Table 6.10). As expected, the top phase (V)

was always the lightest and the bottom phases (L1) the heaviest.

**Table 6.10   Densities for the vapor and the two liquid phases of
CO_2/acetone/TCMTB mixtures**

Pressure (psia/MPa)	Temperature (°C)	ρ^{L1} (g/cm^3)	ρ^{L2} (g/cm^3)	ρ^V (g/cm^3)
766/5.28	35	1.3710	0.7833	0.2673
626/4.32	25	1.6241	0.4517	0.3162
588/4.05	25	1.3161	0.4799	0.4504

More experimental measurements than the minimum required number of
measurements (three) for the stoichiometric method were obtained for all the three
conditions studied using the CO_2/acetone/TCMTB mixture. Thus, data analysis was
possible for all the three conditions studied. The relative deviation in the equilibrium
phase compositions was calculated for all the three conditions using the same method as
for the CO_2/methanol system. These deviations were calculated using the total number of
experiments and the total number of experiments minus one at each temperature and
pressure of the system. The purpose of calculating this relative deviation was to
determine if additional experiments were necessary to achieve an acceptable precision in
the equilibrium phase compositions obtained by the stoichiometric method. For the
CO_2/acetone/TCMTB system at 35 °C and 5.28 MPa (766 psia), the relative deviation in
phase compositions was small for all of the compounds in the three phases compared to
those for the binary CO_2/methanol system. The maximum relative deviation for CO_2

composition in all the three phases was 0.11 %, while those for acetone and TCMTB were 0.48 and 1.66 % respectively.

The relative deviation in phase compositions for the other two conditions (at 25 °C and 4.32 or 4.05 MPa), were also insignificant except for the TCMTB in the vapor phase since the mole fraction of TCMTB in this phase was small (0.0311 at 4.32 MPa and 0.0025 at 4.05 MPa). The relative deviation in the TCMTB mole fraction in this phase ranged from 10.14 to 41.46 % at 4.32 MPa (626 psia) and from 0.13 to 45.89 % at 4.05 MPa (588 psia).

Although the number of experimental sets of data for the three pressures differed, a good precision (maximum of 1.66 % relative deviation) was achieved for the phase compositions at each pressure. Moreover, unlike the CO_2/methanol system, all of the calculated phase compositions were feasible (negative phase compositions were not obtained). Therefore, the stoichiometric method provided results that were consistent with our knowledge of the system and had no limitations for the ternary system of interest.

A MATLAB computer program was used to plot triangular phase diagrams (Appendix C) showing the three-phase compositions determined from the regression analysis discussed in Section 2.3 for the ternary mixture of CO_2/acetone/TCMTB (Figures 6.2, 6.3, and 6.4). The three-phase composition points are shown with connecting lines. The overall mixture compositions at which the three equilibrium phases were observed will fall within these lines connecting the three-phase compositions. Figure 6.2 shows phase compositions for the higher purity TCMTB measured at a higher temperature (35 °C) and pressure (5.28 MPa) than those of Figures 6.3 (25 °C and 4.32 MPa) or 6.4. (25

°C and 4.05 MPa). The lines connecting the three-phase compositions in Figure 6.2 show

a small triangle meaning that phase compositions are similar in all the three phases for the

highest temperature and pressure case. Going from the high pressure to the low pressure

system (Figure 6.2 to Figure 6.4), this triangle becomes larger (phase compositions

become wider spread) meaning that phase compositions are more different in the three

phases at a lower pressure than at a higher pressure. Figures 6.3 and 6.4 used the same

TCMTB purity (96.9%) and temperature (25 °C) but different pressures (4.32 and 4.05

MPa respectively), permitting comparisons of the effects of pressure of the

CO_2/acetone/TCMTB system on phase compositions. The wider-spread phase

compositions at the lower pressure compared to those at the higher pressure indicate that

phase separations occur more easily farther from the critical point (lower pressure). This

is in agreement with the physical reality of the critical point since phase compositions

converge as the system approaches the critical point where they become identical.

As explained in Chapter 6, desired amounts of biocide, cosolvent, or a

cosolvent/biocide mixture were first added to the equilibrium cell. Then pressure in the

equilibrium cell was increased through addition of CO_2. The gas would first fill the cell

and then the liquid/gas meniscus would rise in the cell as pressure was increased. A

second meniscus would rise in the cell with increasing pressure through addition of CO_2,

forming the desired three phases. For example, at acetone and TCMTB contents in the

case of Figure 6.4, the second meniscus would be formed at about 3.95 MPa. Only two

phases were possible below this pressure. Since the stoichiometric method for analysis of

the compositions of phases requires that the number of phases be equal to or greater than

the number of components, only observation of two-phase equilibrium was possible for a three component system with the apparatus used in this study.
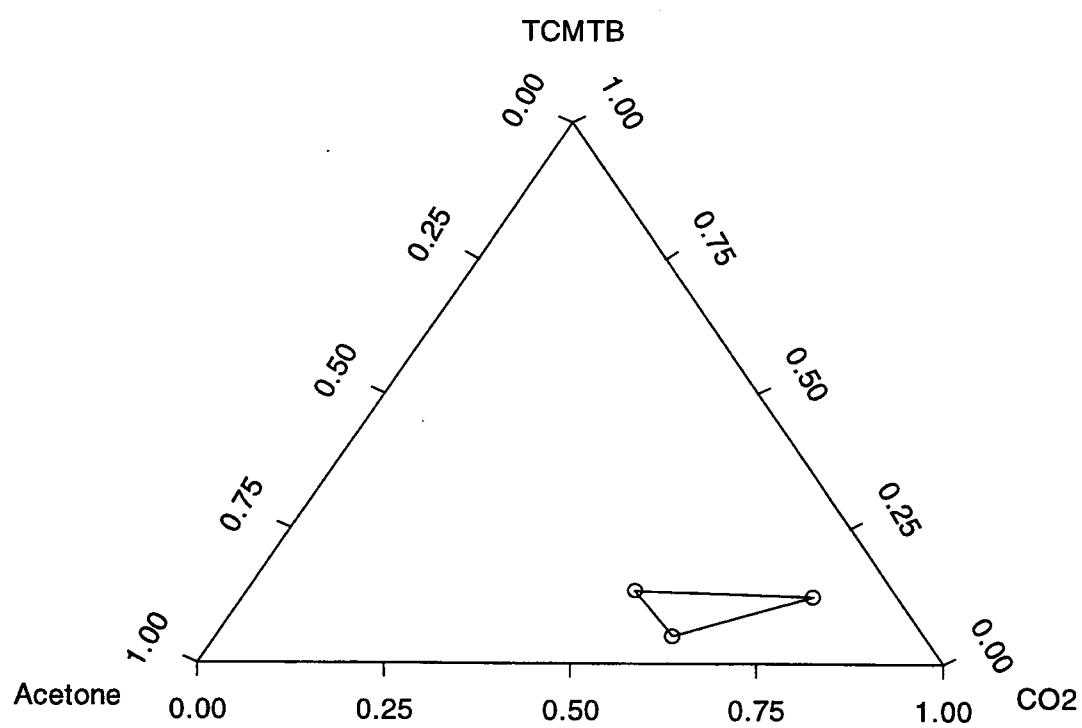
Figure 6.2 Triangular phase diagram representing three-phase behavior for the CO_2/acetone/TCMTB mixture at 35 °C and 5.28 MPa.
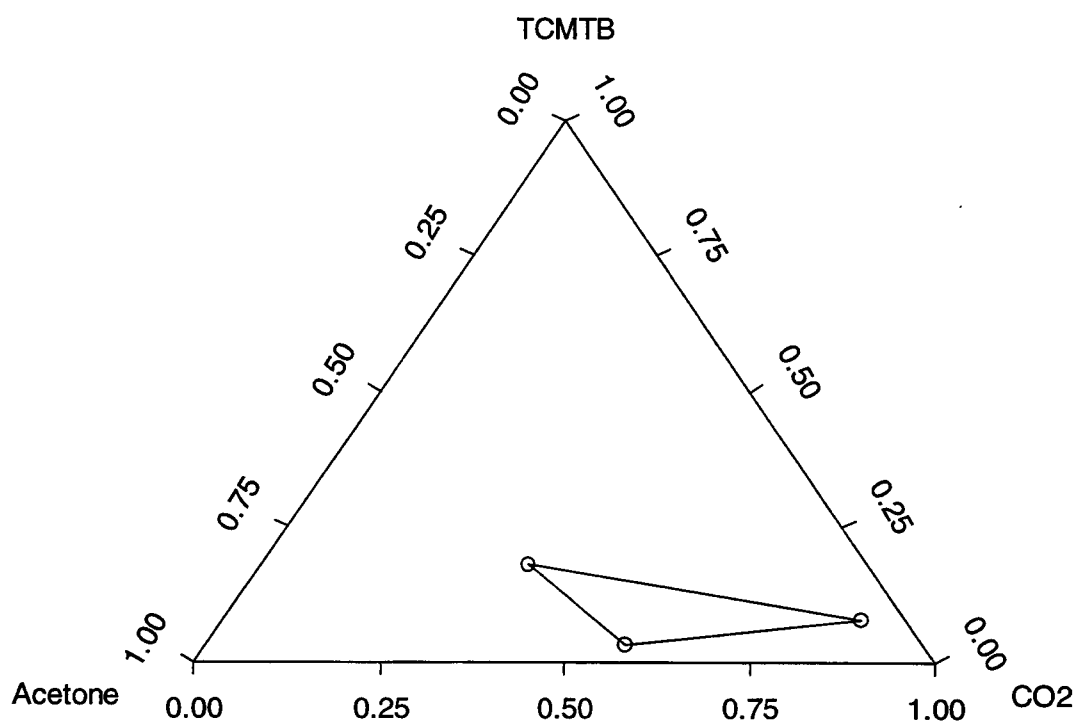
Figure 6.3   Triangular phase diagram representing three-phase behavior for the
CO_2/acetone/TCMTB mixture at 25 °C and 4.32 MPa.
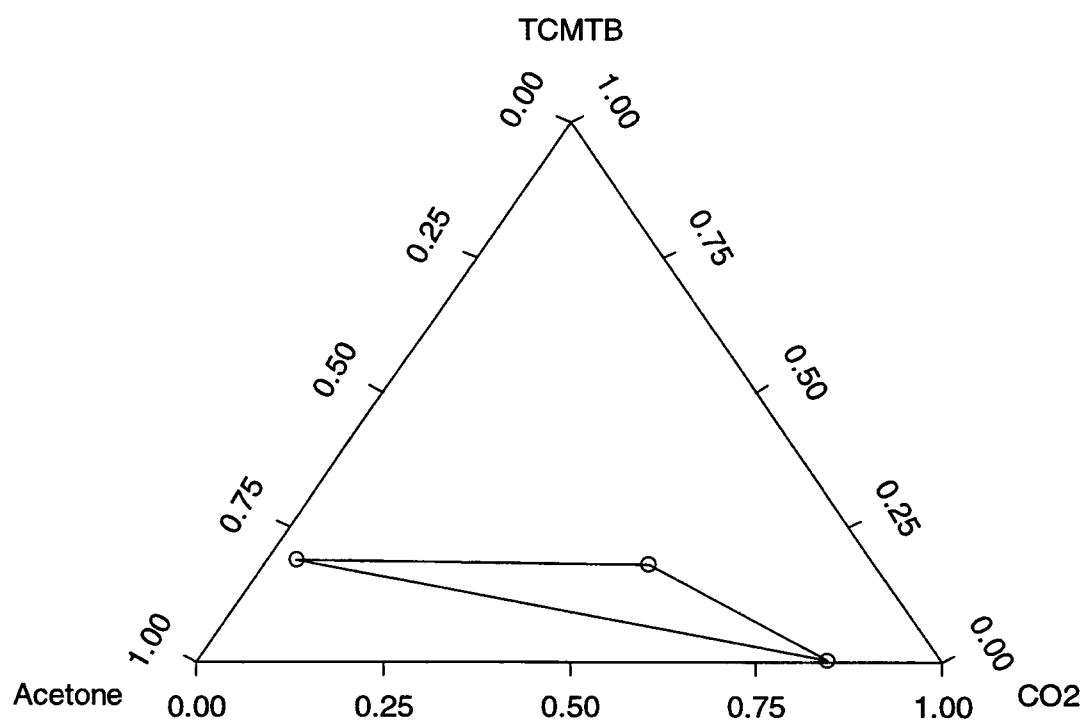
Figure 6.4   Triangular phase diagram representing three-phase behavior for the
CO_2/acetone/TCMTB mixture at 25 °C and 4.05 MPa.

CHAPTER 7

MODEL DEVELOPMENT FOR PHASE EQUILIBRIA AT HIGH PRESSURES

7.1 Introduction

Phase composition measurements are difficult to make without upsetting the phase equilibrium. Such experiments require significant time periods to reach equilibrium, especially near critical conditions. The number of phase equilibria experiments required for process development can be considerably reduced if a mathematical model could be developed to predict reasonably accurate phase compositions. Therefore, the objective of this chapter was to develop a fundamental model with as few parameters as possible for predicting high-pressure phase equilibria of systems containing polar, non-simple molecules. Models used for binary LL and VL equilibria and for ternary VLL equilibria of simple and complex systems are developed in this chapter. Phase compositions in binary and ternary systems were predicted using two different equations of state and three different mixing rules and compared to the experimental values. When critical properties of a compound were not known, they were either estimated using a group contribution method or fitted to phase equilibria data. Results of the biocide systems will be useful for understanding the phenomena that occur during the SC wood treatment process and for improving and scaling up these processes.

7.2 Mathematical Model Used for Phase Equilibria at High Pressure

In order to have thermal and mechanical equilibrium in a heterogeneous, closed system (a system made up of two or more phases where each phase is considered as an

open system within the overall closed system), the temperature (T), the pressure (P) and

the chemical potential (μ_i) (or the partial molar Gibbs free energy) governing mass

transfer of species i must be uniform throughout the system (Prausnitz et al., 1986). The

following necessary conditions for equilibrium for such an n-component p-phase system

can be proved.

$$T_1 = T_2 = \cdots = T_p \tag{7.1}$$

$$P_1 = P_2 = \cdots = P_p \tag{7.2}$$

$$\mu_{i1} = \mu_{i2} = \cdots = \mu_{ip} \quad ; \quad i = 1, n \tag{7.3}$$

In order to relate the chemical potential to physically measurable quantities such

as temperature, pressure and composition (x_i), a function f_i, called the fugacity of species i

in a mixture is defined with reference to the ideal gas mixture (Prausnitz et al., 1986):

$$\ln\left(\frac{\overline{f}_i(T,P,X_i)}{x_i P}\right) = \frac{\mu_i - \mu_i^{IGM}}{RT} \tag{7.4}$$

where superscript IGM denotes the property of an ideal gas mixture. Using equations

(7.3) and (7.4) it can be shown that the fugacity of each species must be the same in all

phases at equilibrium conditions:

$$\overline{f_{i1}} = \overline{f_{i2}} = \cdots = \overline{f_{ip}} \quad ; \quad i = 1, n \tag{7.5}$$

Use of an equation of state is the most common method of computing the fugacity of a species in a gas mixture. Fugacity of a species in a liquid mixture, on the other hand, can be computed using two different methods: one based on an equation of state (EOS) model for the liquid phase or a second based on an activity coefficient model. In this study, equations of state were used for the vapor phase in all equilibrium studies and for the liquid phases in VLL equilibria. Activity coefficient models were used for the liquid phases in LL and VL equilibria. The equation of state and the activity coefficient models are two different methods and will be considered separately.

7.2.1 Equation of State Approach

The fugacity of a species in a gaseous mixture (Sandler, 1989, pp. 308-310) is obtained from

$$\overline{f_i}^V = y_i P \Phi_i^V \tag{7.6}$$

where the fugacity coefficient (Φ_i^V) is calculated from

$$\ln\Phi_i^V = \ln\frac{\overline{f_i}^V}{y_i P} = \frac{1}{RT} \int\limits_{\underline{V}=\infty}^{\underline{V}=Z^V RT/P} \left[\frac{RT}{\underline{V}} - N(\frac{\partial P}{\partial N_i})_{T,V,N_{j \neq i}} \right] d\underline{V} - \ln Z^V \tag{7.7}$$

Volumetric EOSs can be used to compute the fugacity coefficient. Among different volumetric EOSs, the Peng-Robinson (PR) (1976) and the Redlich-Kwong (RK) (1949) EOS with van der Waals mixing rules are the most commonly used equations for multicomponent phase equilibria studies at high pressures. In this study, the PR and RK equations of state with three different mixing rules were evaluated. The mixing rules used in these models were (1) van der Waals mixing rules with one interaction parameter per binary, (2) van der Waals mixing rules with two interaction parameters per binary (Panagiotopoulos and Reid, 1987), and (3) Kwak and Mansoori's mixing rules (1986). The Kwak and Mansoori's mixing rules were attractive because of their correct theoretical basis. With Kwak and Mansoori's mixing rules, the RK-EOS requires fewer interaction parameters (one per binary) than the PR-EOS (three per binary) and therefore the RK-EOS was paired with Kwak and Mansoori's mixing rules while the PR-EOS was used with van der Waals mixing rules having one or two interaction parameters per binary. First the PR and then the RK-EOS are discussed. The PR-EOS is:

$$P = \frac{RT}{\underline{V} - b} - \frac{a(T)}{\underline{V}(\underline{V} + b) + b(\underline{V} - b)} \tag{7.8}$$

with pure component parameters

$$a(T) = 0.45724 \frac{R^2 T_c^2}{P_c} \alpha(T) \tag{7.9}$$

$$\sqrt{\alpha} = 1 + \kappa \left(1 - \sqrt{\frac{T}{T_c}} \right) \tag{7.10}$$

$$\kappa = 0.37464 + 1.54226\,\omega - 0.26992\,\omega^2 \tag{7.11}$$

$$b = 0.07780\,\frac{RT_c}{P_c} \tag{7.12}$$

In the case of mixtures, the parameters a and b depend on the mixture composition. These mixture parameters, can be obtained from van der Waals mixing rules:

$$a = \sum_i^n \sum_j^n y_i\, y_j\, a_{ij} \tag{7.13}$$

$$b = \sum_i^n y_i\, b_i \tag{7.14}$$

In these equations, a_{ij} ($i=j$) and b_i are parameters corresponding to pure component (i) while a_{ij} ($i \neq j$) are called the "unlike-interaction parameters". The unlike-interaction parameters are related to the pure-component parameters by the following expressions:

$$a_{ij} = \left(1 - \delta_{ij}\right)\sqrt{a_{ii}\, a_{jj}} \tag{7.15}$$

where the δ_{ij} values are fitting parameters and $\delta_{ij} = \delta_{ji}$, thus there is only one fitting parameter per binary. If the unlike-interaction parameter is related to the pure-component

parameters by the expressions proposed by Panagiotopoulos and Reid (1987), there will

be two fitting parameters (k_{ij} and k_{ji} where $k_{ij} \neq k_{ji}$) per binary:

$$a_{ij} = \left[1 - k_{ij} + \left(k_{ij} - k_{ji}\right)x_i\right]\sqrt{a_{ii}\,a_{jj}} \qquad (7.16)$$

By using equations (7.8)-(7.15), to evaluate the derivative $(\partial P/\partial N_i)_{T, V, Nj \neq i}$, which

appears in equation (7.7), the fugacity coefficient based on the PR-EOS with van der

Waals mixing rules having one interaction parameter can be determined:

$$\ln \Phi_i^{V} = \frac{B_i}{B}\left(Z^{V}-1\right)-\ln\left(Z^{V}-B\right)$$

$$-\frac{A}{2\sqrt{2}B}\left[\frac{2\sum_j y_j A_{ij}}{A} - \frac{B_i}{B}\right]\ln\left[\frac{Z^{V}+\left(\sqrt{2}+1\right)B}{Z^{V}-\left(\sqrt{2}-1\right)B}\right] \qquad (7.17)$$

where

$$A = \frac{aP}{\left(RT\right)^2} \qquad (7.18)$$

$$B = \frac{bP}{RT} \qquad (7.19)$$

and the superscript V denotes vapor phase property. The compressibility factor, $Z = P\underline{V}/RT$, can be obtained by solving the cubic equation (7.20) (Sandler, 1989, pp. 148-149), which is an equivalent rearrangement of equation (7.8).

$$Z^3 +(B - 1)Z^2 +\left(A - 3B^2 - 2B\right)Z +\left(-AB + B^2 + B^3\right) = 0 \qquad (7.20)$$

The largest real value of Z corresponds to the vapor phase compressibility and the smallest real value to the liquid compressibility. The intermediate value is an extraneous root to the cubic equation with no direct physical meaning. For multicomponent phase equilibria, the appropriate value of Z for each phase is determined by calculating the Gibbs free energy associated with each root of the cubic equation of state. The correct value of Z for each phase is always the root of the cubic EOS giving the lowest Gibbs free energy.

An equation similar to equation (7.17) can be obtained when the PR-EOS with van der Waals mixing rules having two interaction parameters (equation 7.16) is used (Panagiotopoulos and Reid, 1987):

$$\ln \Phi_i{}^V = \frac{B_i}{B}\left(Z^V - 1\right) - \ln\left(Z^V - B\right)$$

$$-\frac{A}{2\sqrt{2}\,B}\ln\left[\frac{Z^V + \left(\sqrt{2}+1\right)B}{Z^V - \left(\sqrt{2}-1\right)B}\right] \times \qquad (7.21)$$

$$\left[\frac{\sum_j x_j\left(A_{ji} + A_{ij}\right) - \sum_j \sum_k x_j^2 x_k\left(k_{jk} - k_{kj}\right)\sqrt{A_{jj}A_{kk}} + x_i \sum_j x_j\left(k_{ij} - k_{ji}\right)\sqrt{A_{ii}A_{jj}}}{A} - \frac{B_i}{B}\right]$$

where A, B, and Z^V are given by equations 7.18, 7.19, and 7.20 respectively.

The RK-EOS is:

$$P = \frac{RT}{\underline{V}-b} - \frac{a}{T^{1/2}\,\underline{V}\left(\underline{V}+b\right)} \qquad (7.22)$$

with pure component parameters

$$a = 1.2828\,R\,T_c^{1.5}\,\underline{V}_c \qquad (7.23)$$

$$b = 0.26 \underline{V}_c \tag{7.24}$$

In the case of mixtures, the parameters a and b depend on the mixture composition and can be obtained from Kwak and Mansoori's mixing rules (1986):

$$a = \frac{\left(\sum_i^n \sum_j^n x_i x_j a_{ij}^{2/3} b_{ij}^{1/3} \right)^{1.5}}{\left(\sum_i^n \sum_j^n x_i x_j b_{ij} \right)^{1/2}} \tag{7.25}$$

$$b = \sum_i^n \sum_j^n x_i x_j b_{ij} \tag{7.26}$$

In these equations, again a_{ij} and b_{ij} ($i=j$) are parameters corresponding to pure component (i) while a_{ij} and b_{ij} ($i \neq j$) are the unlike-interaction parameters and related to the pure-component parameters by the following expressions:

$$a_{ij} = \left(1 - \delta_{ij}\right)\sqrt{a_{ii} a_{jj}} \tag{7.27}$$

$$b_{ij} = \left(\frac{b_{ii}^{1/3} + b_{jj}^{1/3}}{2} \right)^3 \tag{7.28}$$

where the δ_{ij} values are fitting parameters and $\delta_{ij} = \delta_{ji}$. Of course, numerical values of these parameters will be different from those of the PR-EOS (equation 7.15).

Following the same development as for the PR-EOS, the fugacity coefficient based on RK-EOS and Kwak and Mansoori's mixing rules is given by:

$$\ln \Phi_i^V = \ln\left(\frac{V}{V-b}\right) + \frac{2\sum y_j b_{ij} - b}{V-b} - \ln Z$$

$$+ \left[\frac{a\left(2\sum y_j b_{ij} - b\right)}{b^2 RT^{1.5}}\right]\left[\ln\left(\frac{V+b}{V}\right) - \frac{b}{V+b}\right]$$

$$- \left[\frac{\dfrac{3\alpha^{1/2}\left(\sum y_j a_{ij}^{2/3} b_{ij}^{1/3}\right)}{b^{1/2}} - \dfrac{\alpha^{3/2}\left(\sum y_j b_{ij}\right)}{b^{3/2}}}{bRT^{1.5}}\right]\ln\left(\frac{V+b}{V}\right) \qquad (7.29)$$

where

$$\alpha = \sum_i \sum_j y_i y_j a_{ij}^{2/3} b_{ij}^{1/3} \qquad (7.30)$$

Again the compressibility factor, $Z = PV/RT$, can be obtained by solving the cubic

equation (7.31) (Sandler, 1989, pp. 148-149), which is an equivalent rearrangement of

equation (7.22).

$$Z^3 - Z^2 + \left(A - B - B^2\right)Z - AB = 0 \qquad (7.31)$$

where

$$A = \frac{aP}{(RT)^2 \sqrt{T}} \qquad (7.32)$$

$$B = \frac{bP}{RT} \qquad (7.33)$$

As for the case of the PR-EOS, the correct value of Z for each phase in a multicomponent

phase equilibria is always the root of the cubic EOS giving the lowest Gibbs free energy.

As mentioned in section 7.2, the fugacity of a species in a liquid mixture can be

obtained using two different methods: one based on an equation of state model for the

liquid phase and another based on an activity coefficient model. In the first method, an equation similar to equations (7.17), (7.21), and (7.29) will result, except that the liquid phase, rather than vapor phase compressibility factor must be used in the calculations. For multicomponent phase equilibria, the correct value of Z for each phase is always the root of the cubic EOS giving the lowest Gibbs free energy.

7.2.2 Activity Coefficient Methods

The fugacities of species in liquid mixtures (Sandler, 1989, p. 321), are obtained from

$$\bar{f}_i^L\left(T,P,x_i\right) = x_i\,\gamma_i\left(T,P,x_i\right)f_i^L\left(T,P\right) \tag{7.34}$$

where γ_i is the activity coefficient of species i and $f_i^L(T, P)$ is the fugacity of pure species i as a liquid at the temperature and pressure of the mixture. In this study, the van Laar activity coefficient model was used. Using this method, the activity coefficients for species 1 and 2 in a binary mixture are obtained from the following equations:

$$\ln\gamma_1 = \frac{\alpha}{\left[1 + \dfrac{\alpha}{\beta}\dfrac{x_1}{x_2}\right]^2} \tag{7.35}$$

$$\ln\gamma_2 = \frac{\beta}{\left[1 + \dfrac{\beta}{\alpha}\dfrac{x_2}{x_1}\right]^2} \tag{7.36}$$

where α and β are fitting parameters. The activity coefficient for species I in a ternary mixture using the van Laar equation can be obtained from the following equation:

$$\ln\gamma_1 = \frac{x_2{}^2\,\alpha_{12}\left(\dfrac{\beta_{12}}{\alpha_{12}}\right)^2 + x_3{}^2\,\alpha_{13}\left(\dfrac{\beta_{13}}{\alpha_{13}}\right)^2 + x_2\,x_3\dfrac{\beta_{12}}{\alpha_{12}}\dfrac{\beta_{13}}{\alpha_{13}}\left(\alpha_{12}+\alpha_{13}-\alpha_{23}\dfrac{\alpha_{12}}{\beta_{12}}\right)}{\left[x_1 + x_2\left(\dfrac{\beta_{12}}{\alpha_{12}}\right)+x_3\left(\dfrac{\beta_{13}}{\alpha_{13}}\right)\right]^2} \tag{7.37}$$

where $\alpha_{ji} = \beta_{ij}$ and $\beta_{ji} = \alpha_{ij}$. The expression for $\ln\gamma_2$ is obtained by interchanging the subscripts I and 2 in equation (7.37) and for $\ln\gamma_3$ by interchanging the subscripts I and 3. Note that there are two parameters, α_{ij} and β_{ij} for each pair of components in the mixture.

For incompressible pure liquids, the fugacity, f_i^L, which appears in equation (7.34) can be estimated from

$$f^L(T,P) = P^{vap}\left(\frac{f}{P}\right)_{sat}\exp\left[\frac{\underline{V}^L\left(P-P^{vap}\right)}{RT}\right] \tag{7.38}$$

If at least one of the components in a liquid mixture is a solid or a vapor at mixture temperature and pressure, the mixture is non-simple (Sandler, 1989, pp. 351-359). For a non-simple liquid mixture, the pure component fugacities of the nonexistent liquids can be estimated by simple extrapolation procedures. The fugacity of a pure liquid in a non-simple liquid mixture can be estimated to be equal to the product of its vapor pressure, P^{vap}, and the fugacity coefficient of the pure liquid at saturated conditions, $(f/P)_{sat}$. This means that the exponential term of equation (7.38) can be ignored.

The fugacity coefficient of a pure saturated liquid, $(f/P)_{sat}$, is computed at the vapor pressure of the liquid

$$\left(\frac{f}{P}\right)_{sat} = \left(\frac{f}{P}\right)\bigg|_{P = P^{vap}}$$
(7.39)

and can be obtained by using the following equation based on PR-EOS

$$\ln\left(\frac{f}{P}\right) = Z - 1 - \ln(Z - B) - \frac{A}{2\sqrt{2}\,B}\ln\left[\frac{Z + (\sqrt{2} + 1)B}{Z - (\sqrt{2} - 1)B}\right]$$
(7.40)

or using equation (7.41) which is based on RK-EOS

$$\ln\left(\frac{f}{P}\right) = Z - 1 - \ln Z + \ln\left(\frac{V}{V - b}\right) - \frac{a}{b\,R\,T^{1.5}}\ln\left(\frac{V + b}{V}\right)$$
(7.41)

The liquid molar volume which appears in equation (7.38) can be estimated from the following equation (Perry, 1984, p. 3-273):

$$V^L = \frac{R\,T_c\,Z_{RA}^{\left[1 + (1 - T_r)^{2/7}\right]}}{P_c}$$
(7.42)

where Z_{RA} is a constant determined from experimental saturated-liquid densities. If Z_{RA} cannot be determined from experimental data, then the value of the critical compressibility factor, Z_c, may be used for Z_{RA}.

The vapor pressure in equation (7.38) can be estimated from the widely used Antoine correlation

$$\ln P^{sat} = A - \frac{B}{(T+C)}$$

(7.43)

This equation can be used for the components whose constants are tabulated in the literature. If Antoine constants are not known, but the critical pressure, P_c, and critical temperature, T_c, and one other vapor-pressure point, such as the normal boiling point are known, the following equation (Perry, 1984, p. 3-274) can be used:

$$\ln P_r^{sat} = A° - \frac{B°}{T_r} + C° \ln T_r + D° T_r^6$$

(7.44)

where

P_r^{sat}	= reduced vapor pressure = P^{sat} / P_c
T_r	= reduced temperature = T / T_c
$A°$	= $-35Q$
$B°$	= $-36Q$
$C°$	= $42Q + \alpha_c$
$D°$	= $-Q$
Q	= $0.0838 (3.758 - \alpha_c)$

α_c can be determined by inserting the one known vapor-pressure (P_1^{sat}, T_1) into equation (7.44) and solving for α_c:

$$\alpha_c = \frac{0.315 \psi_1 - \ln P_{1r}^{sat}}{0.0838 \psi_1 - \ln T_{1r}}$$

(7.45)

where

$$\psi_1 = -35 + \frac{36}{T_{1r}} + 42\ln T_{1r} - T_{1r}{}^6 \tag{7.46}$$

7.2.3 Computer Algorithm

As mentioned in section 7.2, the necessary condition for equilibrium for an n-component p-phase system is that

$$\overline{f_{i1}} = \overline{f_{i2}} = \cdots = \overline{f_{ip}} \quad ; \quad i = 1, n \tag{7.47}$$

There are $np+2$ state variables: the set $\{x_{ij}\}$, the temperature (T), and pressure (P). Following Heidemann's method (1983) for flash calculations, one of the phases is chosen as a "reference phase". The reference phase can be different for each of the components, depending on convenience; certainly a component must be present in its own reference phase and the reference phase has to be present at equilibrium. Equation (7.47) can be written as

$$\overline{f_{ij}} = \overline{f_{ir_i}} \tag{7.48}$$

where r_i is the index of the reference phase for component i. Equation (7.48) can be written for n components and p-1 nonreference phases to obtain $n(p$-1) equations. Since it is necessary that mole fractions in each phase sum to unity, one additional equation for each of the p phases can be written

$$\sum_i x_{ij} = 1 \tag{7.49}$$

There are a total of $n(p-1)+p$ equations in $np+2$ variables and it is necessary to fix $n-p+2$ variables. If the number of phases, p, is equal to the number of components, n, as in this study, the total number of equations would be n^2 and total number of variables n^2+2. By fixing two variables (such as T and P), the state of the system will be fixed and the phase compositions can be calculated from n^2 equations and n^2 unknowns. In the CO_2-cosolvent-biocide system we are studying three-phase behavior ($n=p=3$), thus by fixing T and P the state of the system will be fixed and the phase compositions can be calculated from 9 equations (6 from equation (7.48) plus 3 from equation (7.49)) in 9 unknowns (the set $\{x_{ij}\}$).

The following convergence criterion (DiAndreth and Paulaitis, 1989) was used for the fugacity equations (equilibrium conditions):

$$\sum_i \sum_j \left[\ln\left(\frac{\overline{f_{ij}}}{\overline{f_{i\,r_i}}} \right) \right]^2 \le \epsilon \tag{7.50}$$

where the logarithm of fugacities represents the gradient of the Gibbs free energy with respect to composition and ϵ is a convergence limit. The gas phase was chosen to be the reference phase and a value of 10^{-8} was used for ϵ. An initial estimate of phase compositions was obtained from either the measured phase compositions at the temperature and pressure of interest, or from previous calculations at similar temperature and pressure. If trivial solutions giving two phases of identical compositions were obtained, a larger ϵ limit was chosen.

In all of the systems studied, parameters (interaction parameters and activity coefficient parameters) were fitted to the experimental data by minimizing the following objective function:

$$f_{obj} = \sum_k \sum_j \sum_i \left(\frac{x_{ij}^{exp} - x_{ij}^{cal}}{x_{ij}^{exp} + x_{ij}^{cal}} \right)^2 \tag{7.51}$$

where x^{exp}_{ij} is the experimental, x^{cal}_{ij} the calculated mole fraction of component i in phase j, and k refers to the data points used in the fitting.

7.2.4 Results and Discussion

The VLL phase equilibria of the ternary systems of interest (CO_2-cosolvent-

biocide) were expected to be complex and possibly difficult to model. Therefore, the

models were first applied to LLE and VLE of simple binary systems and VLLE of ternary

systems consisting of molecules more simple than the molecules in the system of interest.

Three modeling methods were applied to data in the literature. The method numbers

correspond to the number of fitting parameters for binary mixtures.

Method 1:   An equation of state (PR or RK EOS) for both the vapor and the liquid
             phases. This model has 1 fitting parameter for a binary system and 3 for a
             ternary system.

Method 2:   Van Laar activity coefficient model for both the vapor and the liquid
             phases. This method has 2 fitting parameters for a binary system and 6 for
             a ternary system.

Method 3:   An equation of state (PR or RK EOS) for the vapor phase and van Laar
             activity coefficient model for the liquid phase. This method has 3 fitting
             parameters for a binary system and 9 for a ternary system.

The systems studied are summarized in Table 7.1 where "Best" implies the most

successful method for each system. Table 7.1 also shows the conditions (number of

temperatures and pressures) at which phase composition data were available and used in

the fitting.

Figure 7.1 summarizes the overall algorithm for calculating the adjustable

parameters using Powell's minimization method. Figure 7.2 shows the routine for

calculating the objective function used in the composition matching algorithm when an

equation of state is used to calculate the fugacities. The algorithm outlined in Figure 7.2

is for fugacities of the vapor phase in VLE and all phases in VLLE. For the liquid phase in VLE and the two phases of LLE, the mixture fugacities were calculated using activity coefficients and pure component fugacities instead of using mixture parameters. In calculating pure component fugacities, pure component parameters were used to solve the cubic EOS and to find the appropriate value of compressibility factor corresponding to the lowest Gibbs free energy.

The models were solved using a SUN FORTRAN compiler 4.1.4 on a SUN SPARC station 10 model 40 (S10GX-40-32-P46) with one SuperSPARC processor or Microsoft FORTRAN compiler 4.1 on a 486 Gateway 2000 personal computer (4DX2-66V). Since calculations for the adjustable parameters using Powell's minimization method were complex, the 486 personal computer (PC) could not be used to solve the problem due to its memory limitations. The range of time required to do these calculations using the SUN SPARC station was less than a minute to a few minutes depending on the number of phase composition data used in the fitting. Prediction of phase compositions using the fitted parameters obtained from Powell's minimization method required less memory and could be done on either the SUN SPARC station or the PC in less than a minute. The computer programs used for these models are presented in Appendix C. Results of the LLE, VLE, and VLLE modeling are discussed in sections 7.2.4.1, 7.2.4.2, and 7.2.4.3 respectively. A criteria of 10^{-8} was chosen for ϵ in equation (7.50) unless mentioned otherwise.

Table 7.1   **A summary of the systems studied for modeling phase equilibria at high pressures**

Phase	System	Conditions	Method 1	Method 2	Method 3
LL	n-butane/H_2O	4 T, 8 P		Best	
LL	Propylene/H_2O	1 T, 4 P		Best	
LL	n-butyl alcohol/H_2O	9 T, 1 P		Best	
VL	CO_2/methanol	1 T, 9 P			Best
VLL	CO_2/isopropanol/H_2O	1 T, 3 P	Best		
VLL	CO_2/H_2O/C_4E_1	1 T, 3 P	Best		
VLL	CO_2/H_2O/C_8E_3	1 T, 3 P	Best		
VLL	CO_2/acetone/TCMTB	1 T, 2 P	Best		

```
┌─────────┐      ┌──────────────────────────────────────────┐
│  Begin  │─────▶│  Read component properties and constants │
└─────────┘      └──────────────────────────────────────────┘
```

$$\text{Read } T_k, P_k, x^{exp}_{i,j,k}$$

i = component, j = phase,
k = experimental data to be fitted

$$\text{Set } x_{initial,i,j,k} = x^{exp}_{i,j,k}$$

Input initial guess for model parameters

Call POWELL to minimize the objective
function outlined in Fiqure 7.2

Output the fitted parameters

End
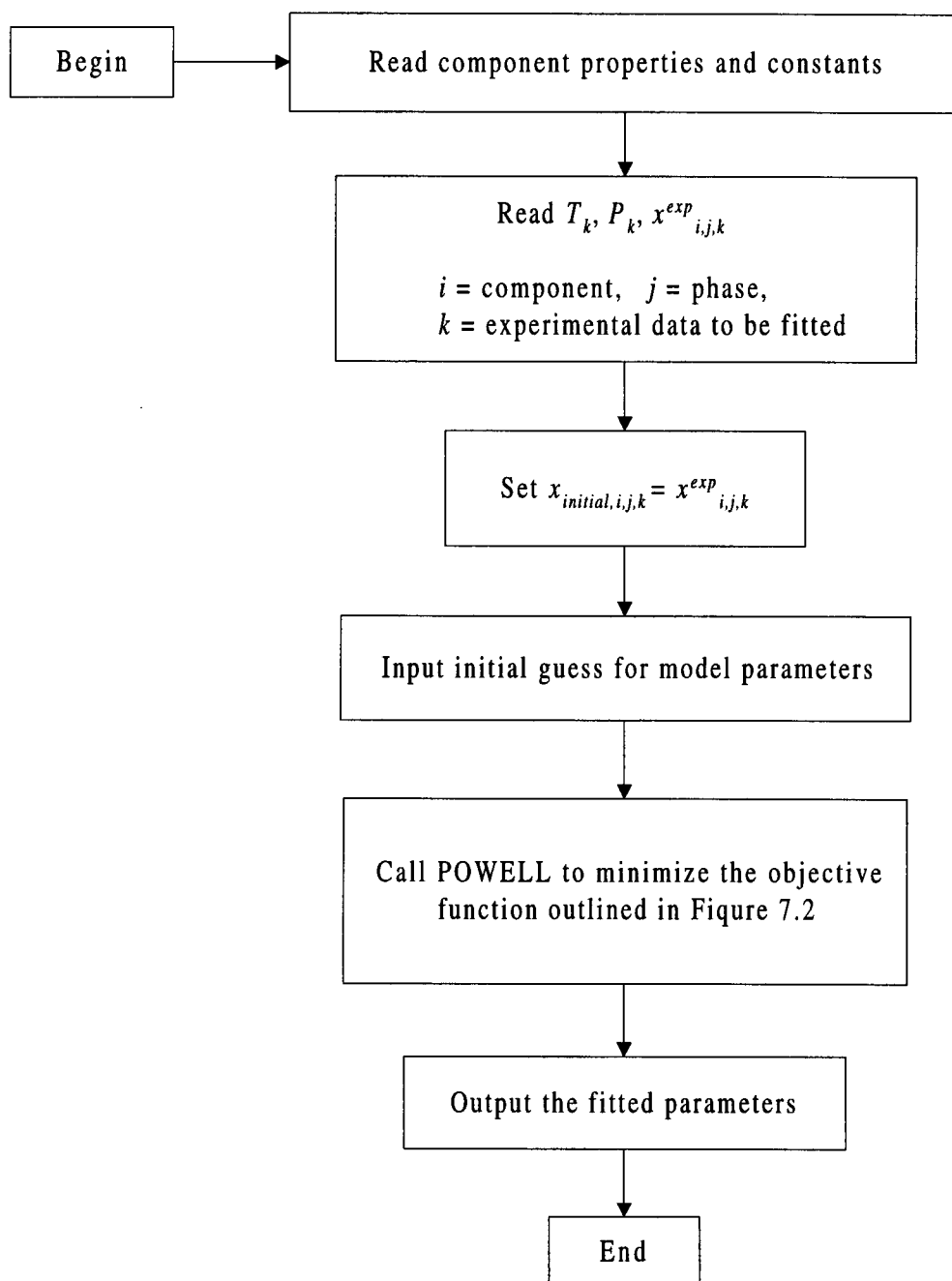
Figure 7.1   Flowchart showing the process for calculation of the adjustable parameters by fitting to experimental data.

Begin → Input values for adjustable parameters

Call PARAM to calculate pure component parameters (a, b) of the EOS

Set $x_{i,j,k} = x_{initial,i,j,k}$

i = component, j = phase,
k = experimental data to be fitted

update k

Use $x_{i,j,k}$ to find mixture parameters (a, b) of the EOS

update j

Solve the cubic EOS for each i to find the three roots Z_1, Z_2 and Z_3

Call GIBENG to find the appropriate value of Z corresponding to the lowest Gibbs free energy

Calculate the fugacity of each component i in phase j for data k

Use Powell's method to find new adjustable parameters

Maximum number of iterations reached ?

No

Fugacities in all j phases calculated ?

No

Yes

Yes

Stop

Use successive substitution method to find new $x_{i,j,k}$

No

Fugacity criteria (Eq. 7.50) satisfied ?

Yes

No

Objective function calculated from Eq. 7.51 minimized ?

No

Yes

All k experimental data used ?

Yes

No

Yes

Output the fitted parameters

End

Figure 7.2   Flowchart showing the process for calculation of the objective function used in the composition matching algorithm.

7.2.4.1 Liquid-Liquid Equilibria

The three modeling methods discussed in section 7.2.4 were applied to three sets

of binary LLE data. Since these are LLE systems, method 2 which uses an activity

coefficient model for the phases would be most applicable. Since the liquid phases could

be treated as compressed gases, method 1 and 3 were also applied. However modeling

efforts using these methods failed or yielded unsatisfactory results. Therefore, only

results obtained from method 2 will be presented here. The problem to be solved then

consists of two liquid phases in equilibrium at a fixed T and P. The mole fractions of one

component in the two phases are the two unknowns once van Laar parameters α and β

have been fitted to phase composition data (Figure 7.3).

Reamer et al. (1952) reported LLE data for the n-butane/water system at 4

temperatures (137.8 to 237.8 °C) and 8 pressures (3.45 to 68.95 MPa / 500 to 10,000

psia). This data was used to test the accuracy of method 2 when the fitting parameters α

and β were considered to depend on T and P. Thus at each condition of known T and P,

the model could be fitted exactly to the data since there were two known mole fractions

and two unknowns (α, β) (Figures 7.4 through 7.9). The parameters α and β decreased

nearly linearly with temperature at pressures of 6.89 MPa (1000 psia) and above (Figures

7.4 and 7.5). These are promising results, since they show that a parameters' dependency

on temperature can be obtained from data at only two temperatures for any pressure in

this range of temperatures and pressures. Once parameters α and β are known, phase

compositions can be accurately predicted at other temperatures in this range.

At lower pressures (3.45 or 4.14 MPa / 500 or 600 psia) linear fits were not as

good but low-order polynomials (third-order for α and second-order for β) were adequate

(Figures 7.6 and 7.7). As shown in Figures 7.8 and 7.9, α and β were strongly dependent on pressure, contrary to the normal assumptions when using the van Laar activity coefficient model. Third-order polynomials are shown as representing the parameters' dependency on the reciprocal of pressure. Curves in the above Figures, are shown only to reflect the fits to the phase composition data and to show that parameters α and β are strongly dependent on temperature and pressure.

A similar analysis using method 2 for LLE isothermal data for propylene/water system (Li and McKetta, 1963) at a temperature of 71.11 °C and pressures from 6.89 to 27.58 MPa (1000 to 4000 psia) showed α *decreased* less than 5 percent while β *increased* by less than 5 percent (Figures 7.10 and 7.11 respectively). A third set of LLE data used was at atmospheric pressure for the n-butyl alcohol/water binary (Hill and Malisoff, 1926) at 9 temperatures from 5 to 80 °C. In this case α exhibited a slight maximum in the middle of the temperature range, only about 7 percent above the minimum value (Figure 7.12). On the other hand β again demonstrated a very nearly linear decrease with increased temperature (Figure 7.13).

For all the three binary LLE systems studied, results showed that van Laar parameters α and β were strongly dependent on temperature and pressure and cannot be treated as constants. Results from binary LLE data also showed that method 2 was applicable to binary LLE systems for a wide range of temperatures and pressures. Van Laar parameters α and β can be obtained as a function of temperature and pressure with only a limited number of data points. These parameters can then be used in method 2 to predict phase compositions at other temperatures and pressures for binary LLE systems.

$$T, P$$
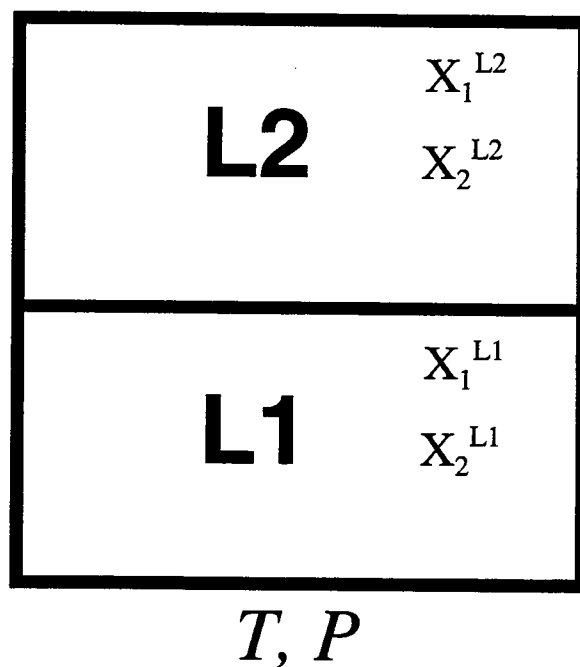
Unknowns $\quad X_1^{L1}, X_1^{L2}$

Model Parameters $\quad \alpha, \beta$

Figure 7.3 Modeling LLE using method 2.
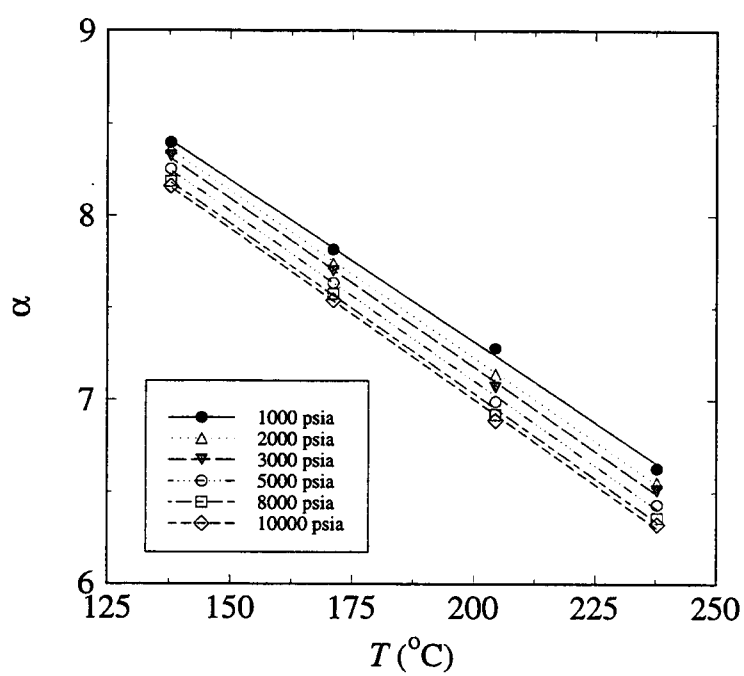
Figure 7.4 Parameter α vs. T for LLE of n-butane/water system at high pressures.
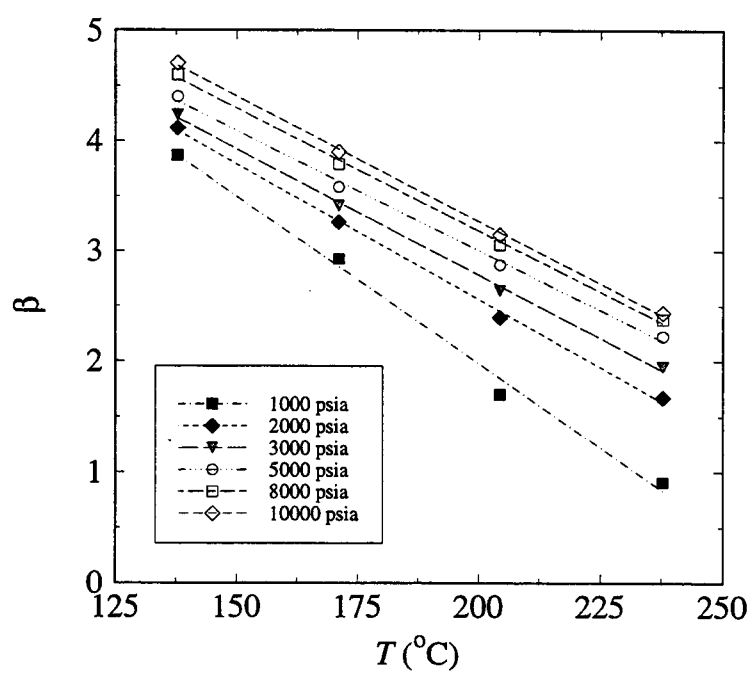
Figure 7.5   Parameter β vs. T for LLE of n-butane/water system at high pressures.
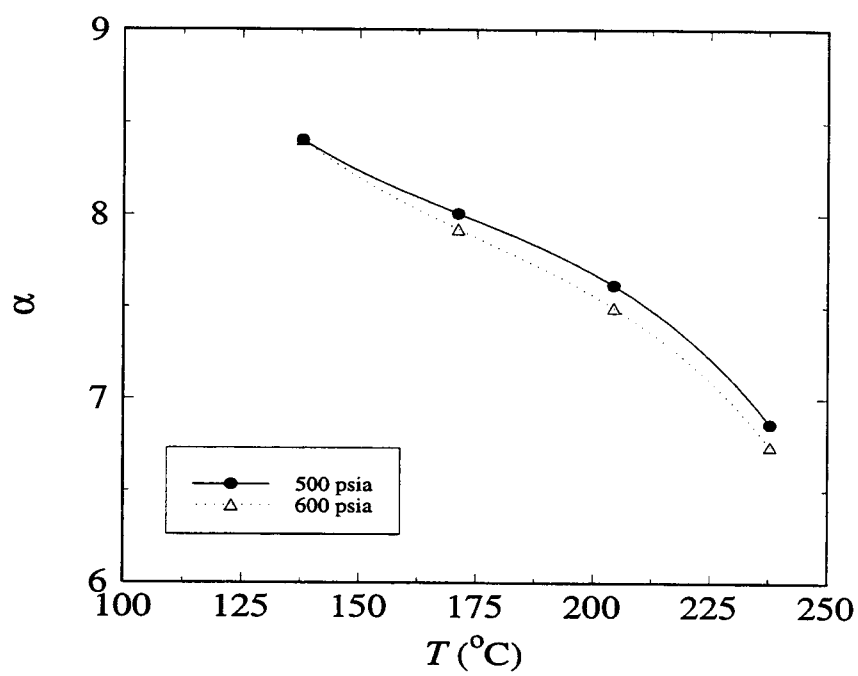
Figure 7.6 Parameter α vs. T for LLE of n-butane/water system at low pressures.
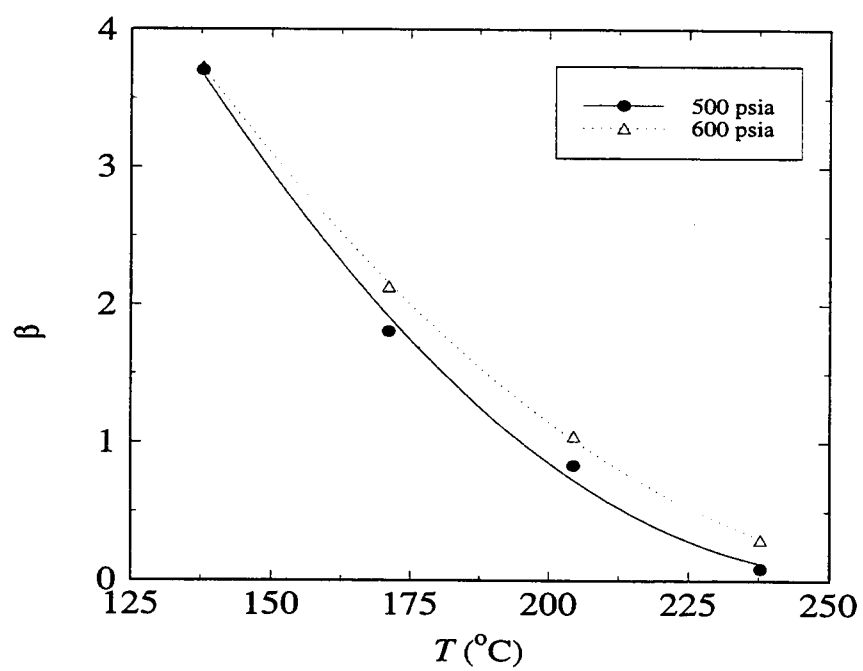
Figure 7.7   Parameter β vs. T for LLE of n-butane/water system at low pressures.
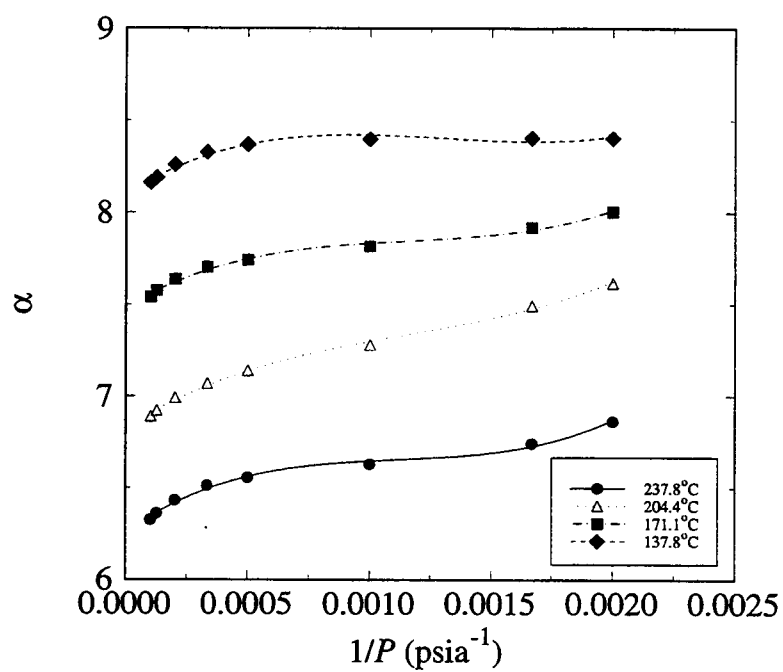
Figure 7.8 Parameter α vs. $1/P$ for LLE of n-butane/water system.
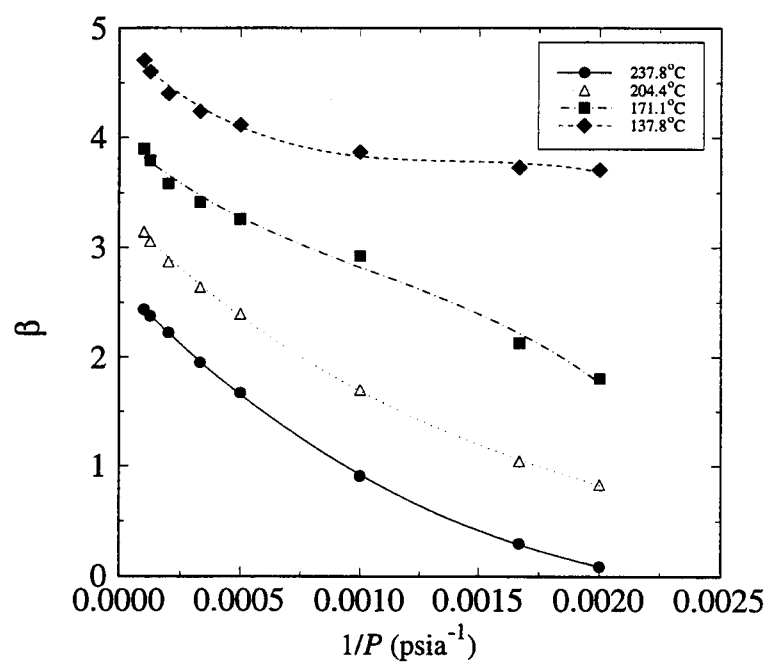
Figure 7.9   Parameter β vs. $1/P$ for LLE of n-butane/water system.
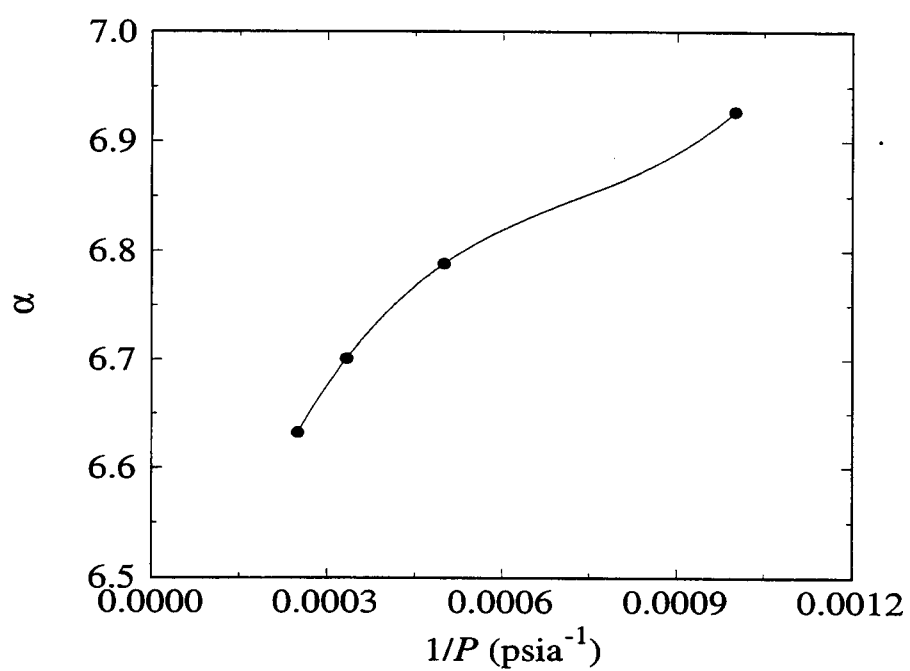
Figure 7.10 Parameter α vs. $1/P$ for LLE of propylene/water system at 71.11 °C.
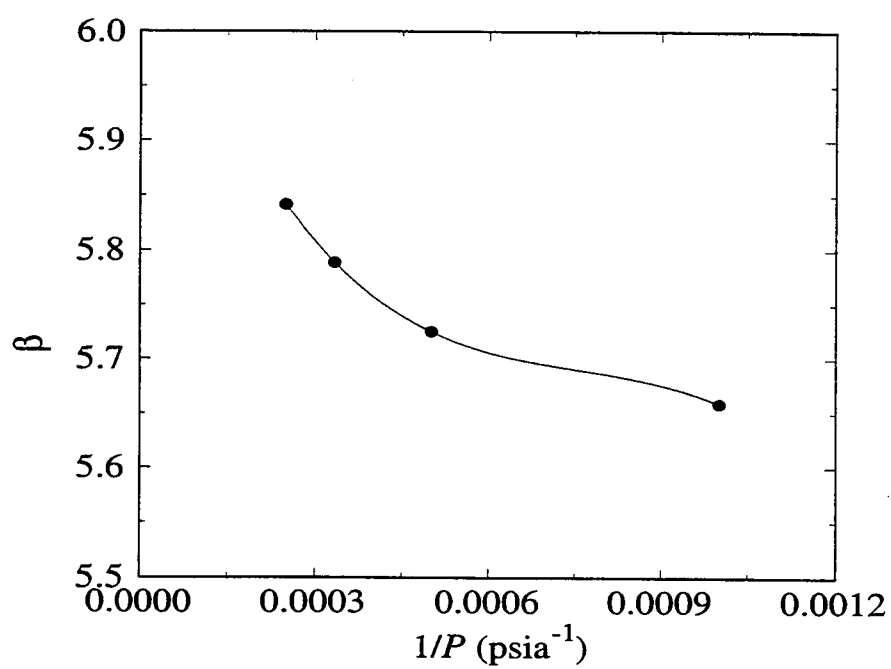
Figure 7.11   Parameter β vs. $1/P$ for LLE of propylene/water system at 71.11 °C.
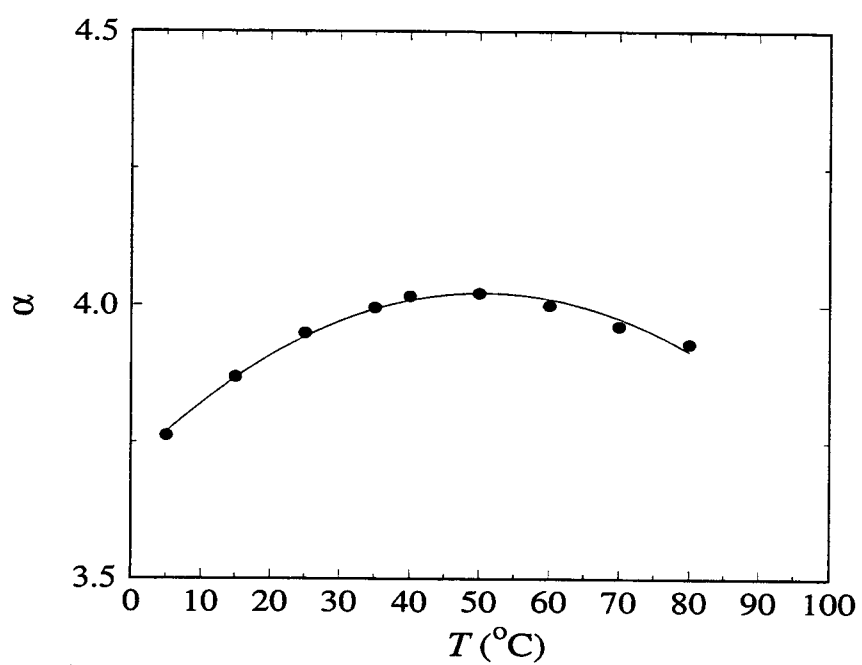
Figure 7.12   Parameter α vs. T for LLE of n-butyl alcohol/water system at 0.101 MPa (1 atm).
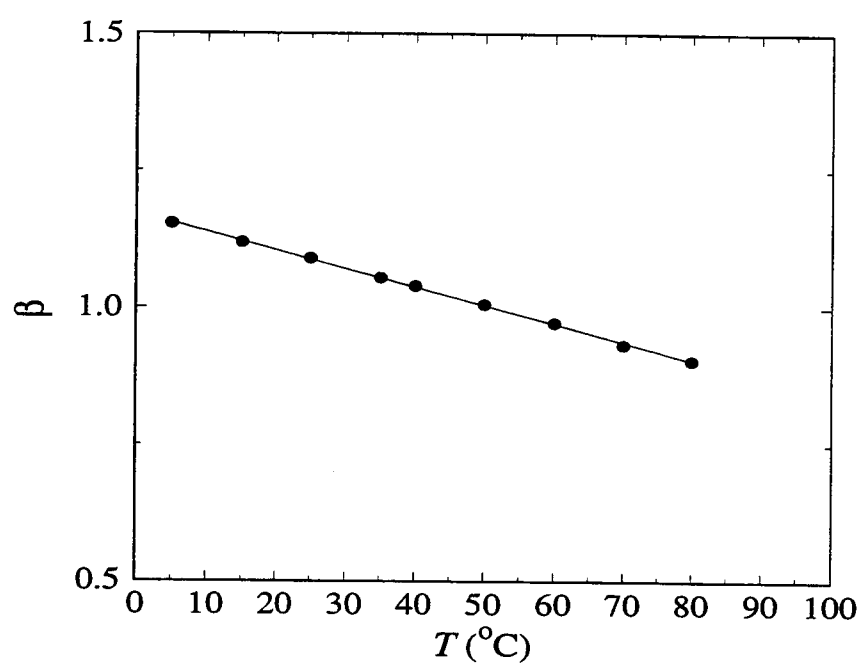
Figure 7.13   Parameter β vs. T for LLE of n-butyl alcohol/water system at 0.101 MPa (1 atm).

7.2.4.2 Vapor-Liquid Equilibria

The VLE data (Katayama et al., 1975) for a CO_2/methanol system at 25 °C and

pressures between 2.76 and 6.21 MPa (400 and 900 psia) were used to test phase

composition models for coexisting vapor and liquid phases. If the liquid phase were

treated as a compressed gas or the vapor phase were treated as an expanded liquid,

method 1 or 2 respectively could be applied. However modeling efforts using method 1

with the Peng-Robinson or Redlich-Kwong equation of state yielded unsatisfactory

results. When method 2 was applied at each T and P, α and β were found to vary greatly:

by 20 percent for α and by over an order of magnitude for β. In using method 3, the RK-

EOS with Kwak and Mansoori's mixing rules was used for the vapor phase and van Laar

activity coefficient model for the liquid phase. As shown in Figure 7.14, this method has

three fitting parameters but only two mole fractions to be fitted for each data point, thus

the problem with data at only one (T, P) set has multiple solutions. To find a single

solution to the problem, two modifications which used two of the data points instead of a

single point were made. Method 3a refers to fitting four experimental mole fractions

from two sets of (T, P) values with three parameters: δ, α and β. Method 3b utilized 4

parameters: δ, β, and an α which was linear in pressure ($\alpha = \alpha_0 + \alpha_1 P$). Values of these

parameters and phase compositions obtained from the model are given in Tables 7.2 and

7.3 respectively. The predictions of methods 3a and 3b were similar (Figure 7.15).

Better matching between the data and model predictions can of course be made by

allowing the parameters to vary with pressure, but the simple 3a method with RK-EOS

and Kwak and Mansoori's mixing rules applied to points 1 and 6 shown in Figure 7.15

represents the simplest method and would require a minimum of data. Results from

$$T, P$$
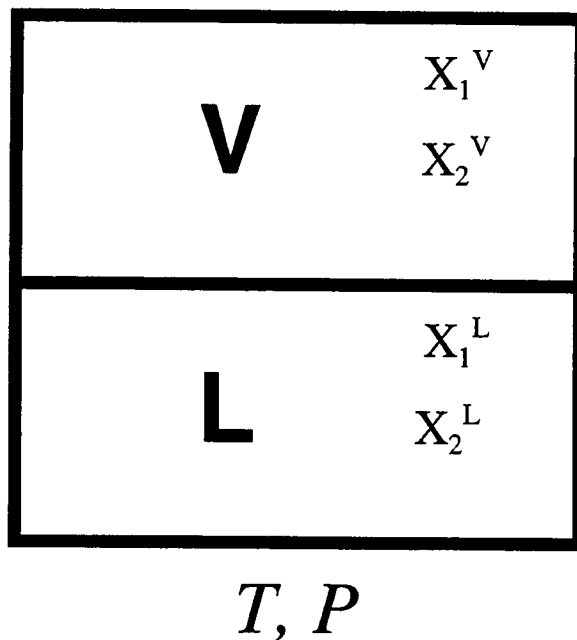
Unknowns $\qquad$ X_1^V, X_1^L

Model Parameters $\quad \delta_{12}, \alpha, \beta$

$\qquad$ **Method 3a** $\qquad$ Constant $\delta_{12}, \alpha, \beta$

$\qquad$ **Method 3b** $\qquad$ Linear α in P, Constant δ_{12}, β

$\qquad$ **Two Points** $\qquad$ 4 Unknowns, 3 Parameters

Figure 7.14 $\quad$ Modeling VLE using method 3.

binary VLE data show that method 3a applied to two sets of (T, P) values can be used to model binary VLE systems. The maximum difference between experimental and predicted phase compositions was about 20%. This difference could be reduced by (1) allowing the parameters to vary with pressure or (2) fitting the parameters to more than two sets of (T, P) values.

Table 7.2   Parameters for VLE of CO_2/methanol system at 25 °C when fitted to two points

Method	δ	α_0	α_1	β
3a	-0.7355	2.8000	-	0.8950
3b	-0.7172	2.2167	0.0100	0.9223

Table 7.3   **Experimental and calculated phase compositions for CO_2/methanol vapor-liquid equilibrium at 25 °C when adjustable parameters were fitted to two data points**

Pressure (psia/MPa)	x^{exp}_{CO2} y^{exp}_{CO2} (x^{cal}_{CO2} y^{cal}_{CO2}) Method 3a [x^{cal}_{CO2} y^{cal}_{CO2}] Method 3b	
888.84/6.13	0.957 0.994 (0.956 0.994) [0.956 0.994]	
873.86/6.02	0.932 0.993 (0.926 0.993) [0.928 0.993]	
867.83/5.98	0.922 0.993 (0.905 0.993) [0.909 0.993]	
849.02/5.85	0.810 0.993 (0.728 0.993) [0.729 0.993]	
819.63/5.65	0.662 0.992 (0.652 0.993) [0.652 0.993]	
791.85/5.46	0.610 0.993 (0.608 0.993) [0.609 0.993]	
690.30/4.76	0.450 0.993 (0.495 0.993) [0.498 0.993]	
599.62/4.13	0.361 0.993 (0.418 0.993) [0.421 0.993]	
435.31/3.00	0.256 0.992 (0.296 0.992) [0.296 0.992]	
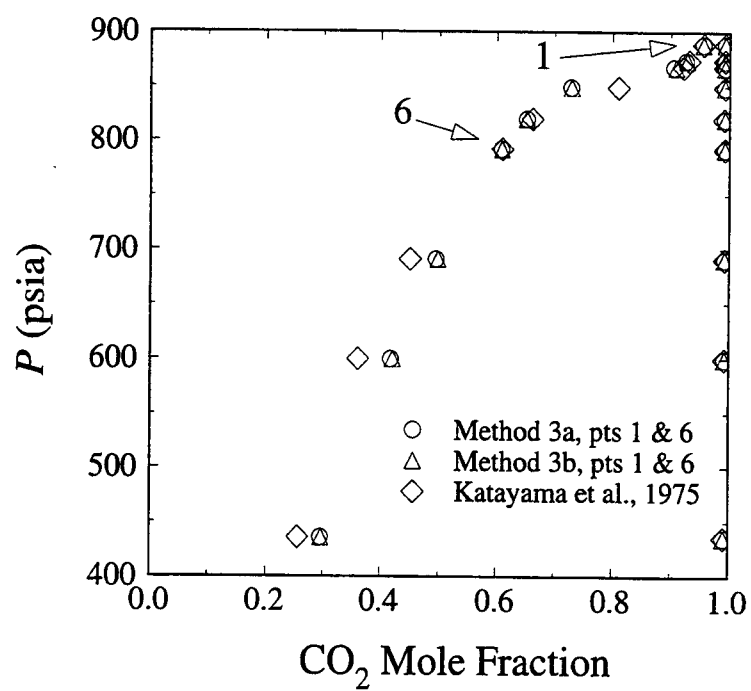
Figure 7.15 Experimental and calculated phase compositions for CO_2/methanol vapor-liquid equilibrium at 25 °C.

7.2.4.3 Vapor-Liquid-Liquid Equilibria

Since gaseous mixtures could not be described by activity coefficient models, only methods 1 and 3 could be applied to the VLLE systems. Method 3 was first applied to the ternary system of CO_2/isopropanol/water at 60 °C. As expected (section 2.4), when different models (method 3) were used for the vapor and liquid phases in equilibrium at high pressures, the properties of the phases did not become identical and thus the program did not find a solution with identical fugacities. Therefore the only choice was to use method 1. Figure 7.16 shows the phases in equilibrium, the six unknowns (mole fraction of two components in each phase at some T, P conditions) and the parameters of the model when method 1 was used.

DiAndreth and Paulaitis (1989) used Peng-Robinson EOS with van der Waals mixing rules and applied method 1 to the VLLE of the simple ternary system of CO_2/isopropanol/water. In this study, three sets of VLLE data were used to investigate the potential for using the simple method 1 with two different equations of state (PR or RK) and three different mixing rules (van der Waals, Panagiotopoulos and Reid, or Kwak and Mansoori) to predict phase compositions of simple and complex systems. Carbon dioxide and water were two of the components in each ternary. The first set of VLLE data (DiAndreth et al., 1987) was for the CO_2/isopropanol/water ternary at 60 °C and three pressures from 11.03 to 12.07 MPa (1600 to 1750 psia). The second set of data at 50 °C and pressure equal to 6.31, 8.03, or 9.76 MPa (915, 1165 or 1415 psia) was for C_4E_1 {CH_3-$(CH_2)_3$-O-$(CH_2)_2$-OH} as the third component. Finally data at 40 °C and pressure equal to 6.31, 8.03, or 9.76 MPa (915, 1165 or 1415 psia) for C_8E_3 {CH_3-

$$V \qquad X_1^V$$
$$X_2^V$$
$$X_3^V$$

$$L2 \qquad X_1^{L2}$$
$$X_2^{L2}$$
$$X_3^{L2}$$

$$L1 \qquad X_1^{L1}$$
$$X_2^{L1}$$
$$X_3^{L1}$$

$$T, P$$
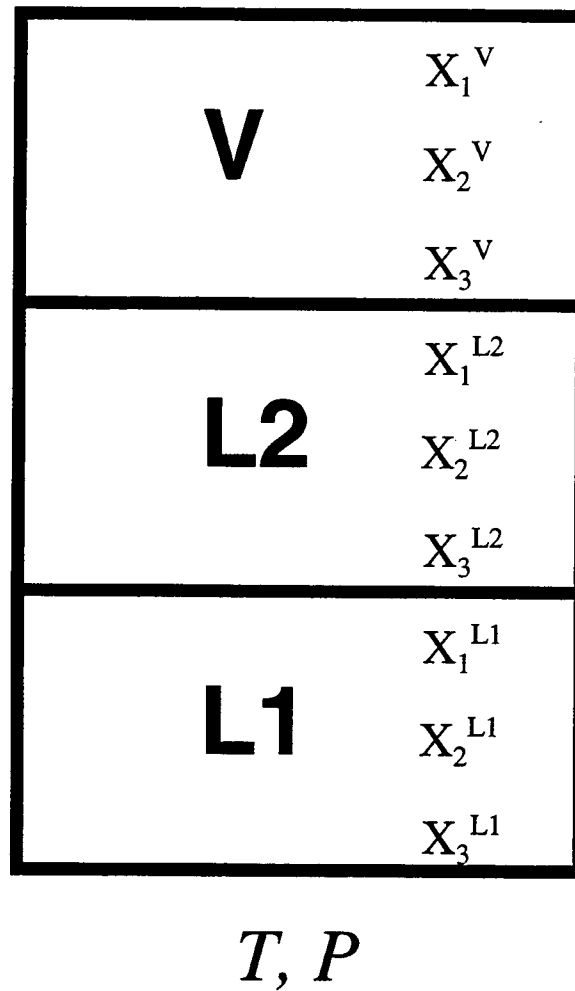
Unknowns $\qquad X_1^V, \; X_2^V, X_1^{L2}, X_2^{L2}, X_1^{L1}, X_2^{L1}$

Model Parameters $\qquad \delta_{12}, \delta_{13}, \delta_{23}$

Figure 7.16 Modeling VLLE using method 1.

$(CH_2)_6$-C-(O-$(CH_2)_2$-OH)$_3$} were also employed to evaluate method 1 when used for VLL

equilibria. The last two systems (Ritter and Paulaitis, 1990) contained more complex

third components than the isopropanol system and should thus give a better indication of

whether these methods could be applied to the complex biocide molecules which would

be used in SCF treatment of wood.

To make sure the computer program was correct, interaction parameters obtained

from the model for the CO_2/isopropanol/water system were compared to those obtained

by DiAndreth and Paulaitis (1989) using the same method. The interaction parameters

obtained from this program were in good agreement with those obtained by DiAndreth

and Paulaitis for the CO_2-isopropanol pair (δ_{12}) and the isopropanol-water (δ_{23}) pair, but

not for the CO_2-water pair (δ_{13}) (Table 7.4). DiAndreth and Paulaitis (1989) stated that

their procedure could result in several different sets of interaction parameters at each

temperature. Their final choice of binary interaction parameters was based on the ability

to predict phase compositions as a function of pressure. In this study the calculated

interaction parameters were used as initial guesses by executing the same program several

times until the value of the objective function described in Chapter 7 did not decrease.

Thus, the method of finding the ultimate values of the adjustable parameters were

different in this study than in the study conducted by DiAndreth and Paulaitis. This

difference might be the reason for the disagreement between this method and that of

DiAndreth and Paulaitis in the final value of the interaction parameter δ_{13}.

Table 7.4   Interaction parameters for VLLE of CO_2 (1), isopropanol (2), water (3) system when fitted to the data at 60 °C and three pressures using the PR-EOS with vdW mixing rules

Source	δ_{12}	δ_{13}	δ_{23}
DiAndreth and Paulaitis (1989)	0.017	- 0.025	- 0.208
This work	0.017	- 0.036	- 0.208

In order to apply method 1, the critical temperature, the critical pressure and the acentric factor of each component were needed. While experimental values of these parameters were available for CO_2, water and isopropanol, the parameters for C_4E_1 and C_8E_3 had to be estimated (Appendix B). When the critical temperature for C_4E_1 or C_8E_3 was treated as an adjustable parameter, the agreement between experimental and calculated phase compositions improved significantly (fitted T_c decreased the objective function, f_{obj}, in equation (7.51) by a factor of 8.0 for C_4E_1 system and by a factor of 66.4 for C_8E_3 system). However, critical pressure (P_c) or acentric factor (ω_c) did not have significant effects on the agreement between experimental and calculated phase compositions (fitted P_c or ω_c decreased the objective function, f_{obj}, in equation (7.51) by a maximum factor of 1.13 for C_4E_1 system and did not have any effects on the objective function for C_8E_3 system). Three methods were used to estimate the critical temperature:

(a)   Lyderson's correlation (Lyman et al., 1982) based on an experimental normal boiling point

(b)   Lyderson's correlation (Lyman et al., 1982) with Miller's method (1984) for estimating normal boiling point

(c)   Critical temperature treated as an adjustable variable when fitting phase compositions (at two extreme pressures) using method 1 with PR-EOS and vdW mixing rules

The fitted T_c (absolute) for isopropanol was identical to its experimental value while absolute T_c estimated from method (a) was about 1.6 % higher than the experimental value and absolute T_c estimated from method (b) about 6.4 % higher (Table 7.5). For C_4E_1, an experimental value for the normal boiling point was available in the literature and thus method (a) could be applied. Again T_c estimated from method (a) was lower than that estimated from method (b). For C_8E_3 and TCMTB experimental values for the normal boiling points were not available in the literature, thus method (a) could not be applied. For all of the four compounds studied, fitted T_c (method c) was lower than that obtained from the estimated normal boiling point (method b). The relative difference between absolute critical temperature obtained from methods (b) and (c) was about 6.4% for isopropanol, 52.3 % for C_4E_1, 93.1 % for C_8E_3 and less than 0.2 % for TCMTB. Thus the relative difference between critical temperatures obtained from methods (b) and (c) increased with the complexity of the compound (Table 7.6), except for TCMTB where the difference was small and the fitted T_c did not improve the calculated phase compositions significantly. This small difference for the TCMTB case was believed to be due to the bad fit of the model to the TCMTB data compared to the fit of the model to data in other systems. In the TCMTB case, model predicted trivial solutions where two of the three phases had identical compositions at the convergence.

Table 7.5   **Critical temperatures of selected compounds obtained by different methods**

Compound	Method	T_c (°C/K)
isopropanol	Experimental*	235.18/508.33
	Method a	242.87/516.02
	Method b	267.81/540.96
	Method c	235.18/508.33
C_4E_1	Method a	326.83/599.98
	Method b	381.70/654.85
	Method c	156.75/429.90
C_8E_3	Method b	589.57/862.72
	Method c	173.58/446.73
TCMTB	Method b	486.80/759.95
	Method c**	485.50/758.65
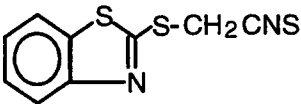
* = FLOWTRAN database

** = Critical temperature is fitted to only one data point (99.6 wt% pure TCMTB at 35 °C and 5.28 MPa / 766 psia). This fitted T_c is not realistic since a trivial solution giving three phases of identical compositions was obtained at the convergence as explained in more details later in this Chapter. Trivial solutions were also resulted when the other two data points (at the lower TCMTB purity of 96.9 wt%) were used in method (c). Therefore, only the fitted T_c obtained from the high purity TCMTB data point is reported here.

Values of the interaction parameters and T_c of isopropanol, C_4E_1 or C_8E_3 obtained for the three ternary systems containing one of these compounds when fitted to the data at the two extreme pressures of each system (using PR-EOS with vdW mixing rules) are given in Table 7.7. In all the three systems, the interaction parameter between CO_2 and isopropanol, C_4E_1 or C_8E_3 (δ_{12}) was positive, the interaction parameter between CO_2 and

water (δ_{13}) was negative, and the interaction parameter between water and isopropanol, C_4E_1 or C_8E_3 (δ_{23}) was also negative. Phase compositions calculated using the fitted T_c values for isopropanol (Tables 7.8 through 7.10), C_4E_1 (Tables 7.11 through 7.13) or C_8E_3 (Tables 7.14 through 7.16) as the third component are compared to experimental values in Figures 7.17 through 7.19 respectively. While parameters of the model were fitted to phase compositions at the two extreme pressures, the phase compositions at the intermediate pressure were predicted in all three systems. As expected for more complicated molecules, the simple method 1 did not fit as well as for the CO_2/isopropanol/water ternary (the largest and important relative deviation between experimental and calculated phase compositions was that of CO_2 in the middle phase (L2) and was only 16.4 % for the isopropanol system while it was 79.6 and 125.2 % for C_4E_1 and C_8E_3 systems respectively). Although relative deviation between experimental and calculated phase compositions for water in the top phase (V) was larger than that of CO_2 in the middle phase (L2) for all the three ternary systems, the larger relative deviations of water were because of the small compositions of water in the top phase and thus were not as important as those of CO_2 in the middle phase (L2). As seen on Figures 7.18 and 7.19, method 1 fitted the CO_2-rich phase (top=V) and water-rich phase (bottom=L1) almost exactly while it did not fit the third phase (middle=L2) well. Moreover, the difference between the experimental and calculated phase compositions for the middle phase (L2) was smaller for the system containing the simpler molecule C_4E_1 compared to the system containing C_8E_3 (79.6 % maximum relative deviation for C_4E_1 system while 125.2 % for C_8E_3 system). Another point is that at lower pressures the agreement between experimental and calculated phase compositions was better for all systems studied.

Table 7.6   **Molecular structure of compounds studied for the VLL equilibrium**

Compound	Molecular Mass	Molecular Structure
Isopropanol	60	$CH_3-\overset{\overset{\displaystyle OH}{\mid}}{C}H-CH_3$
C_4E_1	118	$CH_3-CH_2-CH_2-CH_2-O-CH_2-CH_2-OH$
C_8E_3	294	$CH_3-CH_2-CH_2-CH_2-CH_2-CH_2-CH_2-C\overset{\displaystyle O-CH_2-CH_2-OH}{\underset{\displaystyle O-CH_2-CH_2-OH}{-O-CH_2-CH_2-OH}}$
TCMTB	238	

Table 7.7 Interaction parameters and T_c of isopropanol, C_4E_1 or C_8E_3 for VLLE of three ternary systems when fitted to the data at the two extreme pressures of each system using the PR-EOS with vdW mixing rules

System	δ_{12}	δ_{13}	δ_{23}	T_c (2) (°C/K)
CO_2 (1), isopropanol (2), water (3)	0.013	- 0.047	- 0.210	235.18/508.33
CO_2 (1), C_4E_1 (2), water (3)	0.217	- 0.104	- 0.371	156.75/429.90
CO_2 (1), C_8E_3 (2), water (3)	0.310	- 0.080	- 0.570	173.58/446.73

Table 7.8 Experimental and calculated phase compositions for VLL: CO_2/isopropanol/water at 60 °C and 11.03 MPa using the PR-EOS with van der Waals mixing rules

Phase	x^{exp}_{CO2} (x^{cal}_{CO2})	$x^{exp}_{isopropanol}$ $(x^{cal}_{isopropanol})$	x^{exp}_{water} (x^{cal}_{water})
G	0.790 (0.817)	0.094 (0.104)	0.116 (0.079)
L2	0.313 (0.269)	0.224 (0.217)	0.463 (0.514)
L1	0.064 (0.063)	0.132 (0.103)	0.804 (0.833)

Table 7.9 Experimental and calculated phase compositions for VLL: CO_2/isopropanol/water at 60 °C and 11.55 MPa using the PR-EOS with van der Waals mixing rules

Phase	x^{exp}_{CO2} (x^{cal}_{CO2})	$x^{exp}_{isopropanol}$ $(x^{cal}_{isopropanol})$	x^{exp}_{water} (x^{cal}_{water})
G	0.758 (0.755)	0.102 (0.132)	0.139 (0.112)
L2	0.334 (0.303)	0.235 (0.221)	0.431 (0.476)
L1	0.065 (0.061)	0.128 (0.100)	0.807 (0.839)

Table 7.10 Experimental and calculated phase compositions for VLL: CO_2/isopropanol/water at 60 °C and 12.07 MPa using the PR-EOS with van der Waals mixing rules

Phase	x^{exp}_{CO2} (x^{cal}_{CO2})	$x^{exp}_{isopropanol}$ $(x^{cal}_{isopropanol})$	x^{exp}_{water} (x^{cal}_{water})
G	0.757 (0.710)	0.138 (0.151)	0.105 (0.139)
L2	0.357 (0.336)	0.257 (0.223)	0.386 (0.442)
L1	0.062 (0.059)	0.102 (0.097)	0.836 (0.844)

Table 7.11   Experimental and calculated phase compositions for VLL: CO_2/C_4E_1/water at 50 °C and 6.31 MPa using the PR-EOS with van der Waals mixing rules

Phase	x^{exp}_{CO2} (x^{cal}_{CO2})	x^{exp}_{water} (x^{cal}_{water})	x^{exp}_{C4E1} (x^{cal}_{C4E1})
G	0.949 (0.973)	0.021 (0.005)	0.030 (0.022)
L2	0.223 (0.185)	0.495 (0.516)	0.283 (0.299)
L1	0.017 (0.022)	0.973 (0.970)	0.010 (0.008)

Table 7.12   Experimental and calculated phase compositions for VLL: CO_2/C_4E_1/water at 50 °C and 8.03 MPa using the PR-EOS with van der Waals mixing rules

Phase	x^{exp}_{CO2} (x^{cal}_{CO2})	x^{exp}_{water} (x^{cal}_{water})	x^{exp}_{C4E1} (x^{cal}_{C4E1})
G	0.951 (0.967)	0.018 (0.007)	0.031 (0.026)
L2	0.336 (0.235)	0.384 (0.485)	0.280 (0.280)
L1	0.023 (0.025)	0.969 (0.967)	0.008 (0.008)

Table 7.13   Experimental and calculated phase compositions for VLL: CO_2/C_4E_1/water at 50 °C and 9.76 MPa using the PR-EOS with van der Waals mixing rules

Phase	x^{exp}_{CO2} (x^{cal}_{CO2})	x^{exp}_{water} (x^{cal}_{water})	x^{exp}_{C4E1} (x^{cal}_{C4E1})
G	0.959 (0.935)	0.020 (0.021)	0.021 (0.044)
L2	0.483 (0.269)	0.278 (0.462)	0.240 (0.268)
L1	0.026 (0.028)	0.967 (0.965)	0.008 (0.007)

Table 7.14   Experimental and calculated phase compositions for VLL: CO_2/C_8E_3/water at 40 °C and 6.31 MPa using the PR-EOS with van der Waals mixing rules

Phase	x^{exp}_{CO2} (x^{cal}_{CO2})	x^{exp}_{water} (x^{cal}_{water})	x^{exp}_{C8E3} (x^{cal}_{C8E3})
G	0.990 (0.993)	0.005 (0.003)	0.005 (0.004)
L2	0.250 (0.196)	0.575 (0.424)	0.175 (0.380)
L1	0.017 (0.013)	0.983 (0.987)	0.000 (0.000)

Table 7.15 Experimental and calculated phase compositions for VLL: CO_2/C_8E_3/water at 40 °C and 8.03 MPa using the PR-EOS with van der Waals mixing rules

Phase	x^{exp}_{CO2} (x^{cal}_{CO2})	x^{exp}_{water} (x^{cal}_{water})	x^{exp}_{C8E3} (x^{cal}_{C8E3})
G	0.983 (0.989)	0.009 (0.005)	0.009 (0.005)
L2	0.436 (0.228)	0.364 (0.411)	0.200 (0.361)
L1	0.013 (0.014)	0.998 (0.986)	0.000 (0.000)

Table 7.16 Experimental and calculated phase compositions for VLL: CO_2/C_8E_3/water at 40 °C and 9.76 MPa using the PR-EOS with van der Waals mixing rules

Phase	x^{exp}_{CO2} (x^{cal}_{CO2})	x^{exp}_{water} (x^{cal}_{water})	x^{exp}_{C8E3} (x^{cal}_{C8E3})
G	0.993 (0.979)	0.004 (0.016)	0.003 (0.005)
L2	0.536 (0.238)	0.258 (0.408)	0.207 (0.354)
L1	0.013 (0.015)	0.988 (0.985)	0.000 (0.000)

11.03 MPa (1600 psia)

11.55 MPa (1675 psia)

12.07 MPa (1750 psia)
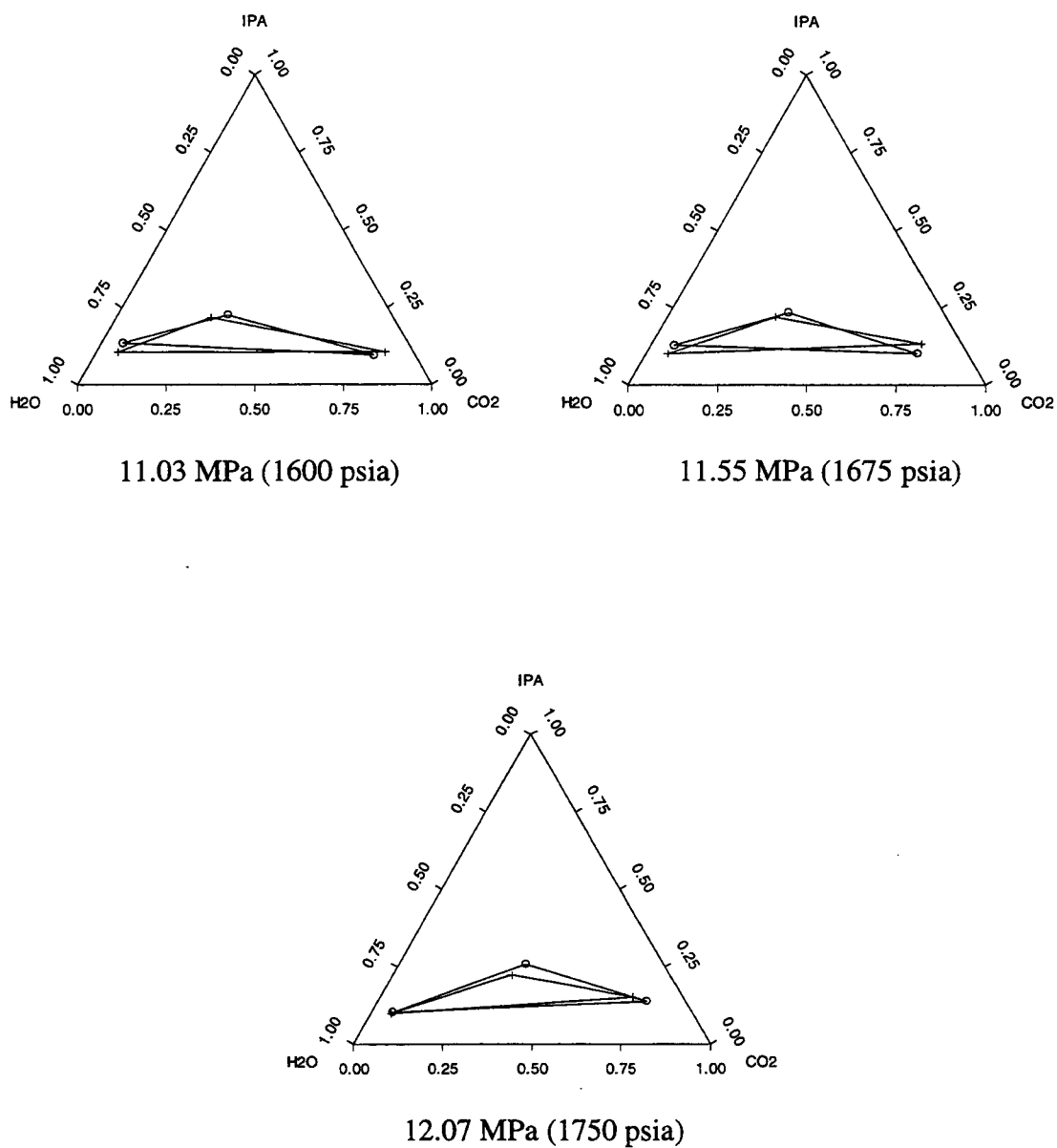
Figure 7.17 Experimental and fitted phase compositions for VLL: CO_2/isopropanol/water at 60 °C using the PR-EOS with van der Waals mixing rules (o = data, + = fitted).

6.31 MPa (915 psia)

8.03 MPa (1165 psia)

9.76 MPa (1415 psia)
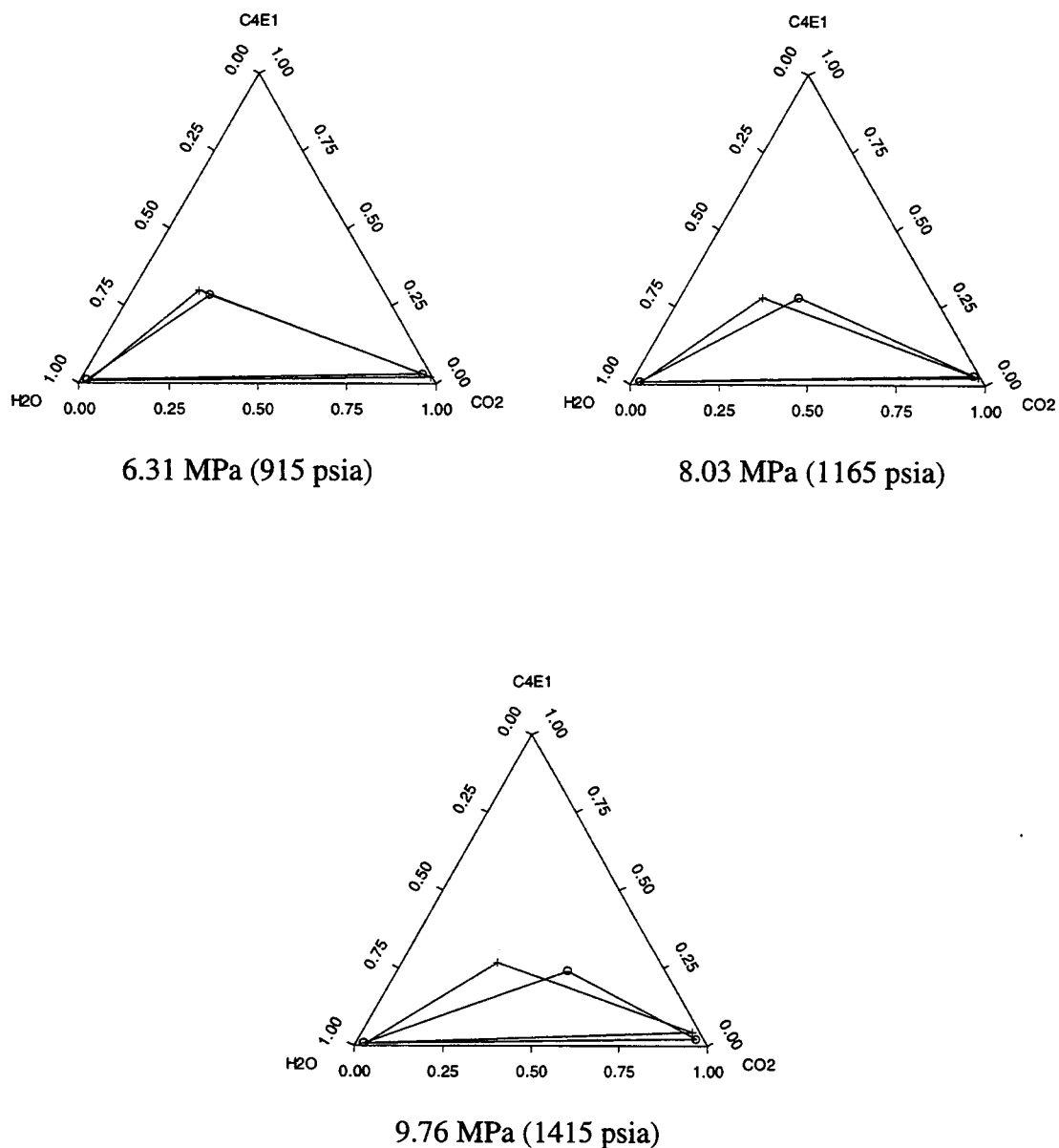
Figure 7.18 Experimental and fitted phase compositions for VLL: CO_2/C_4E_1/water at 50 °C using the PR-EOS with van der Waals mixing rules (o = data, + = fitted).

6.31 MPa (915 psia)

8.03 MPa (1165 psia)

9.76 MPa (1415 psia)
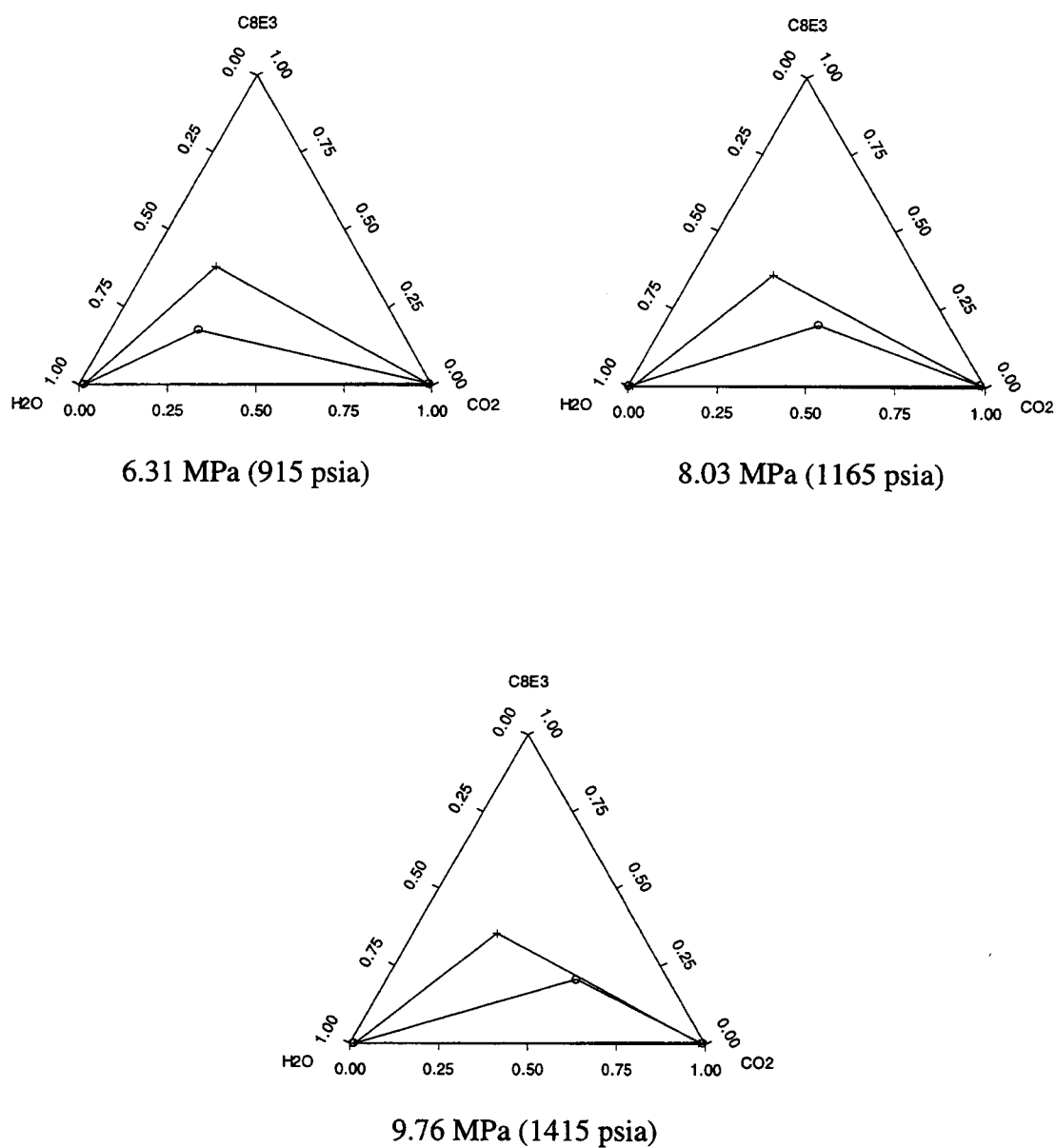
Figure 7.19 Experimental and fitted phase compositions for VLL: CO_2/C_8E_3/water at 40 °C using the PR-EOS with van der Waals mixing rules (o = data, + = fitted).

To compare the phase compositions obtained by Redlich-Kwong EOS with

Kwak-Mansoori's mixing rules with experimental values, method 1 was applied to the

CO_2/isopropanol/water system and the results are shown in Figure 7.20. The interaction

parameters were fitted to the compositions at the two extreme pressures and the

compositions at the intermediate pressure were predicted. Interaction parameters and

calculated phase compositions are tabulated in Tables 7.17 through 7.20. Although the

agreement between the experimental and calculated phase compositions is not bad, it is

not as good as that seen with the Peng-Robinson EOS with van der Waals mixing rules

(Figure 7.17). Because RK-EOS with Kwak-Mansoori's mixing rules did not fit the data

as well as the PR-EOS with van der Waals mixing rules for this simple ternary system,

more complicated ternary systems were not modeled with RK-EOS with Kwak-

Mansoori's mixing rules.

Table 7.17   **Interaction parameters for VLL: CO_2 (1), water (2) and isopropanol (3) system when fitted to the data at the two extreme pressures using the RK-EOS with Kwak and Mansoori's mixing rules**

δ_{12}	δ_{13}	δ_{23}
0.1962	-0.1153	-0.0744

Table 7.18 Experimental and calculated phase compositions for VLL: CO_2/isopropanol/water at 60 °C and 11.03 MPa using the RK-EOS with Kwak and Mansoori's mixing rules

Phase	x^{exp}_{CO2} (x^{cal}_{CO2})	$x^{exp}_{isopropanol}$ $(x^{cal}_{isopropanol})$	x^{exp}_{water} (x^{cal}_{water})
G	0.790 (0.725)	0.094 (0.141)	0.116 (0.134)
L2	0.313 (0.223)	0.224 (0.249)	0.463 (0.528)
L1	0.064 (0.065)	0.132 (0.086)	0.804 (0.850)

Table 7.19 Experimental and calculated phase compositions for VLL: CO_2/isopropanol/water at 60 °C and 11.55 MPa using the RK-EOS with Kwak and Mansoori's rules

Phase	x^{exp}_{CO2} (x^{cal}_{CO2})	$x^{exp}_{isopropanol}$ $(x^{cal}_{isopropanol})$	x^{exp}_{water} (x^{cal}_{water})
G	0.758 (0.706)	0.102 (0.148)	0.139 (0.146)
L2	0.334 (0.229)	0.235 (0.249)	0.431 (0.522)
L1	0.065 (0.065)	0.128 (0.085)	0.807 (0.850)

Table 7.20   Experimental and calculated phase compositions for VLL:
CO$_2$/isopropanol/water at 60 °C and 12.07 MPa using the RK-EOS
with Kwak and Mansoori's rules

Phase	x^{exp}_{CO2} (x^{cal}_{CO2})	$x^{exp}_{isopropanol}$ ($x^{cal}_{isopropanol}$)	x^{exp}_{water} (x^{cal}_{water})
G	0.757 (0.692)	0.138 (0.153)	0.105 (0.155)
L2	0.357 (0.233)	0.257 (0.249)	0.386 (0.518)
L1	0.062 (0.066)	0.102 (0.085)	0.836 (0.849)

11.03 MPa (1600 psia)

11.55 MPa (1675 psia)

12.07 MPa (1750 psia)
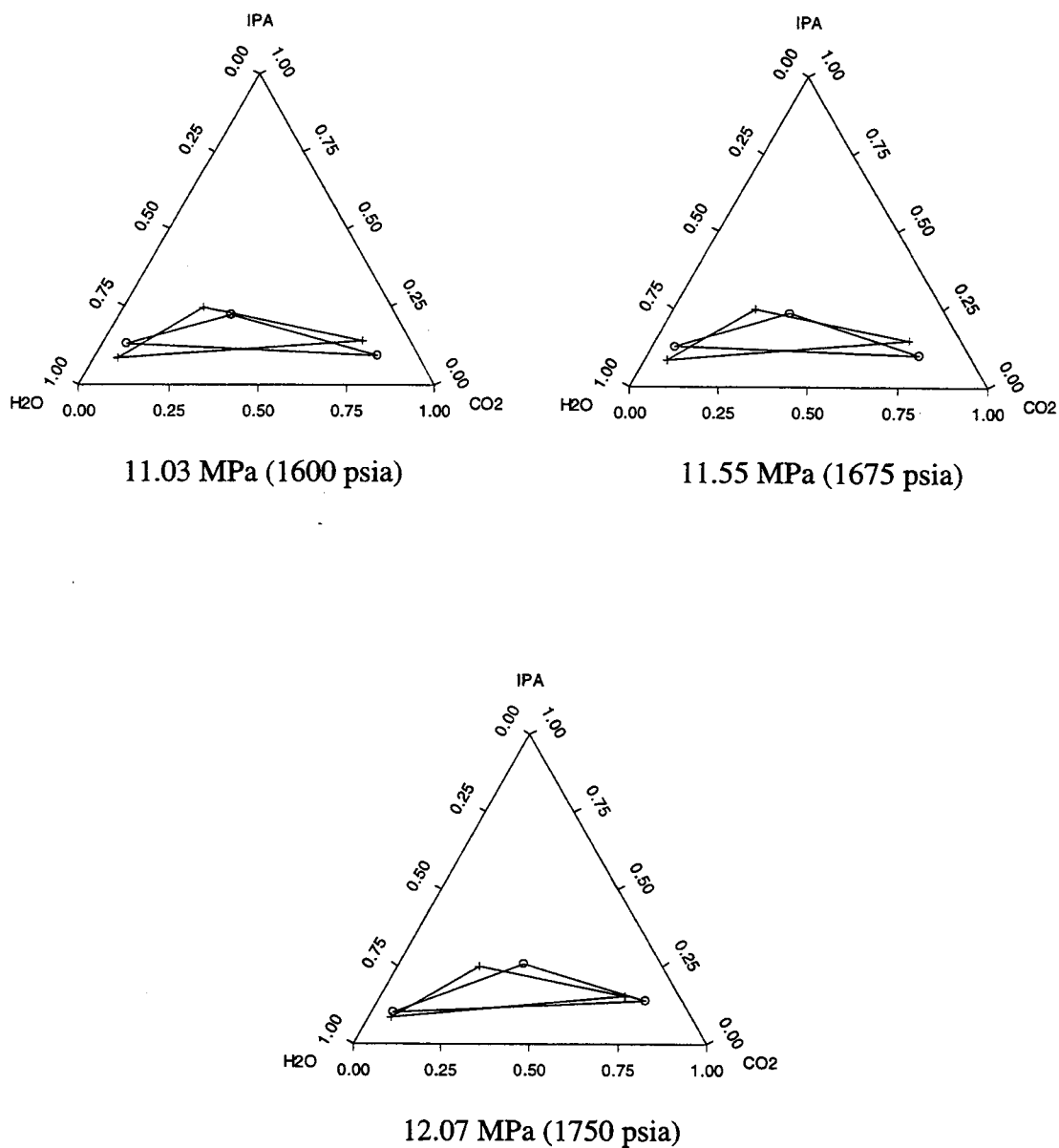
Figure 7.20 Experimental and fitted phase compositions for VLL: CO_2/isopropanol/water at 60 °C using the RK-EOS with Kwak-Mansoori's mixing rules (o = data, + = fitted).

The VLLE ternary system of interest for wood preservation is the CO_2/acetone/TCMTB. Data for the highest purity of TCMTB (99.6 wt %) was obtained as phase compositions at 35 °C and 5.28 MPa (766 psia). As a first effort in analyzing these compositions, the Peng-Robinson equation of state with van der Waals mixing rules was used to model the vapor and both liquid phases (method 1) and the parameters including the critical temperature were fitted to the data. When the same criteria for the equality of the fugacities (10^{-8}) as in other ternary systems was used, only a trivial solution giving three phases of identical compositions was obtained at the convergence. When a less stringent criteria (10^{-4}) was used, two of the phases still had identical compositions. In all cases the experimental phase compositions were chosen as the initial guesses for the phase composition used in Heidemann's successive substitution algorithm discussed earlier in this Chapter. Since the successful convergence of this method depended on the initial phase compositions, sometimes the modified phase compositions had to be used as initial guesses in order for the model to converge to a realistic solution.

A new mixing rule (Panagiotopoulos and Reid, 1987) having more adjustable parameters was tested in order to improve the results. Before applying this mixing rule to the biocide system, it was first applied to the simpler ternary systems to see if any improvements were possible. Therefore, Peng-Robinson EOS and Panagiotopoulos and Reid's mixing rules were applied to the second most complex system (CO_2/C_8E_3/water) studied. Interaction parameters and calculated phase compositions are tabulated in Tables 7.21 through 7.24. Results obtained from the new 6-parameter mixing rules allowed a better fit between experimental and calculated phase compositions (Figure 7.21) than those obtained from the 3-parameter mixing rules of van der Waals (Figure 7.19) (the

largest and important relative deviation between experimental and calculated phase compositions was 54.2 % with the new 6-parameter mixing rule compared to the 125.2 % with the 3-parameter mixing rule). Fitted T_c obtained from PR-EOS with van der Waals mixing rules was used in the new modeling method (PR-EOS with Panagiotopoulos and Reid's mixing rules). When the new mixing rule was applied to the system of interest (CO_2/acetone/TCMTB) at 35 °C and 5.28 MPa (766 psia), no significant improvements were observed (like in the case of the 3-parameter mixing rule, a trivial solution giving three phases of identical compositions was obtained at the convergence).

Table 7.21   **Interaction parameters for VLL: CO_2 (1), water (2) and C_8E_3 (3) system at 40 °C when fitted to each of the data using the PR-EOS with Panagiotopoulos and Reid's mixing rules and T_c=173.58 °C (446.73 K)**

Pressure (psia/MPa)	δ_{12}	δ_{13}	δ_{23}	δ_{21}	δ_{31}	δ_{32}
915 / 6.31	-0.0918	0.7636	-0.9902	-0.1940	-0.0679	-0.5898
1165 / 8.03	-0.0735	-0.2615	-0.6857	-0.0194	0.0370	-0.6130
1415 / 9.76	-0.0760	-1.0940	-0.6351	0.1800	0.0913	-0.6211

Table 7.22 Experimental and calculated phase compositions for VLL: CO_2/C_8E_3/water at 40 °C and 6.31 MPa using the PR-EOS with Panagiotopoulos and Reid's mixing rules

Phase	x^{exp}_{CO2} (x^{cal}_{CO2})	x^{exp}_{water} (x^{cal}_{water})	x^{exp}_{C8E3} (x^{cal}_{C8E3})
G	0.990 (0.991)	0.005 (0.004)	0.005 (0.005)
L2	0.250 (0.265)	0.575 (0.532)	0.175 (0.203)
L1	0.017 (0.016)	0.983 (0.984)	0.000 (0.000)

Table 7.23 Experimental and calculated phase compositions for VLL: CO_2/C_8E_3/water at 40 °C and 8.03 MPa using the PR-EOS with Panagiotopoulos and Reid's mixing rules

Phase	x^{exp}_{CO2} (x^{cal}_{CO2})	x^{exp}_{water} (x^{cal}_{water})	x^{exp}_{C8E3} (x^{cal}_{C8E3})
G	0.983 (0.986)	0.009 (0.006)	0.009 (0.008)
L2	0.436 (0.600)	0.364 (0.236)	0.200 (0.163)
L1	0.013 (0.013)	0.998 (0.987)	0.000 (0.000)

Table 7.24 Experimental and calculated phase compositions for VLL: CO_2/C_8E_3/water at 40 °C and 9.76 MPa using the PR-EOS with Panagiotopoulos and Reid's mixing rules

Phase	x^{exp}_{CO2} (x^{cal}_{CO2})	x^{exp}_{water} (x^{cal}_{water})	x^{exp}_{C8E3} (x^{cal}_{C8E3})
G	0.993 (0.993)	0.004 (0.004)	0.003 (0.003)
L2	0.536 (0.536)	0.258 (0.258)	0.207 (0.207)
L1	0.013 (0.013)	0.988 (0.988)	0.000 (0.000)
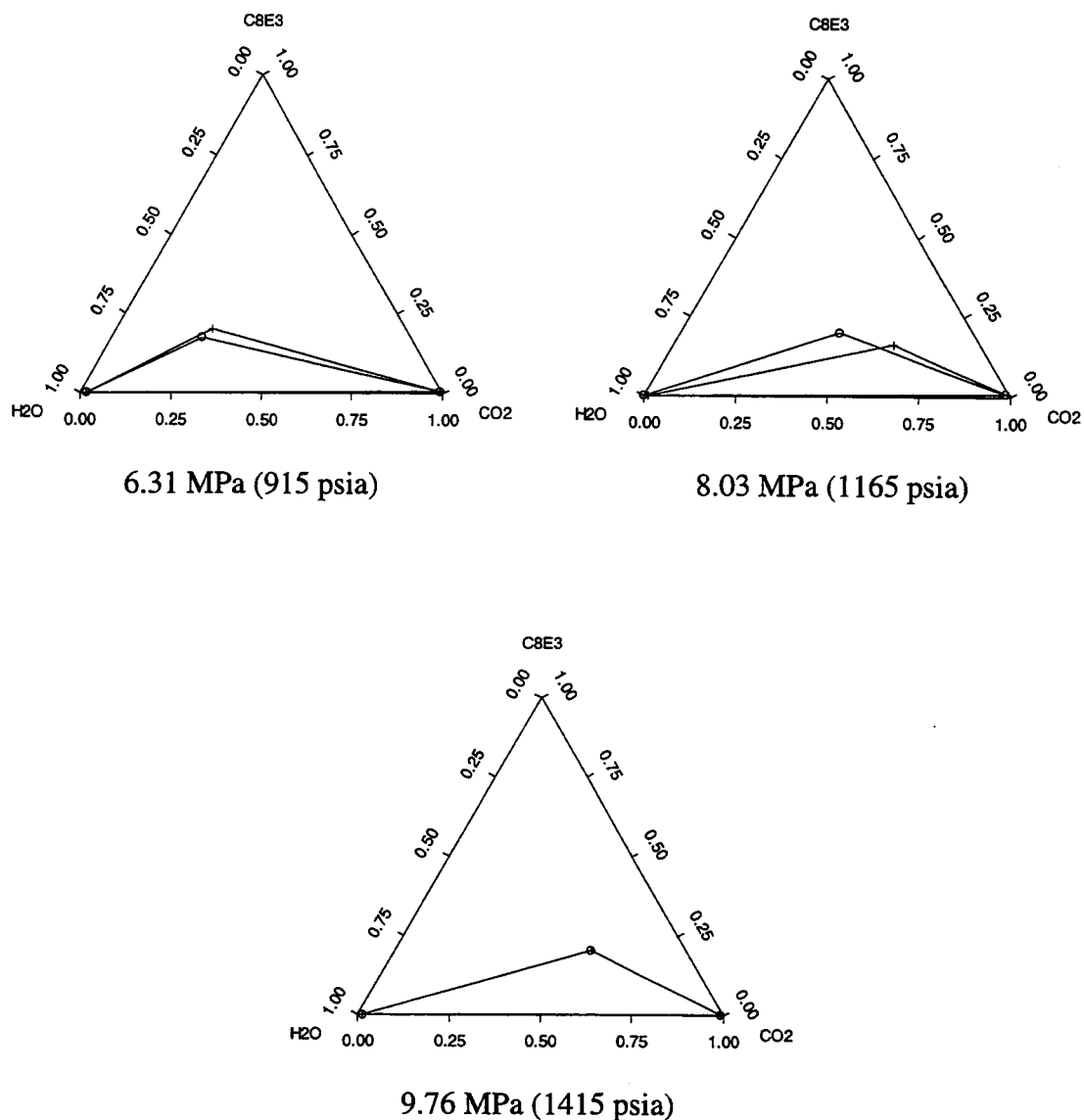
Figure 7.21 Experimental and fitted phase compositions for VLL: CO_2/C_8E_3/water at 40 °C using the PR-EOS with Panagiotopoulos and Reid's mixing rules (o = data, + = fitted).

There were a few differences between the system containing TCMTB at 35 °C and 5.28 MPa (766 psia) (Figure 6.2) with other ternary systems studied. These differences may explain the failure of the model for the TCMTB system. Probably the most important difference between the TCMTB system and the C_4E_1 or C_8E_3 system is that in the later two systems two of the three phases are pure or almost pure. This makes separations and modeling easier. The third phase of the C_4E_1 or C_8E_3 system contains significant amounts of each component and the model did not fit compositions of this phase as accurately. In the case of TCMTB system, due to the miscibilities of the molecules, none of the three phases are pure and this makes modeling more difficult than with the other ternary systems. Although none of the phases are pure in the simplest ternary system (CO_2/isopropanol/water), (like the TCMTB system), the properties of isopropanol are well known, and the molecular interactions might be different than those of the TCMTB system. These differences could be the reasons that modeling efforts were successful for the isopropanol system but not for the TCMTB system.

In the isopropanol, C_4E_1 or C_8E_3 systems, the compositions of the three phases were widely spread (Figures 7.17 through 7.19) while in the TCMTB system at 35 °C and 5.28 MPa (766 psia) (Figure 6.2), the compositions are close to each other and thus different phase compositions are difficult to obtain. Therefore trivial solutions were found that gave satisfactory fits to the phase compositions. In order to test the model for wider spread phase compositions in the TCMTB system, a second data set for phase compositions at a lower temperature (25 °C) and pressure (4.05 MPa) was used. This data was obtained with a lower purity TCMTB (96.9 wt %). The model converged to a nontrivial solution (calculated phase compositions were not identical) when a fugacity

criteria of 10^{-8} was used and T_c was fitted. Interaction parameters and fitted phase

compositions are tabulated in Tables 7.25 and 7.26 and Figure 7.22 shows a comparison

between experimental and fitted phase compositions for the CO_2/acetone/TCMTB

system. This model fitted the top phase (V) of the TCMTB system almost exactly but it

did not fit the middle (L2) and the bottom (L1) phases as good as it fitted these phases for

the simpler system of C_8E_3 (the largest important relative deviation in the middle and

bottom phases of the TCMTB system were 57.1 and 113.3 % respectively, compared to

54.2 and 1.1 % in the middle and bottom phases respectively for the C_8E_3 system). Even

though the fit to the TCMTB data was not as good as that for the systems containing

simpler molecules, the model fitted the data at 25 °C and 4.05 MPa (588 psia) much

better than it fitted the data at the higher temperature and pressure. Therefore it seems

that for systems containing complex molecules, this method is good when a good

separation between the phases exists. In other words phase compositions should be

widely spread for the model to converge to a nontrivial solution. Since the method gave a

better fit at the lower temperature and pressure (25 °C instead of 35 °C and 4.05 MPa /

588 psia instead of 5.28 MPa / 766 psia), the method seems to be good for conditions far

from the critical region.

Table 7.25 Interaction parameters and fitted T_c for VLL: CO_2 (1), acetone (2) and TCMTB (3) system at 25 °C and 4.05 MPa using the PR-EOS with Panagiotopoulos and Reid's mixing rules

δ_{12}	δ_{13}	δ_{23}	δ_{21}	δ_{31}	δ_{32}	T_c (°C / K)
0.3070	1.0364	-0.9876	0.1617	0.7190	-0.0440	32.02 / 305.17

Table 7.26 Experimental and calculated phase compositions for VLL: CO_2/acetone/TCMTB at 25 °C and 4.05 MPa using the PR-EOS with Panagiotopoulos and Reid's mixing rules

Phase	x^{exp}_{CO2} (x^{cal}_{CO2})	$x^{exp}_{acetone}$ ($x^{cal}_{acetone}$)	x^{exp}_{TCMTB} (x^{cal}_{TCMTB})
G	0.846 (0.855)	0.152 (0.142)	0.003 (0.003)
L2	0.039 (0.099)	0.769 (0.601)	0.191 (0.300)
L1	0.516 (0.264)	0.302 (0.644)	0.182 (0.092)
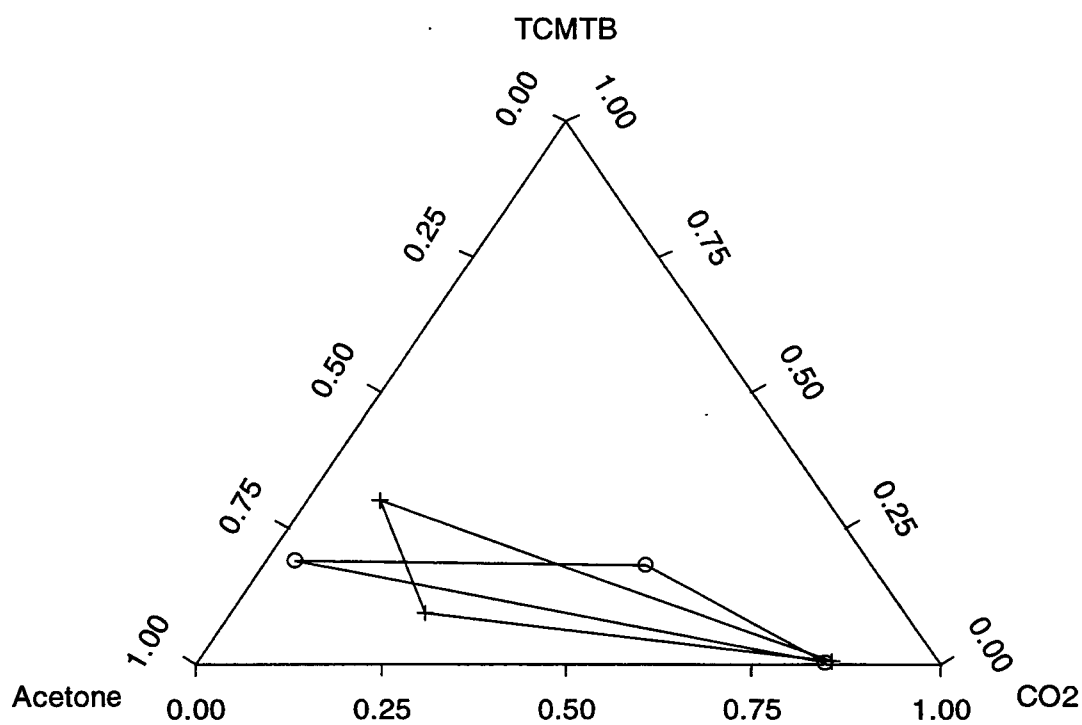
Figure 7.22   Experimental and fitted phase compositions for VLL:
CO₂/acetone/TCMTB at 25 °C and 4.05 MPa with the 96.9 wt% pure
TCMTB using the PR-EOS with Panagiotopoulos and Reid's mixing rules
(o = data, + = fitted).

Figure 7.22   Experimental and fitted phase compositions for VLL:
CO_2/acetone/TCMTB at 25 °C and 4.05 MPa with the 96.9 wt% pure
TCMTB using the PR-EOS with Panagiotopoulos and Reid's mixing rules
(o = data, + = fitted).

As mentioned earlier in this section, the relative difference between fitted T_c (using the PR-EOS with vdW mixing rules) and that obtained from the estimated normal boiling point increased with the complexity of compounds, except for TCMTB where the difference was small (Table 7.4). A bad fit of the model to the TCMTB data was believed to be the reason for this small difference between the fitted and estimated T_c. As shown above, using the same EOS (PR), but with Panagiotopoulos and Reid's mixing rules, a better fit to the TCMTB data was possible and a much different fitted T_c was obtained for TCMTB (32.02 °C / 305.17 K compared to 485.50 °C / 758.65 K obtained using vdW mixing rules). The relative difference between this new fitted T_c (305.17 K) and that obtained from the estimated normal boiling point (759.95 K) is about 149 % which follows the trend mentioned above (the relative difference between fitted and estimated T_c increases with the complexity of compounds studied here). Since the new value obtained for fitted T_c (32.02 °C / 305.17 K) for TCMTB follows this trend better than the T_c reported in Table 7.4 (485.50 °C / 758.65 K) and also gives a better fit to the TCMTB data, the new T_c is expected to be more realistic than the T_c reported in Table 7.4.

An effort to use the PR-EOS with Panagiotopoulos and Reid's mixing rules with the estimated T_c (486.80 °C / 759.95 K) in modeling the TCMTB system at 25 °C and 4.05 MPa (588 psia) was not successful (a trivial solution giving three phases of identical compositions was obtained). Moreover, no improvement occurred when critical pressure or the acentric factor of TCMTB were used as adjustable parameters. Thus as in other ternary systems (modeled with PR-EOS and van der Waals mixing rules), it is recommended that only the T_c be treated as an additional fitting parameter for modeling

the TCMTB system with PR-EOS and Panagiotopoulos and Reid's mixing rules.

As shown in Figure 7.22, the agreement between experimental and calculated phase compositions is not as good as that seen for other systems. The most important reason for this difference might be the fact that this system is more complex (it involves a large polar molecule) than the other ternary systems (Table 7.5). Therefore, the interactions between the molecules might be different in the TCMTB system than that in the other ternary systems. The fact that none of the phases in the TCMTB system are pure while two of the phases in the C_4E_1 or C_8E_3 systems are pure or almost pure shows the more complex nature of the TCMTB system compared to the C_4E_1 and C_8E_3 systems. The wood treatment process requires that the components of the mixture be relatively miscible in one another so that enough biocide could be dissolved in the supercritical phase and deposited in the wood structure. Acetone was chosen as the cosolvent so that molecular interactions between the components of the mixture would enhance miscibilities of components in one another. Presence of 3.1 wt% impurities in the TCMTB (96.9 wt%) might be another reason for the poor fit of the model for the TCMTB system compared to the other ternary systems. Any amount of impurities may affect the critical point of mixtures (as demonstrated by Figure 5.3 in section 5.3) as well as on equilibrium phase compositions.

When the fugacity criteria was less stringent (0.1 instead of 10^{-8}), the model predicted a better fit for the TCMTB system at 25 °C and 4.05 MPa (588 psia). Interaction parameters and fitted phase compositions are tabulated in Tables 7.27 and 7.28 and Figure 7.23 shows a comparison between experimental and fitted phase compositions for this system. When the fugacity criteria was set equal to or less than one,

a "perfect" fit was obtained and the fugacity criteria at convergence was 0.8931. This

was done as a check for errors in the program. Since the model predicted a better fit as

the fugacity criteria was relaxed, the program behaved as expected. Moreover earlier

results obtained by this method for the CO_2/isopropanol/water system at 60 °C and three

pressures (11.03, 11.55 and 12.07 MPa / 1600, 1675 and 1750 psia) agreed with the

results obtained by DiAndreth and Paulaitis (1989) for the same system using the same

method as shown in Table 7.3. Therefore, the reasons for the poor fit of the model for the

TCMTB system are believed to be due to the complexity of the molecules and possibly

the impurities of TCMTB.

Table 7.27 **Interaction parameters for VLL: CO_2 (1), acetone (2) and TCMTB (3) system at 25 °C and 4.05 MPa using the PR-EOS with Panagiotopoulos and Reid's mixing rules when T_c = 32.02 °C and fugacity criteria is 0.1**

δ_{12}	δ_{13}	δ_{23}	δ_{21}	δ_{31}	δ_{32}
0.370	0.217	-1.051	0.123	0.693	-0.032

Table 7.28 Experimental and calculated phase compositions for VLL: CO_2/acetone/TCMTB at 25 °C and 4.05 MPa using the PR-EOS with Panagiotopoulos and Reid's mixing rules when $T_c = 32.02$ °C and fugacity criteria is 0.1

Phase	x^{exp}_{CO2} (x^{cal}_{CO2})	$x^{exp}_{acetone}$ $(x^{cal}_{acetone})$	x^{exp}_{TCMTB} (x^{cal}_{TCMTB})
G	0.846 (0.822)	0.152 (0.176)	0.003 (0.003)
L2	0.039 (0.168)	0.769 (0.607)	0.191 (0.225)
L1	0.516 (0.350)	0.302 (0.559)	0.182 (0.090)
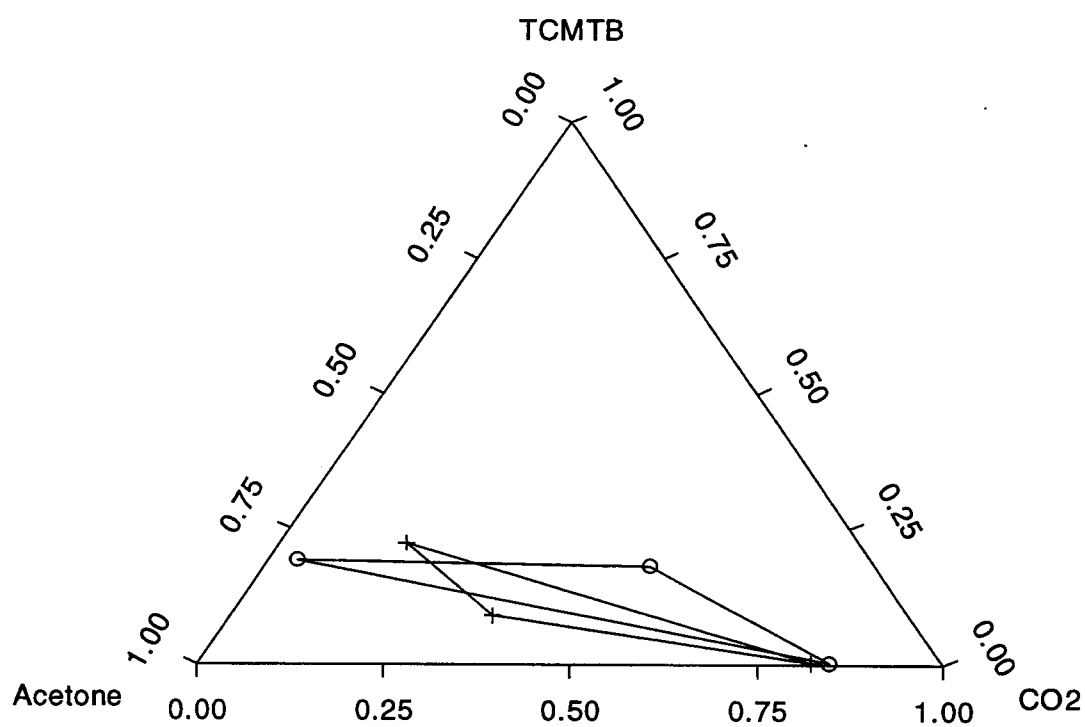
Figure 7.23 Experimental and fitted phase compositions for VLL:
CO₂/acetone/TCMTB at 25 °C and 4.05 MPa with the 96.9 wt% pure
TCMTB using the PR-EOS with Panagiotopoulos and Reid's mixing rules
with a fugacity criteria of 0.1 (o = data, + = fitted).

CHAPTER 8

CONCLUSIONS AND RECOMMENDATIONS

8.1 Conclusions

The work presented in this thesis could be used to improve supercritical wood treatment technology. Knowledge of the operating conditions which ensure a single phase in the treatment process and of the phases which might exist in different sections of the process can be useful for reliable scale-up of the technology and design of a recovery system. Conclusions of this thesis are as follows:

1. Experimental equipment was designed and used to measure the critical loci of binary (CO_2 and biocide) and ternary (CO_2, cosolvent and biocide) mixtures and the phase compositions of ternary (CO_2, cosolvent and biocide) mixtures.

2. Critical temperature and pressure of CO_2/propiconazole mixture increased by about 3.5 °C and 0.21 MPa (30 psia) respectively as propiconazole wt% was increased from 0.5 to 1.0.

3. Critical temperatures and pressures of CO_2/acetone/TCMTB mixtures increased by about 1.0 °C and 0.12 MPa (17 psia) respectively as the acetone content was increased from 3.2 to 3.7 wt% at a constant TCMTB level of 0.95 wt%. Critical temperature and pressure of this system, however, decreased by less than 1.0 °C and less than 0.03 MPa (5 psia) when TCMTB content was increased from 0.24 to 0.95 wt%.

4. Critical temperatures and pressures of the CO_2/methanol/tebuconazole mixtures increased by about 9 °C and 0.90 MPa (130 psia) as the mole fraction of cosolvent (methanol) was increased from about 0.7 to 3.7 wt% at a constant tebuconazole level of 0.44 wt%. The presence of tebuconazole at 0.44 wt% had little effect on the critical temperature but it increased the critical pressure by about 0.07 MPa (10 psia).

5. Measured vapor/liquid/liquid phase compositions for a CO_2/acetone/TCMTB mixture at 25 °C and 4.05 MPa (588 psia) (which was considered far from the critical point of the mixture) were widely spread. At a temperature of 25 °C and a pressure of 4.32 MPa (626 psia), the phase spread was not as wide as that at 588 psia. At a higher temperature and pressure (35 °C and 5.28 MPa / 766 psia), the phase compositions were more similar, which suggested closeness to the critical point of the mixture. Measured phase compositions for the three conditions studied for this ternary system show that substantial amounts of each compound were present in each of the three phases. The SC wood treatment process, requires the biocide-cosolvent pairs to be miscible in one another as well as in SC-CO_2 to a large extent to facilitate a high deposition of the biocide in the wood structure. Results from this ternary system show that the miscibilities of the compounds used in this system are in agreement with the miscibility requirement of the SC wood treatment process and thus the TCMTB-acetone pair has the potential to be a successful candidate in this technology.

6. Mathematical models were developed to describe high-pressure LL, VL and VLL

    equilibria of binary and ternary systems. A Van Laar activity coefficient model

    for both liquid phases was used to model LLE data in the literature for three

    binary systems. Results showed that van Laar activity coefficient parameters were

    functions of temperature and pressure and should not be considered as constants.

    In the case of VLE, the Redlich-Kwong equation of state and Kwak and

    Mansoori's mixing rules for the vapor phase and van Laar activity coefficient

    model for the liquid phase gave good fits to binary data from the literature. At

    least two data points were necessary for the purpose of fitting the parameters.

7. For VLLE, the Peng-Robinson equation of state with van der Waals mixing rules

    for the vapor and the liquid phases represented the system well for the simple

    system of CO_2/isopropanol/water but was less useful for the more complex

    systems when the critical temperature of one component was estimated from

    Lyderson's correlation (Lyman et al., 1982) based on the normal boiling point.

    The critical temperature was found to be a useful fitting parameter and when

    applied to data for the CO_2/isopropanol/water system, the fitted T_c was closer to

    the known experimental value of T_c than Lyderson's correlations. When neither

    critical temperature nor normal boiling point are known (or perhaps do not exist)

    it is recommended that T_c be simply treated as an additional fitting parameter.

    With the fitted T_c, the model was good for all ternary systems chosen from the

    literature but not for the CO_2/acetone/TCMTB data reported here.

8. The agreement between calculated and experimental phase compositions was better at lower pressures when the system was farther from the critical region.

9. The Redlich-Kwong equation of state with Kwak and Mansoori's mixing rules was tested in presenting VLLE of the CO_2/isopropanol/water system and found to be less useful than the Peng-Robinson equation of state with van der Waals mixing rules.

10. Results for the biocide system improved when the PR-EOS with Panagiotopoulos and Reid's mixing rules were used and T_c was fitted, but the fit was not as good as that achieved for other ternary systems (in the simple ternary systems, model fits were almost exact for two or all of the phases while it was only exact for one phase in the TCMTB system). Therefore the new mixing rules of Panagiotopoulos and Reid were superior to that of van der Waals for fitting the VLLE data of ternary systems. The new mixing rule had six adjustable parameters (three parameters more than the van der Waals mixing rules) and was only good for the biocide system at conditions farthest from the critical region.

11. The complexity of the biocide molecule and impurities in the raw material might be reasons for not obtaining better agreement between the experimental and calculated phase compositions. Thus, the phase composition estimation problem for practical wood preservatives at near critical conditions continues to be a challenge.

8.2 Recommendations

Although this work answered many questions regarding the phase behavior of mixtures used in the SC wood treatment process, additional studies will be needed to better understand and improve the process. Future work should include the following studies:

1. Results obtained for the CO_2/acetone/TCMTB system show that a good phase separation is possible at 25 °C and 4.05 MPa (588 psia). This is promising if a recovery system is to be designed for the wood treatment process. The separation section in the recovery system of a wood treatment process should be operated at a temperature of 25 °C or below and a pressure at 3.45 MPa (500 psia) or below to recycle acetone and TCMTB.

2. One limitation of the phase composition measurements used in this work is that the number of phases must be equal to the number of components. When experiments are to be made at conditions where this requirement does not hold, it is recommended to modify the experimental equipment and use a sampling method such as that used by Panagiotopoulos and Reid (1987), Suzuki and Sue (1990), Ohgaki and Katayama (1975) or Brunner et al. (1987) instead of a stoichiometric method. A variable volume cell should be used in order to vary temperature or pressure to obtain phase equilibria measurements at constant pressure or constant temperature respectively for constant total composition.

3. Another limitation of this method is that overall phase compositions of each component in the mixture cannot be significantly different (35% maximum relative difference) in one experiment than those in another experiment at a constant temperature and pressure if the same number of phases (i.g. three phases) are to be obtained in the visible range of the view cell. Consequently, the measured phase volumes cannot be significantly different (95% maximum relative difference) in one experiment than those in another experiment at a constant temperature and pressure. This might cause the stoichiometric method to be less reliable. If the stoichiometric method is to be used for phase composition measurements, a longer view cell (about three times longer than the 210-mm long cell used in this study) should be used. Another limitation of the stoichiometric method is that it might give unfeasible phase compositions (i.e. negative phase compositions) if number of experiments are limited.

4. Previous solubility studies (Sahle, 1994) have shown that even presence of 1.1 mole% of cosolvents can significantly increase the solubility of biocides in SC-CO_2. Sahle reported an order of magnitude increase in the solubility of tebuconazole in SC-CO_2 in the presence of 1.1 mole% methanol. Since water and wood extracts would most likely be present in the supercritical fluid during wood treatment process, phase behavior studies should be conducted with water and wood extracts as additional components to the ternary mixture. Type(s) of possible wood extracts present in the SC wood treatment process should be determined by wood extraction experiments using SCfs.

5.   Mixing rules and equations of state had significant effects on the performance

of the model. Thus, other mixing rules and equations of state may improve model

performance and should be investigated. Biocide molecules might react or

associate with other molecules in the mixture because of their complex molecular

structure, therefore, the performance of association models (i.g. Chapman et al.,

1990; Huang and Radosz, 1990; Jennings et al., 1993) in predicting phase

equilibria compositions should be investigated.

6.   In the CO_2/acetone/TCMTB system studied here, each of the VLL phases

contained significant amounts (more than 0.15 mole fractions) of two or all

components of the mixture and the model derived here could not fit the data. It

would be interesting to find a biocide and/or cosolvent which would form at least

one nearly pure phase to see if the current model is any more appropriate for such

a system.

The first recommendation applies to the operation of the SC wood treatment

equipment. Operating the separation section in the recovery system of the wood

treatment process when CO_2/acetone/TCMTB mixture is used at a temperature of 25 °C

or below and a pressure at 3.45 MPa (500 psia) or below, would ensure a good phase

separation. A good phase separation would be useful for recycling purposes and

operating the separation system at this range of temperatures and pressures would keep

the cost of recompression low. The second recommendation requires the equipment to be

modified but it would have three advantages: (1) it would allow experiments to be done at

a wider range of temperatures and pressures, (2) it would be more time efficient than the constant volume cell since with the variable volume cell, measurements at different pressures would be possible with a single cell loading, and (3) it would not require the number of phases to be equal to the number of components. The third recommendation is also a modification to the equipment and may improve reliability of the stoichiometric method. The fourth recommendation is also important since water and wood extracts are expected to be present in the SCF during the treatment process. Although phase behavior of ternary systems are complex, phase behavior of five and more-component systems can become even more complex, therefore, this recommendation is challenging. Even though the fifth recommendation is not as urgent as the first four, the quality of the models depend on the mixing rules and the equations of state, therefore, other mixing rules and equations of state may improve model performance, especially if the model takes into account the physical reality of the phenomena. The sixth recommendation will answer the applicability of the current model to the complex biocide systems of interest. If a model can be successfully applied to these biocide systems, the number of phase equilibria experiments required for process development can be considerably reduced. This recommendation is also challenging, but least urgent, since it is time consuming to find a biocide and/or a cosolvent that would form at least one nearly pure phase.

REFERENCES

Andrews, T.,"The Bakerian Lecture. On the Continuity of the Gaseous and Liquid States of Matter," *Phil. Trans.* **1869**, *159*, 575-590.

Anonymous, "3 Supercritical Fluid Extraction Strategies,"*R & D Magazine*, April 1995, 59-60.

Beret, Samil and Prausnitz, J. M., "Perturbed Hard-Chain Theory: An Equation of State for Fluids Containing Small or Large Molecules," *AIChE J.* **1975,** *21*(6), 1123-1132.

Brennecke, Joan F. and Eckert, Charles A., "Phase Equilibria for Supercritical Fluid Process Design," *AIChE J.* **1989,** *35*(9), 1409-1427.

Brunner, Erwin, "Fluid Mixtures at High Pressures, I. Phase Separation and Critical Phenomena of 10 Binary Mixtures of (a Gas + Methanol)," *J. Chem. Thermodynamics* **1985,** *17*, 671-679.

Brunner, E.; Hultenschmidt, W.; Schlichtharle, G. J., "Fluid Mixtures at High Pressures, IV. Isothermal Phase Equilibria in Binary Mixtures Consisting of (Methanol + Hydrogen or Nitrogen or Methane or Carbon Monoxide or Carbon Dioxide)," *Chem. Thermodynamics* **1987,** *19*, 273-291.

Calimli, A. and Olcay, A., "Supercritical Dioxane Extraction of Spruce Wood and Dioxane-Lignin and Comparison of the Extracts with the Pyrolysis Products," *Separation Sci. and Technol.* **1983,** *17*(1), 183-197.

Carnahan, Norman F. and Starling, Kenneth E., "Intermolecular Repulsions and the Equation of State for Fluids," *AIChE J.* **1972,** *18*(6), 1184.

Chapman, W. G.; Gubbins, K. E.; Jackson, G.; Radosz, M., "New Reference Equation of State for Associating Liquids," *Ind. Eng. Chem. Res.* **1990,** *29*, 1709.

DiAndreth, J. R.; Ritter, J. M.; Paulaitis, M. E., "Experimental Technique for Determining Mixture Compositions and Molar Volumes of Three or More Equilibrium Phases at Elevated Pressures," *Ind. Eng. Chem. Res.* **1987,** *26*(2), 337-343.

DiAndreth, J. R. and Paulaitis, M. E., "Multiphase Behavior in Ternary Fluid Mixtures: A Case Study of the Isopropanol-Water-CO_2 System at Elevated Pressures," *Chemical Engineering Science* **1989,** *44*(5), 1061-1069.

Dobbs, Joseph M. and Johnston, Keith P., "Selectivities in Pure and Mixed Supercritical Fluid Solvents," *Ind. Eng. Chem. Res.* **1987,** *26,* 1476-1482.

Ekart, Michael P.; Brennecke, Joan F.; Eckert, Charles A., "Molecular Analysis of Phase Equilibria in Supercritical Fluids," In *Supercritical Fluid Technology: Reviews in Modern Theory and Applications,* Thomas J. Bruno and James F. Ely, CRC Press, Inc., Boco Raton, FL., 1991; 163-192.

Fall, David J. and Luks, Kraemer D., "Phase Equilibria Behavior of the Systems Carbon Dioxide + n-Dotriacontane and Carbon Dioxide + n-Docosane," *Journal of Chemical and Engineering Data* **1984,** *29,* 413-417.

Gurdial, G. S.; Foster, N.R.; Yun, S. L. J.; Tilly, K. D., "Phase Behavior of Supercritical Fluid-Entrainer Systems," In *Supercritical Fluid Engineering Science;* E. Kiran and J. F. Brenneke, Eds.; ACS Symposium Series 514; American Chemical Society: Washington, D.C., 1993; 34-45.

Heidemann, R. A., "Computation of High Pressure Phase Equilibria," *Fluid Phase Equilibria* **1983,** *14,* 55-78.

Hill, Arthur E. and Malisoff, William M., "The Mutual Solubility of Liquids. III. The Mutual Solubility of Phenol and Water. IV. The Mutual Solubility of Normal Butyl Alcohol and Water," *J. Am. Chem. Soc.* **1926,** *48,* 918-927.

Huang, S. H. and Radosz, M., "Equation of State for Small, Large, Polydisperse, and Associating Molecules," *Ind. Eng. Chem. Res.* **1990,** *29,* 2284.

Huang, Hai and Sandler, Stanley I., "Prediction of Vapor-Liquid Equilibria at High Pressures Using Activity Coefficient Parameters Obtained from Low-Pressure Data: A Comparison of Two Equation of State Mixing Rules," *Ind. Eng. Chem. Res.* **1993,** *32,* 1498-1503.

Hutchenson, Keith W. and Foster, Neil R., "Innovations in Supercritical Fluid Science and Technology," In *Innovations in Supercritical Fluids Science and Technology;* Keith W. Hutchenson and Neil R. Foster, Eds.; ACS Symposium Series 608; American Chemical Society: Washington D.C., 1995; 1-31.

Jennings, David W.; Lee, Rong-Jwyn; Teja, Amyn S., "Vapor-Liquid Equilibria in the Carbon Dioxide + Ethanol and Carbon Dioxide + 1-Butanol Systems," *Journal of Chemical and Engineering Data* **1991,** *36,* 303-307.

Jennings, David W.; Gude, Michael T.; Teja, Amyn S., "High-Pressure Vapor-Liquid Equilibria in Carbon Dioxide and 1-Alkanol Mixtures," In *Supercritical Fluid Engineering Science;* E. Kiran and J. F. Brenneke, Eds.; ACS Symposium Series 514; American Chemical Society: Washington, D.C., 1993; 10-33.

Johnston, Keith P. and Eckert, C. A., "An Analytical Carnahan-Starling-van der Waals Model for Solubility of Hydrocarbon Solids in Supercritical Fluids," *AIChE J.* **1981,** *27*(5), 773.

Johnston, Keith P.; Ziger, David H.; Eckert, C. A., "Solubilities of Hydrocarbon Solids in Supercritical Fluids. The Augmented van der Waals Treatment," *Ind. Eng. Chem. Fundam.* **1982,** *21*, 191-197.

Johnston, Keith P.; Kim, Sunwook; Wong, Joseph M., "Local Composition Models for Fluid Mixtures Over a Wide Density Range," *Fluid Phase Equilibria* **1987,** *38*, 39-62.

Katayama, Takashi; Ohgaki, Kazunari; Maekawa, Goro, Motojiro; Nagano, Tamon, "Isothermal Vapor-Liquid Equilibria of Acetone-Carbon Dioxide and Methanol-Carbon Dioxide Systems at High Pressures," *Journal of Chemical Engineering of Japan* **1975,** *8*(2), 89-92.

Kay, Webster B., "The Critical Locus Curve and the Phase Behavior of Mixtures," *Accounts Chem. Res.* **1968,** *1*, 344-351.

King, Jr., A. D. and Robertson, W. W., "Solubility of Naphthalene in Compressed Gases," *J. Chem. Phys.* **1962,** *37*(7), 1453.

Knobler, C. M. and Scott, R. L., "Indirect Determination of Concentrations in Coexisting Phases," *Journal of Chem. Phys.* **1980,** *73*, 5390-5391.

Kuenen, J. P., *Commun. phys. Lab. Univ. Leiden*, **1892,** No. 4B, 7.

Kumar, Sanat K.; Suter, Ulrich W.; Reid, Robert C., "A Statistical Mechanics Based Lattice Model Equation of State," *Ind. Eng. Chem. Res.* **1987,** *26*, 2532-2542.

Kwak, T. Y. and Mansoori, G. A., "Van Der Waals Mixing Rules for Cubic Equations of State. Applications for Supercritical Fluid Extraction Modeling," *Chemical Engineering Science* **1986,** *41*(5), 1303-1309.

Lee, B. I. and Kesler, M. G., "A Generalized Thermodynamic Correlation Based on Three-Parameter Corresponding States," *AIChE J.* **1975,** *21*(3), 510-527.

Li, C. C. and McKetta, John J., "Vapor-Liquid Equilibrium in the Propylene-Water System," *Journal of Chemical and Engineering Data* **1963,** *8*(2), 271-275.

Lyman, W. J.; Reehl, W. F.; Rosenblatt, D. H., *Handbook of Chemical Property Estimation Methods: Environmental Behavior of Organic Compounds*, McGraw-Hill, New York, NY, 1982; 12-16 to 12-39.

Mackay, M. E. and Paulaitis, M. E., "Solid Solubilities of Heavy Hydrocarbons in Supercritical Solvents," *Ind. Eng. Chem. Fund.* **1979,** *18*(2), 149.

Miller, C. O. M., In *Perry's Chemical Engineers' Handbook*, 6th ed., Perry, R. H.; Green, D., Eds.; McGraw-Hill, New York, NY, 1984; 3-265 to 3-267.

Morrell, J.J.; Levien, K.L.; Sahle-Demessie, E; Kumar, S.; Smith, S.; Barnes, H.M., "Treatment of Wood Using Supercritical Fluid Processes," 14th Annual Meeting of the Canadian Wood Preservation Association, Vancouver, B.C., Nov. 2-4, 1993.

Najour, G. C. and King, A. D., Jr., "Solubility of Anthracene in Compressed Methane, Ethylene, Ethane, and Carbon Dioxide: The Correlation of Anthracene-Gas Second Cross Virial Coefficients Using Pseudocritical Parameters," *J. Chem. Phys.* **1970,** *52*(10), 5206.

Nitta, T.; Ikeda, K.; Katayama, T., "Calculation of Solid-Fluid Phase Equilibria and Three- Dimensional Phase Diagrams for Binary Systems of Naphthalene and Supercritical Fluids," *International Chemical Engineering* **1993,** *33*(2), 257-264.

Ohgaki, K. and Katayama, T., "Isothermal Vapor-Liquid Equilibria for Systems Ethyl Ether-Carbon Dioxide and Methyl Acetate-Carbon Dioxide at High Pressures," *J. Chem. Eng. Data* **1975,** *20*(3), 264-267.

Panagiotopoulos, Athanassios Z., "Direct Determination of Phase Coexistence Properties of Fluids by Monte Carlo Simulation in a New Ensemble," *Molecular Physics* **1987,** *61*(4), 813-826.

Panagiotopoulos, A. Z. and Reid, R. C., "High-Pressure Phase Equilibria in Ternary Fluid Mixtures with a Supercritical Component," In *Supercritical Fluids: Chemical Engineering Principles and Applications*; T. G. Squires and M. E. Paulaitis, Eds.; ACS Symposium Series 329; American Chemical Society, Washington DC., 1987; 115-129.

Panagiotopoulos, A. Z., "Gibbs-Ensemble Monte Carlo Simulations of Phase Equilibria in Supercritical Fluid Mixtures," In *Supercritical Fluid Science and Technology*; K. P. Johnston and J. Penninger, Eds.; ACS Symposium Series 406, American Chemical Society: Washington D.C., 1989; 39-51.

Patel, N. C. and Teja, A. S., "A New Cubic Equation of State for Fluids and Fluid Mixtures," *Chem. Eng. Sci.* **1982,** *37*(3), 463-473.

Peng, D. Y. and Robinson, D. B., "A New Two-Constant Equation of State," *Ind. Eng. Chem. Fund.* **1976,** *15*(1), 59.

Perry's Chemical Engineers' Handbook, 6th ed., Perry, R. H.; Green, D., Eds.; McGraw-Hill, New York, NY, 1984; 3-265 to 3-275.

Prausnitz, John M.; Lichtenthaler, Ruediger N.; de Azevedo, Edmundo G., *Molecular Thermodynamics of Fluid-Phase Equilibria*, 2nd ed., Prentice-Hall, Englewood Cliffs, NJ, 1986; 8-32.

Reamer, H. H.; Sage, B. H.; Lacey, W. N., "Phase Equilibria in Hydrocarbon Systems," *Industrial and Engineering Chemistry* **1952**, *44*(3), 609-615.

Redlich, O. and Kwong, J. N. S., "On the Thermodynamics of Solutions. V. An Equation of State: Fugacities of Gaseous Solutions," *Chem. Rev.* **1949**, *44*, 233-244.

Ritter, J.M. and Paulaitis, M.E., "Multiphase Behavior in Ternary Mixtures of CO_2, H_2O, and Nonionic Amphiphiles at Elevated Pressures,"*Langmuir* **1990**, *6*(5), 934-941.

Ritter, D. C. and Campbell, A. G., "Supercritical Carbon Dioxide Extraction of Southern Pine and Ponderosa Pine," *Wood and Fiber Science* **1991**, *23*(1), 98-113.

Rössling, G. L. and Franck, E. U., "Solubility of Anthracene in Dense Gases and Liquids to 200 °C and 2000 Bar," *Ber Bunsenges. Phys. Chem.* **1983**, *87*, 882.

Saad, H. and Gulari, E., "Diffusion of Liquid Hydrocarbons in Supercritical CO_2 by Photon Correlation Spectroscopy," *Ber. Bunseges, Phys. Chem.* **1984**, *88*, 834-841.

Sahle-Demessie, E., "Deposition of Chemicals in Semi-porous Solids Using Supercritical Fluid Carriers," Ph. D. Thesis, Oregon State University, 1994.

Sandler, Stanley I., *Chemical and Engineering Thermodynamics*, 2nd ed., Wiley, New York, NY, 1989; 146-149, 219-226, 308-311, 316-345, 351-359, 371, 382.

Shing, K. S. and Chung, S. T., "Computer Simulation Methods for the Calculation of Solubility in Supercritical Extraction Systems," *J. Phys. Chem.* **1987**, *91*, 1674-1681.

Shing, K. S., "Application of Molecular Simulation to the Study of Supercritical Extraction," In *Supercritical Fluid Technology: Reviews in Modern Theory and Applications*; Thomas J. Bruno and James F. Ely; CRC Press, Inc., Boco Raton, FL., 1991; 227-244.

Singh, Harcharan; Yun, S. L. Jimmy; Macnaughton, Stuart J.; Tomasko, David L.; Foster, Neil R., "Solubility of Cholesterol in Supercritical Ethane and Binary Gas Mixtures Containing Ethane," *Ind. Eng. Chem. Res.* **1993**, *32*, 2841-2848.

Soave, Giorgio, "Equilibrium Constants from a Modified Ridlich-Kwong Equation of State," *Chemical Engineering Science* **1972,** *27,* 1197-1203.

Suleiman, David; Gurdial, Gurdev S.; Eckert, Charles A., "An Apparatus for Phase Equilibria of Heavy Paraffins in Supercritical Fluids," *AIChE Journal* **1993,** *39*(7), 1257-1260.

Suzuki, Kazuhiko and Sue, Haruhusa, "Isothermal Vapor-Liquid Equilibrium Data for Binary Systems at High Pressures: Carbon Dioxide-Methanol, Carbon Dioxide Ethanol, Carbon Dioxide-1-Propanol, Methane-Ethanol, Methane-1-Propanol, Ethane-Ethanol, and Ethane-1-Propanol Systems," *Journal of Chemical and Engineering Data* **1990,** *35*(1), 63-66.

Tour, C. de la, *Annales de Chimie* **1822,** *21,* 127-132.

Traub, Peter and Stephan, Karl, "High-Pressure Phase Equilibria of the System CO_2-Water-Acetone Measured with a New Apparatus," *Chemical Engineering Science* **1990,** *45*(3), 751-758.

Tsekhanskaya, Y. V., "Diffusion of Naphthalene Solution in Carbon Dioxide Near the Liquid-Gas Critical Point," *Russ. J. Phys. Chem.* **1971,** *45,* 744.

Vetere, A., In *Perry's Chemical Engineers' Handbook*, 6th ed., Perry, R. H.; Green, D., Eds.; McGraw-Hill, New York, NY, 1984; 3-265 to 3-267.

Vezzetti, D. J., "Solubility of Solids in Supercritical Gases. II. Extension to molecules of differing sizes," *J. Chem. Phys.* **1984,** *80*(2), 868-871.

Ward, D.; Dinatelli, T.; Sunol, A. K., "Supercritical Fluid Aided Wood-Polymer Composite Manufacture," AIChE Meeting, Orlando, FL, Spring, 1990.

Wong, J. M.; Pearlman, R. S.; Johnston, K. P., "Supercritical Fluid Mixtures: Prediction of the Phase Behavior," *J. Phys. Chem.* **1985,** *89,* 2671-2675.

APPENDICES

Appendix A

Phase Composition Calculations Using the Stoichiometric Technique

As explained in Chapter 2, the stoichiometric method for determining the compositions of equilibrium phases requires the number of phases to be equal to or greater than the number of components. This method involves a mole balance for each component at a constant temperature and pressure and can be written as:

$$VC=n \tag{A.1}$$

where C is an array of unknown phase compositions, V is a 2-dimensional matrix containing the measured phase volumes and n is an array containing the total number of moles of the compounds. For a two component system forming two equilibrium phases at constant temperature and pressure, equation (A.1) can be written as:

$$C_1^L V_k^L + C_1^G V_k^G = n_{1,k} \tag{A.2}$$

$$C_2^L V_k^L + C_2^G V_k^G = n_{2,k} \tag{A.3}$$

where C_i^α is an unknown molar compositions of component i in the α phase, V_k^α is the measured volume of α phase in experiment k, and $n_{i,k}$ is the total number of moles of component i in experiment k. Since there are two equations and four unknown (C_i^α), at least two sets of experiments at the same temperature and pressure but with different overall mole fractions will be necessary to solve for the unknowns. Let the following V

and n be the two sets of measured volumes, and total number of moles:

	V^G (cm^3)	V^L (cm^3)	n_{CO_2} (mole)	$n_{methanol}$ (mole)
Experiment 1:	23.0158	16.4842	0.4654	0.0099
Experiments 2:	27.6652	11.8348	0.3975	0.0074

Based on these data, the following four equation in four unknowns can be solved for the concentration of each component in each phase.

$$(16.4842)\, C_1^L + (23.0158)\, C_1^G = 0.4654 \tag{A.4}$$

$$(11.8348)\, C_1^L + (27.6652)\, C_1^G = 0.3975 \tag{A.5}$$

$$(16.4842)\, C_2^L + (23.0158)\, C_2^G = 0.0099 \tag{A.6}$$

$$(11.8348)\, C_2^L + (27.6652)\, C_2^G = 0.0074 \tag{A.7}$$

Compositions can then be calculated from the ratio of concentration for each component to the total concentration in each phase:

$$x_1^\alpha = \frac{C_1^\alpha}{C_1^\alpha + C_2^\alpha} \tag{A.8}$$

$$x_2^\alpha = \frac{C_2^\alpha}{C_1^\alpha + C_2^\alpha} \qquad (A.9)$$

To calculate density of phase α, the following equation can be used:

$$\rho^\alpha = C_1^\alpha \, wt_1 + C_2^\alpha \, wt_2 \qquad (A.10)$$

where ρ^α is the density of phase α and wt_i is the molecular weight of component i.

Appendix B

Properties Estimated Using Group Contribution Methods

The critical volume of organic compounds can be estimated using the Vetere (1984) group contribution method

$$V_c = 33.04 + \left(\sum_i M_i \times \Delta_{V_i} \right)^{1.029} \tag{B.1}$$

where M_i is the molecular weight of group i and Δ_{vi} is the volume contribution of group i. V_c is calculated in units of cm^3/mole. The critical pressure of organic compounds can be estimated from Lyderson's group contribution method (Lyman et al., 1982)

$$P_c = \frac{M}{\left(0.34 + \sum_i \Delta_{P_i} \right)^2} \tag{B.2}$$

where M is the molecular weight of the compound and Δ_{Pi} is the pressure contribution of group i. P_c is calculated in atm. The critical temperature of organic compounds can be estimated from Lyderson's correlation

$$T_c = \frac{T_b}{0.567 + \sum_i \Delta_{T_i} - (\sum_i \Delta_{T_i})^2} \tag{B.3}$$

where T_b is the normal boiling point and Δ_{T_i} is the temperature contribution of group i.

Both T_c and T_b are calculated in absolute temperature, K (or °R). If T_b is not available, it can be estimated using Miller's correlation (1984).

$$T_b = 0.012186 \ \theta \, e^{\beta} \qquad (B.4)$$

where

$$\theta = \frac{T_b}{T_c} \qquad (B.5)$$

$$\beta = \frac{[(1-\theta)^{2/7} - 0.048] \ln V_c + (1-\theta)^{2/7} \ln P_c + 1.255}{(1-\theta)^{2/7}} \qquad (B.6)$$

Acentric factor can be estimated using Lee and Kesler's correlation (1975)

$$\omega = \frac{-\ln P_c - 5.92714 + 6.09648 \, \theta^{-1} + 1.28862 \ln\theta - 0.169347 \, \theta^6}{15.2518 - 15.6875 \, \theta^{-1} - 13.4721 \ln\theta + 0.43577 \, \theta^6} \qquad (B.7)$$

Isopropanol

$$CH_3 - \overset{\overset{\displaystyle OH}{|}}{CH} - CH_3$$
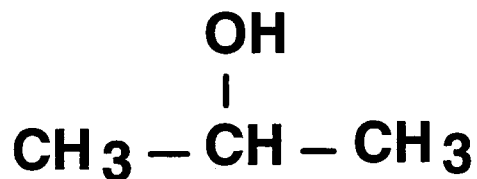
Group	Quantity	Δ_{ti}	Δ_{pi}	Δ_{vi}
—CH$_3$	1	0.020	0.227	3.360
—CH$_2$ (nonring)	2	2(0.020) = 0.040	2(0.227) = 0.454	2(3.360) = 6.720
—OH (alcohols)	1	0.082	0.060	0.704
	Total:	0.142	0.741	10.784

$V_c = 214.54$ cm^3/mole $= 2.1454 \times 10^{-4}$ m^3/mole

$P_c = 51.427$ atm $= 5.211 \times 10^6$ Pa

$T_b = 372.63$ K $= 99.48$ °C

$T_c = 540.96$ K $= 267.81$ °C

$\omega = 0.61754$

If experimental $T_b = 82.30$ °C (355.45 K) is used, the following values are obtained:

$V_c = 214.54$ cm^3/mole $= 2.1454 \times 10^{-4}$ m^3/mole

$P_c = 51.427$ atm $= 5.211 \times 10^6$ Pa

$T_c = 516.02$ K $= 242.87$ °C

$\omega = 0.61754$

C$_4$E$_1$ (2-Butoxyethanol= Ethylene glycol monobutyl ether)

$$CH_3 - CH_2 - CH_2 - CH_2 - O - CH_2 - CH_2 - OH$$
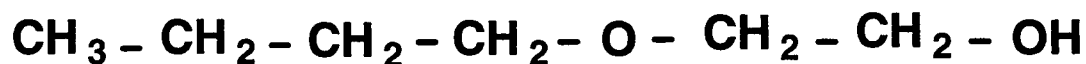
Group	Quantity	Δ_{ti}	Δ_{pi}	Δ_{vi}
—CH$_3$	1	0.020	0.227	3.360
—CH$_2$ (nonring)	5	5(0.020) = 0.100	5(0.227) = 1.135	5(3.360) = 16.800
—OH (alcohols)	1	0.082	0.060	0.704
—O— (nonring)	1	0.021	0.160	1.075
	Total:	0.223	1.582	21.939

V_c = 405.64 cm^3/mole = 4.0564x10^{-4} m^3/mole

P_c = 31.99 atm = 3.2415x10^6 Pa

T_b = 484.76 K = 211.61 °C

T_c = 654.85 K = 381.70 °C

ω = 0.8657

If experimental T_b = 171.00 °C (444.15 K) is used, the following values are obtained:

V_c = 405.64 cm^3/mole = 4.0564x10^{-4} m^3/mole

P_c = 31.99 atm = 3.2415x10^6 Pa

T_c = 599.98 K = 326.83 °C

ω = 0.8657

C₈E₃ (*n-Octyl tri(oxyethylene) mono ether*)

$$CH_3-CH_2-CH_2-CH_2-CH_2-CH_2-CH_2-C \begin{cases} O-CH_2-CH_2-OH \\ O-CH_2-CH_2-OH \\ O-CH_2-CH_2-OH \end{cases}$$
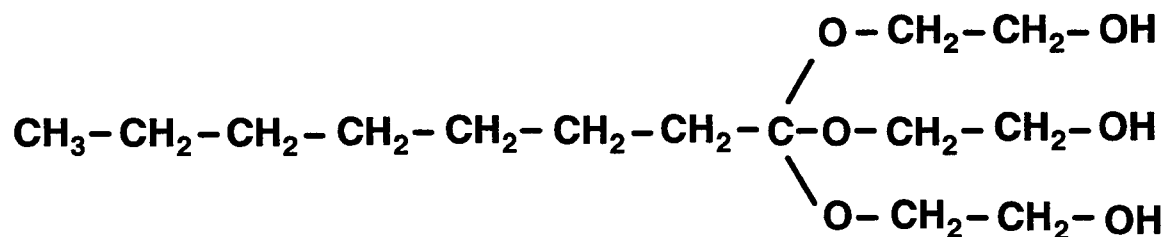
Group	Quantity	Δ_{ti}	Δ_{pi}	Δ_{vi}
—CH₃	1	0.020	0.227	3.360
—CH₂ (nonring)	12	12(0.020) = 0.240	12(0.227) = 2.724	12(3.360) = 40.32
—C— (nonring)	1	0.000	0.210	3.360
—OH (alcohols)	3	3(0.082) = 0.246	3(0.060) = 0.180	3(0.704) = 2.112
—O— (nonring)	3	3(0.021) = 0.063	3(0.160) = 0.480	3(1.075) = 3.225
	Total:	0.569	3.821	52.377

$V_c = 934.236 \ cm^3/mole = 9.34236 \times 10^{-4} \ m^3/mole$

$P_c = 17.003 \ atm = 1.7229 \times 10^6 \ Pa$

$T_b = 700.73 \ K = 427.58 \ ^\circ C$

$T_c = 862.72 \ K = 589.57 \ ^\circ C$

$\omega = 1.3841$

TCMTB (2-(*Thiocyanomethylthio*) *benzothiazole*)
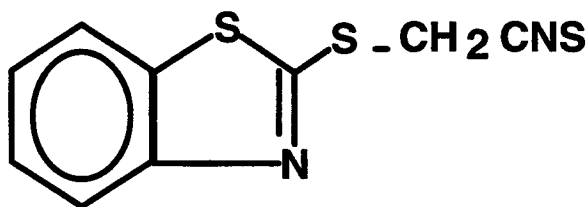
Group	Quantity	Δ_{ti}	Δ_{pi}	Δ_{vi}
= CH (ring)	4	4(0.011) = 0.044	4(0.154) = 0.616	4(2.538) = 10.152
= C— (ring)	3	3(0.011) = 0.033	3(0.154) = 0.462	3(2.538) = 7.614
—CH$_2$ (nonring)	1	0.020	0.227	3.360
—N = (ring)	1	0.007	0.130	1.883
—CN	1	0.060	0.360	2.784
—S— (nonring)	1	0.015	0.270	0.591
= S	1	0.003	0.240	0.591
—S— (ring)	1	0.008	0.240	0.911
	Total:	0.190	2.545	27.886

$V_c = 553.88 \text{ cm}^3/\text{mole} = 5.5388 \times 10^{-4} \text{ m}^3/\text{mole}$

$P_c = 28.595 \text{ atm} = 2.8974 \times 10^6 \text{ Pa}$

$T_b = 547.85 \text{ K} = 274.70 \text{ °C}$

$T_c = 759.95 \text{ K} = 486.80 \text{ °C}$

$\omega = 0.62233$

Appendix C

Listings of Computer Programs

Two MATLAB program and two FORTRAN programs are presented here. DTFTPHAS.M which is a MATLAB program calculates phase compositions in an N-component and N-phase equilibria system using the stoichiometric method discussed in section 2.4. The program requires meniscus levels of the phases at equilibrium and the volumes or amount of the components used. TRIAPLOT.M is also written using MATLAB and generates a triangular plot from a data set of compositions in a ternary system. ACTLLE.FOR is a FORTRAN program which calculates phase compositions of LL equilibria in a binary mixture at a specified temperature and pressure. Van Laar activity coefficient model is used and its parameters are fitted to the data. The successive substitution algorithm discussed by Heidemann (1983) is used in the calculations. PREOSVLL.FOR is the second FORTRAN program and calculates phase compositions of VLL equilibria in a ternary mixture at a specified temperature and pressure. Peng-Robinson equation of state is used and the binary interaction parameters as well as the critical temperature of the third component are fitted to the data. Like in the ACTLLE.FOR program, in PREOSVLL.FOR program the successive substitution algorithm of Heidemann (1983) is used to obtain a solution. In the PREOSVLL.FOR program, the mixing rule suggested by Panagiotopoulos and Reid (1987) was used, but with minor changes to the program, van der Waals mixing rules could be used in the calculations.

```
%************************************************************
%                                                          *
%                        DTFTPHAS.M                        *
%_____*
%                                                          *
%    This program calculates phase compositions in an N-component and N-phase   *
%    equilibria system using a stoichiometric method from measured phase volumes. *
%    The program requires the meniscus levels and the volumes or amounts of the   *
%    components used.  The program treats the Nth component as a solid for which   *
%    amounts (gram) and molecular wt. is needed to calculate its moles. Up to the  *
%    N-1 component, volume and density will be used.                             *
%    Vmole (exp,phase) in cm3/mole is the molar volume of phase "phase" in        *
%    experiment "exp". dphase (exp,phase) in g/cm3 is density of phase "phase" and *
%    experiment "exp". mole (com,exp) is number of mole of component "com" in      *
%    experiment "exp".                                                           *
%                                                          *
%************************************************************


N = input (' Number of variables must be equal to number of equations. Enter number of ...
        variables, N: ');

m = input (' Enter number of experiments, m: ');

%XLLALL=[12.41,22.58;12.53,18.68;12.83,18.58;13.12,20.73;13.48,20.63;11.88,22.96]
XLLALL=[12.79,22.38;13.36,22.12;12.57,21.60;12.59,22.82;12.02,23.02;12.57,22.13;...
        11.98,21.47;12.52,21.23;12.40,21.97;12.69,21.10;12.27,21.88;12.30,21.88]
%XLLALL=[12.15,21.09;13.34,21.26;13.89,20.62;12.51,22.02;12.66,20.98;11.96,20.61;...
%        12.34,20.68;11.55,21.61;12.92,21.74;13.56,22.82]

%xvolall=[8.0,7190.0;7.0,6855.0;7.0,6635.0;8.0,7712.0;8.0,7801.0;10.0,8237.0]
xvolall=[9.5,6033.0;9.5,5325.719;9.0,4956.55;10.0,4926.12;9.0,6342.42;9.0,3450.96;...
        8.0,5292.79;8.0,3420.03;8.5,3244.42;8.0,3348.19;8.5,5075.285;8.5,4659.225]
%xvolall=[10.0,4925.6;10.0,5185.5;9.5,4354.91;10.0,2947.09;9.5,3977.77;9.0,3821.119;...
%        9.0,4369.879;10.0,3973.77;9.5,4035.63;10.0,4155.36]

%xgramall=[9.7297,10.0010,10.0034,10.5008,11.0936,10.1060]
xgramall=[11.0203,11.8386,10.5558,10.7548,10.0096,11.0192,10.0339,10.5179,10.5072,...
        10.7600,10.2848,10.2846]
%xgramall=[10.0106,11.0715,11.6085,10.6664,10.5630,9.8371,10.0446,9.7010,11.0296,...
%        12.0081]

disp(' Enter the experiment numbers: ')
for i=1:m
        i
        mm(i)=input(' mm(i): ');
end
```

```
%disp(' Enter liquid levels in each exp., XLL(exp.,phase)')

for i=1:m
        for j=1:N-1
%       ij=[i j]
%       XLL(i,j) = input (' XLL(i,j): ');
        XLL(i,j)=XLLALL(mm(i),j);
        end
end
XLL
for i=1:m
Vlowliq=0.0;
Vallliq=0.0;
        for j=1:N-1
%       V(i,j)=-13.34+1.89*XLL(i,j)-Vlowliq;
        V(i,j)=-14.04+1.88*XLL(i,j)-Vlowliq;
        Vlowliq=V(i,j);

        end
                for k=1:N-1

                Vallliq=V(i,k)+Vallliq;

                end

%V(i,N)=39.5-Vallliq;
V(i,N)=38.6-Vallliq;
end
V
%InversV=inv(V)
%Pinv1=pinv(V)
%Pinv2=(inv(V'*V))*V'
%cond(pinv(V))
for i=1:N-1
disp(' Component # i')
i
disp(' Enter density d in g/cm^3 and molecular weight of ith component')
d(i)=input(' d(i): ');
wt(i)=input(' wt(i): ');
%disp(' Enter amount of this component xvol (cm^3) in each experiment')
        for j=1:m
%       j
%       xvol(j)=input('xvol(j): ');
        xvol(j)=xvolall(mm(j),i);
        bn(j)=(xvol(j)*d(i))/wt(i);
        end
```

```
xvol
bn'
ccomp=((inv(V'*V))*V')*bn'
f=V*ccomp-bn'
        for j=1:N
                c(i,j)=ccomp(j);
        end
end
for i=N
disp(' Component # i')
i
disp(' Enter molecular weight of ith component')
wt(i)=input(' wt(i): ');
%disp(' Enter amount of this component xgram (g) in each experiment')
        for j=1:m
%       j
%       xgram(j)=input('xgram(j): ');
        xgram(j)=xgramall(mm(j));
        bn(j)=(xgram(j))/wt(i);
        end
xgram
bn'
ccomp=((inv(V'*V))*V')*bn'
f=V*ccomp-bn'
        for j=1:N
        c(i,j)=ccomp(j);
        end
end
c
for k=1:m
        for j=1:N
                molesum=0.0;
                gramsum=0.0;
                for i=1:N
                        molesum=c(i,j)*V(k,j)+molesum;
                        gramsum=c(i,j)*V(k,j)*wt(i)+gramsum;
                        moleij(i,j)=c(i,j)*V(k,j);
                end
                Vmole(k,j)=V(k,j)/molesum;
                dphase(k,j)=gramsum/V(k,j);
        end
        for ii=1:N
                moleik=0.0;
                for jj=1:N
                        moleik=moleij(ii,jj)+moleik;
                end
```

```
                    mole(ii,k)=moleik;
        end
end
for i=1:N
ctot(i)=0.0;
        for j=1:N
        ctot(i)=c(j,i)+ctot(i);
        end
end
ctot
[u s v]=svd(pinv(V))
CondV=cond(pinv(V))
disp(' mole fractions x(comp.,phase) are as follows:')
for i=1:N
        for j=1:N
        x(j,i)=c(j,i)/ctot(i);
        end
end
x
Vmole
dphase
 mole
%******************** END OF PROGRAM        *************
```

```
%**********************************************************************
%                                                                     *
%                          TRIAPLOT.M                                 *
%_____*
%                                                                     *
%       This program generates a triangular plot from a data set of   *
%       compositions in a ternary system.  Compositions should add    *
%        up to unity.  Only compositions of two of the components are  *
%       needed.  Component "A" will be ploted on the left corner of   *
%       the plot, "B" on the right corner, and "C" on the top corner. *
%       The user should only provid the compositions of components    *
%       "A" and "C" (XA and XC).                                      *
%                                                                     *
%       Variables:                                                    *
%                                                                     *
%       kx         x position of the left corner of the plot on       *
%                  the screen                                         *
%       ky         y position of the right corner of the plot on      *
%       m          number of data points                             *
%       Nt         number of thick marks on each side of the plot     *
%                  the screen                                         *
%       Px(i)      x position of one point of line i in               *
%                  constructing the triangular shape                  *
%       P2x(i)     x position of second point of line i in            *
%                  constructing the triangular shape                  *
%       Py(i)      y position of one point of line i in               *
%                  constructing the triangular shape                  *
%       P2y(i)     y position of second point of line i in            *
%                  constructing the triangular shape                  *
%       X(i)       x position of experimental data i on a             *
%                  triangular plot                                    *
%       Xcal(i)    x position of data i from calculations on a        *
%                  triangular plot                                    *
%       XA         a data set containing compositions of component    *
%                  "A" from experiments                               *
%       Xacal      a data set containing compositions of component    *
%                  "A" from calculations                              *
%       XC         a data set containing compositions of component    *
%                  "C" from experiments                               *
%       Xccal      a data set containing compositions of component    *
%                  "C" from calculations                              *
%       Xl(i)      x values of the points in line i in                *
%                  constructing the triangular shape                  *
%       Y(i)       y position of data i on a triangular plot          *
%       Ycal(i)    y position of data i from calculations on a        *
%                  triangular plot                                    *
```

```
%       Yl(i)            y values of the points in line i in              *
%                        constructing the triangular shape                *
%       Tl               length of the thick marks                        *
%       Tw               distance between the two adjacent thick marks     *
%                                                                          *
%**********************************************************************

Nt=5;
Tl=1/50;
Tw=1/(Nt-1);
kx=0.25;
ky=0.25;
Ts=1/20;

Px(1)=kx;
Py(1)=ky;
P2x(1)=kx+0.5;
P2y(1)=ky+(3^0.5)/2;

Px(2)=P2x(1);
Py(2)=P2y(1);
P2x(2)=kx+1;
P2y(2)=ky;

Px(3)=kx;
Py(3)=ky;
P2x(3)=kx+1;
P2y(3)=ky;

for i=1:Nt
        ii=i-1;
        n=4+ii;
        Px(n)=kx+ii*Tw;
        Py(n)=ky;
        P2x(n)=Px(n);
        P2y(n)=Py(n)-Tl;
end

for i=1:Nt
        ii=i-1;
        n=3+Nt+i;
        Px(n)=kx+ii*Tw/2;
        Py(n)=ky+ii*Tw*(3^0.5)/2;
        P2x(n)=Px(n)-Tl*(3^0.5)/2;
        P2y(n)=Py(n)+Tl/2;
end
```

```
for i=1:Nt
        ii=i-1;
        n=3+2*Nt+i;
        Px(n)=kx+1-ii*Tw/2;
        Py(n)=ky+ii*Tw*(3^0.5)/2;
        P2x(n)=Px(n)+Tl*(3^0.5)/2;
        P2y(n)=Py(n)+Tl/2;
end
%Px
%Py
%P2x
%P2y

Xl1=[Px(1) P2x(1)];
Yl1=[Py(1) P2y(1)];
Xl2=[Px(2) P2x(2)];
Yl2=[Py(2) P2y(2)];
Xl3=[Px(3) P2x(3)];
Yl3=[Py(3) P2y(3)];
Xl4=[Px(4) P2x(4)];
Yl4=[Py(4) P2y(4)];
Xl5=[Px(5) P2x(5)];
Yl5=[Py(5) P2y(5)];
Xl6=[Px(6) P2x(6)];
Yl6=[Py(6) P2y(6)];
Xl7=[Px(7) P2x(7)];
Yl7=[Py(7) P2y(7)];
Xl8=[Px(8) P2x(8)];
Yl8=[Py(8) P2y(8)];
Xl9=[Px(9) P2x(9)];
Yl9=[Py(9) P2y(9)];
Xl10=[Px(10) P2x(10)];
Yl10=[Py(10) P2y(10)];
Xl11=[Px(11) P2x(11)];
Yl11=[Py(11) P2y(11)];
Xl12=[Px(12) P2x(12)];
Yl12=[Py(12) P2y(12)];
Xl13=[Px(13) P2x(13)];
Yl13=[Py(13) P2y(13)];
Xl14=[Px(14) P2x(14)];
Yl14=[Py(14) P2y(14)];
Xl15=[Px(15) P2x(15)];
Yl15=[Py(15) P2y(15)];
Xl16=[Px(16) P2x(16)];
Yl16=[Py(16) P2y(16)];
Xl17=[Px(17) P2x(17)];
```

```
Yl17=[Py(17) P2y(17)];
Xl18=[Px(18) P2x(18)];
Yl18=[Py(18) P2y(18)];


%*********************************************************************
%                                                                   *
%       Now converting the composition data to the form used in the *
%       triangular plot and ploting the data.  A=Acetone, C=TCMTB.   *
%                                                                   *
%*********************************************************************


XA=[0.1517 0.7694 0.3019 0.1517];
XC=[0.0025 0.1912 0.1816 0.0025];
XAcal=[0.142 0.601 0.644 0.142];
XCcal=[0.003 0.300 0.092 0.003];
m1=size(XA);
m=m1(2);
for i=1:m
        X(i)=kx+1-XA(i)-XC(i)/2;
        Y(i)=ky+XC(i)*(3^0.5)/2;
        Xcal(i)=kx+1-XAcal(i)-XCcal(i)/2;
        Ycal(i)=ky+XCcal(i)*(3^0.5)/2;
end
axis([0 1.5 0 1.5])
%axis('off')
plot(Xl1,Yl1,'w-',Xl2,Yl2,'w-',Xl3,Yl3,'w-',Xl4,Yl4,'w-',Xl5,Yl5,'w-',...
    Xl6,Yl6,'w-',Xl7,Yl7,'w-',Xl8,Yl8,'w-',Xl9,Yl9,'w-',Xl10,Yl10,'w-',...
    Xl11,Yl11,'w-',Xl12,Yl12,'w-',Xl13,Yl13,'w-',Xl14,Yl14,'w-',Xl15,Yl15,'w-')
hold
%plot(Xl16,Yl16,'w-',Xl17,Yl17,'w-',Xl18,Yl18,'w-',X,Y,'wo',X,Y,'w-')

plot(Xl16,Yl16,'w-',Xl17,Yl17,'w-',Xl18,Yl18,'w-',X,Y,'wo',X,Y,'w-',Xcal,Ycal,'w+',...
    Xcal,Ycal,'w-')

%text('Position',[Px(2)-10*Ts Py(2)+3*Ts],'String','PR, 60 oC, 1600
psi','HorizontalAlignment','center')
%text('Position',[Px(2)-13*Ts Py(2)-1*Ts],'String','o = exp','HorizontalAlignment','center')
%text('Position',[Px(2)-13*Ts Py(2)-3*Ts],'String','+ = cal','HorizontalAlignment','center')
%plot (X,Y,'o')
text('Position',[kx-2*Ts ky-Ts],'String','Acetone','HorizontalAlignment','right')
text('Position',[Px(2) Py(2)+3*Ts],'String','TCMTB','HorizontalAlignment','center')
text('Position',[P2x(3)+2*Ts P2y(3)-Ts],'String','CO2','HorizontalAlignment','left')
text('Position',[Px(4) P2y(4)-Ts],'String','0.00','HorizontalAlignment','center')
text('Position',[Px(5) P2y(5)-Ts],'String','0.25','HorizontalAlignment','center')
text('Position',[Px(6) P2y(6)-Ts],'String','0.50','HorizontalAlignment','center')
text('Position',[Px(7) P2y(7)-Ts],'String','0.75','HorizontalAlignment','center')
```

```
text('Position',[Px(8) P2y(8)-Ts],'String','1.00','HorizontalAlignment','center')
set(gca,'DefaultTextRotation',60)
text('Position',[P2x(9)-Ts P2y(9)+Ts/2],'String','1.00','HorizontalAlignment','center')
text('Position',[P2x(10)-Ts P2y(10)+Ts/2],'String','0.75','HorizontalAlignment','center')
text('Position',[P2x(11)-Ts P2y(11)+Ts/2],'String','0.50','HorizontalAlignment','center')
text('Position',[P2x(12)-Ts P2y(12)+Ts/2],'String','0.25','HorizontalAlignment','center')
text('Position',[P2x(13)-Ts P2y(13)+Ts/2],'String','0.00','HorizontalAlignment','center')
set(gca,'DefaultTextRotation',-60)
text('Position',[P2x(14)+Ts P2y(14)+Ts/2],'String','0.00','HorizontalAlignment','center')
text('Position',[P2x(15)+Ts P2y(15)+Ts/2],'String','0.25','HorizontalAlignment','center')
text('Position',[P2x(16)+Ts P2y(16)+Ts/2],'String','0.50','HorizontalAlignment','center')
text('Position',[P2x(17)+Ts P2y(17)+Ts/2],'String','0.75','HorizontalAlignment','center')
text('Position',[P2x(18)+Ts P2y(18)+Ts/2],'String','1.00','HorizontalAlignment','center')
```

%****************   END OF PROGRAM   ***************

```
C***************************************************************
C                                                              *
C                        ACTLLE.FOR                            *
C_____*
C     This program calculates phase compositions of two-phase LL  *
C     equilibrium in a binary mixture at a specified temperature   *
C     and pressure.  Van Laar activity coefficient model is used   *
C     and its parameters are fitted to the data.  The successive   *
C     substitution algorithm discussed by Heidemann is used to     *
C     converge to a solution representing a local minimum in the   *
C     Gibbs free energy.  An initial guess of mole fractions for   *
C     the two phases is required to initiate the calculations.     *
C                                                              *
C     The elements of all 3x3 arrays except DELT are defined as:   *
C                                                              *
C                   G(ALC)              G(H2O)                 *
C                   L(ALC)              L(H2O)                 *
C                                                              *
C***************************************************************
        DOUBLE PRECISION TC,PC,OMEG,T,P,R,ERROR,FSTX,CALX,SUM,SQRS,XP,
     +  xi(2,2),TO,FTOL,FRET,PS,ALPHG,VC,FPURE(2),ALF,BETA,FUGA

        COMMON /PURE/TC(2),PC(2),OMEG(2),VC(2)
           COMMON / INPT/T,P,R,ERROR
        COMMON / MIX/APUR(2),BPUR(2),ACRS,BCRS,ALPHG,FPURE,ALF,BETA
        COMMON / COMP/FSTX(2,6),CALX(2,6),ICOUNT,SUM,SQRS,K1,PS(3)
        COMMON /VOLUME/VCM3(2),FUGA(2,2)
        DIMENSION XP(2)
        INTEGER NDIM,K1,K2,ILOW,IUP
        PARAMETER(NDIM=2,FTOL=1.0E-6)
        INTEGER i,iter,np
        OPEN(UNIT=74,FILE='rkacfwpl.out')
        np=NDIM
        N=2
        DO 57 I=1,NDIM
           DO 58 J=1,NDIM
              xi(I,J)=0.0
58         CONTINUE
57      CONTINUE
        DO 53 I=1,NDIM
           xi(I,I)=1.0
53      CONTINUE
        CALL DEFDAT
        K1=1
c        K1=3
c        OPEN(UNIT=24,FILE='fholpwl1')
c        OPEN(UNIT=24,FILE='fholbw2')
        OPEN(UNIT=24,FILE='fholmc6')
        READ(24,*) TO,PS(1)
        DO 202 IPHAS=1,2
        READ(24,*) (FSTX(IPHAS,ICOMP),ICOMP=1,2)
202     CONTINUE
        CLOSE(UNIT=24,STATUS='KEEP')

c        OPEN(UNIT=34,FILE='fholpwl2')
c        OPEN(UNIT=34,FILE='fholbw4')
c        OPEN(UNIT=34,FILE='fholmc10')
c        READ(34,*) TO,PS(2)
c        DO 302 IPHAS=1,2
c        READ(34,*) (FSTX(IPHAS,ICOMP),ICOMP=3,4)
```

```
c302     CONTINUE
c        CLOSE(UNIT=34,STATUS='KEEP')
c        OPEN(UNIT=44,FILE='fholpwl2')
c        OPEN(UNIT=44,FILE='fholbw4')
c        OPEN(UNIT=44,FILE='fholmc13')
c        READ(44,*) TO,PS(3)
c        DO 402 IPHAS=1,2
c        READ(44,*) (FSTX(IPHAS,ICOMP),ICOMP=5,6)
c402     CONTINUE
c        CLOSE(UNIT=44,STATUS='KEEP')

c        WRITE(*,1020)
c        READ(*,*) TO,PO
C        P=1.0+(PO/14.696081)
C        T=TO+273.15
         T=TO
c1020    FORMAT(' INPUT THE TEMPERATURE(oC) AND PRESSURE(PSIG):  '$)
         CALL PARAM

         WRITE(*,1035)
1035     format('INPUT VALUES FOR VAN LAAR PARAMETERS, ALF AND BETA:')
         READ(*,*) ALF,BETA

      XP(1)=ALF
      XP(2)=BETA

      call POWELL(XP,xi,NDIM,np,FTOL,iter,fret)
      write(74,'(/1x,a,i3)') 'Iterations:',iter
      write(74,'(/1x,a/1x,2f12.6)') 'Minimum found at: ',
     1(XP(i),i=1,NDIM)
      write(74,'(/1x,a,f12.6)') 'Minimum function value =',fret

         DO 17 K2=1,K1
            ILOW=N*K2-N+1
            IUP=N*K2
            WRITE(74,1005) T,PS(K2)
            WRITE(74,1010)
            WRITE(74,1025)
            WRITE(74,1030) (FSTX(1,ICOMP),ICOMP=ILOW,IUP),(CALX(1,ICOMP),
     1       ICOMP=ILOW,IUP)
            WRITE(74,1050) (FSTX(2,ICOMP),ICOMP=ILOW,IUP),(CALX(2,ICOMP),
     1       ICOMP=ILOW,IUP)
17       CONTINUE
            WRITE(74,1060) ICOUNT
            WRITE(74,1070) SUM
            WRITE(74,1080) SQRS
            WRITE(74,1090) (VCM3(IPHAS),IPHAS=1,2)
1005     FORMAT(/,15X,'  TEMPERATURE = ',F5.1,'  PRESSURE = ',F6.1)
1010     FORMAT(/' PHASE IX(PRA)  IX(H2O)  FX(PRA)
     1    FX(H2O)')
1025     FORMAT(/,2('***********************'))
1030     FORMAT(/,'  LIGHT   ',2(F8.5,3X),6X,2(F8.5,3X))
1050     FORMAT('  HEAVY   ',2(F8.5,3X),6X,2(F8.5,3X))
1060     FORMAT(/,15X,' THE NUMBER OF ITERATION WAS:   ',I3)
1070     FORMAT(15X,'  THE SUM OF THE SQUARES WAS:  ',E15.5)
1080     FORMAT(15X,'  THE SUM OF THE MOLE FRACTION SQUARES WAS: ',E15.5)
1090 FORMAT(5X,'MOLAR VOLUMES (CM3/MOLE)'/5X,' TOP(G)     LOW(L)
     1    '/5X,2(F8.2,3X))

      print 19,APUR(1),BPUR(2),ALPHG
```

```
19      format(1x,'Ap=',e10.3,'Bp=',e10.3,'ALPHG=',e10.3)
        STOP
        END
C********************************************************************
        REAL FUNCTION FUNC(XP)
        DOUBLE PRECISION TC,PC,OMEG,T,P,R,ERROR,APUR,BPUR,ACRS(2,2)
     +  ,FSTX,CALX,SUM,SQRS,EXPX(2,2),DELT(2,2),XP(2)
     +  ,F(8),PS,BCRS(2,2),ALPHG,VC,FPURE(2),ALF,
     +  BETA
        COMMON /PURE/TC(2),PC(2),OMEG(2),VC(2)
        COMMON / INPT/T,P,R,ERROR
        COMMON / MIX/APUR(2),BPUR(2),ACRS,BCRS,ALPHG,FPURE,ALF,BETA
        COMMON / COMP/FSTX(2,6),CALX(2,6),ICOUNT,SUM,SQRS,K1,PS(3)
        INTEGER N

        N=2

        ALF=XP(1)
        BETA=XP(2)
        KK=0
        DO 301 K2=1,K1
           P=PS(K2)
         CALL PUREFU
           DO 201 IPHAS=1,2
              JJ=0
              DO 101 JCOMP=N*K2-N+1,N*K2
                 JJ=1+JJ
                 EXPX(IPHAS,JJ)=FSTX(IPHAS,JCOMP)
101           CONTINUE
201        CONTINUE
           CALL SUCESS(EXPX,ICOUNT,SUM)
           DO 211 IPHAS=1,2
              JJ=0
              DO 111 JCOMP=N*K2-N+1,N*K2
                 JJ=1+JJ
                 CALX(IPHAS,JCOMP)=EXPX(IPHAS,JJ)
111           CONTINUE
211        CONTINUE

           DO 24 J=1,N
              DO 25 I=N*K2-N+1,N*K2
                 KK=KK+1
                 F(KK)=ABS((FSTX(J,I)-CALX(J,I))/(FSTX(J,I)+CALX(J,I)))
25            CONTINUE
24         CONTINUE
301     CONTINUE
         SQRS=0.0
         DO 35 L=1,(N**2)*K1
            SQRS=SQRS+(F(L)*F(L))
35       CONTINUE
         FUNC=SQRS
         RETURN
         END
```

```
C*******************************************************************
C                                                                 *
C     Subroutine DEFDAT asks for a datafile containing the        *
C     critical temperature, critical pressure, acentric factor,   *
C     and gas constant for the three pure components.  A          *
C     convergence criterion is also inputed.                      *
C*******************************************************************
        SUBROUTINE DEFDAT
        DOUBLE PRECISION TC,PC,VC,OMEG,T,P,R,ERROR
        COMMON /PURE/TC(2),PC(2),OMEG(2),VC(2)
        COMMON /INPT/T,P,R,ERROR
c        OPEN(UNIT=26,FILE='FDATPW')
c        OPEN(UNIT=26,FILE='FDATBW')
        OPEN(UNIT=26,FILE='FDATMC')
        READ(26,*) R
        READ(26,*) TC(1),TC(2)
        READ(26,*) PC(1),PC(2)
        READ(26,*) OMEG(1),OMEG(2)
        READ(26,*) VC(1),VC(2)
        CLOSE(UNIT=26,STATUS='KEEP')
        WRITE(*,1020)
        READ*, ERROR
        RETURN
1020    FORMAT('  INPUT THE ERROR CRITERION:   '$)
        END
C*******************************************************************
C                                                                 *
C     Subroutine PARAM calculates the pure component and mixture  *
C     parameters needed by the Peng-Robinson EOS.  The           *
C     temperature dependent of the 'a' parameter can be computed  *
C     using the emperical function of acentric factor developed   *
C     by Peng and Robinson or computed using a quadratic          *
C     function of temperature fitted to the pure component vapor  *
C     pressure curves.  Either isopropanol or ethanol can be      *
C     chosen as the alcohol component.                            *
C*******************************************************************
        SUBROUTINE PARAM
        DOUBLE PRECISION TC,PC,OMEG,T,P,R,ERROR,APUR,BPUR,
     +  BCRS(2,2),ALPHG,VC,FPURE(2),ALF
     +  ,BETA,ACRS(2,2)
        COMMON /PURE/TC(2),PC(2),OMEG(2),VC(2)
        COMMON /INPT/T,P,R,ERROR
        COMMON /MIX/APUR(2),BPUR(2),ACRS,BCRS,ALPHG,FPURE,ALF,BETA
        DO 10 JA=1,2
        APUR(JA)=1.2828*R*(TC(JA)**1.5)*VC(JA)
        BPUR(JA)=0.26*VC(JA)
10        CONTINUE
        DO 20 JB=1,2
            DO 30 JC=1,2
                BCRS(JB,JC)=((BPUR(JB)**(1.0/3.0)+BPUR(JC)**(1.0/3.0))
     +                      /2)**3
30            CONTINUE
20        CONTINUE

        RETURN
        END
```

```
C******************************************************************
C                                                                *
C     Subroutine PUREFU calculates pure component fugacities for  *
C     a given temperature at the vapor pressure of that compound. *
C     The Gibbs free energy associated with each numerical root   *
C     of the cubic equation of state is checked to determine the  *
C     correct numerical root corresponding to the lowest Gibbs    *
C     free energy.                                                 *
C                                                                *
C******************************************************************
          SUBROUTINE PUREFU
          DOUBLE PRECISION T,P,R,ERROR,APUR,BPUR,ACRS(2,2),Z
     +    ,VPCM3,AP,BP,ZMAX,ZCAP,PVAP(2),PRSAT(2),TF,T1,T2,T3,T4
     +    ,FPURE(2),ALF,BETA,A(2),B(2),C(2),TC,PC,FINT
     +    ,ZC(2),VC,VL(2),V,COEFP,TR(2),BCRS(2,2),OMEG,ZRA(2)
     +    ,ALPHG
          COMMON /INPT/T,P,R,ERROR
          COMMON /PURE/TC(2),PC(2),OMEG(2),VC(2)
          COMMON /MIX/APUR(2),BPUR(2),ACRS,BCRS,ALPHG,FPURE,ALF,BETA
          DIMENSION Z(3),COEFP(3),VPCM3(2)
C          OPEN(UNIT=38,FILE='ANTPW')
C          OPEN(UNIT=38,FILE='ANTBW')
          OPEN(UNIT=38,FILE='ANTMC')
          READ(38,*)(A(ICOMP),B(ICOMP),C(ICOMP),ICOMP=1,2)
          CLOSE(UNIT=38,STATUS='KEEP')
          TF=1.8*T-459.67
          DO 10 ICOMP=1,2
              PRSAT(ICOMP)=EXP(A(ICOMP)-B(ICOMP)/(TF+C(ICOMP)))
              PVAP(ICOMP)=PC(ICOMP)*PRSAT(ICOMP)
10        CONTINUE
          DO 15 ICOMP=1,2
              ZC(ICOMP)=PC(ICOMP)*VC(ICOMP)/(R*TC(ICOMP))
              ZRA(ICOMP)=ZC(ICOMP)
              TR(ICOMP)=T/TC(ICOMP)
              IF (TR(ICOMP).GT.1.0) THEN
                  PRINT 1,ICOMP
1                 FORMAT(1X,'MOLAR LIQUID VOUME FOR COMPONENT',I2,' IS ZERO
     +               , FPURE IS VAPOR PRESSURE TIMES THE FUGACITY COEFFICIENT')
                  VL(ICOMP)=0.0
              ELSE
                  VL(ICOMP)=ZRA(ICOMP)**(1.0+(1.0-TR(ICOMP))**(2.0/7.0))
                  VL(ICOMP)=VL(ICOMP)*R*TC(ICOMP)/PC(ICOMP)
              END IF
15        CONTINUE
          DO 20 ICOMP=1,2
              AP=APUR(ICOMP)*PVAP(ICOMP)/(R*R*(T**2.5))
              BP=BPUR(ICOMP)*PVAP(ICOMP)/(R*T)
              COEFP(1)=-1.0
              COEFP(2)=AP-BP-BP*BP
              COEFP(3)=-AP*BP
              CALL CUBIC(IROOT,Z,COEFP)
              ZMAX=0.0
              DO 30 I=1,3
                  IF (Z(I) .GT. ZMAX) ZMAX=Z(I)
30            CONTINUE
              DO 40 I=1,3
                  IF (Z(I) .LE. 0.0) Z(I)=ZMAX
40            CONTINUE
              CALL GIBPUR(Z,ICOMP,PVAP,ZCAP)
              V=ZCAP*R*T/PVAP(ICOMP)
```

```
                 T1=ZCAP-1.0
                 T2=LOG(ZCAP)
                 T3=LOG(V/(V-BPUR(ICOMP)))
                 T4=APUR(ICOMP)/(BPUR(ICOMP)*R*(T**1.5))
               T4=T4*LOG((V+BPUR(ICOMP))/V)
                 FPURE(ICOMP)=T1-T2+T3-T4
                 FPURE(ICOMP)=EXP(FPURE(ICOMP))
               FINT=VL(ICOMP)*(P-PVAP(ICOMP))/(R*T)
               FINT=EXP(FINT)
               FPURE(ICOMP)=PVAP(ICOMP)*FPURE(ICOMP)*FINT
                 VPCM3(ICOMP)=(ZCAP*R*T*1000)/PVAP(ICOMP)
20           CONTINUE
             PRINT 2,(VPCM3(I),I=1,2),(FPURE(I),I=1,2),(PVAP(I),I=1,2)
     +       ,(VL(I),I=1,2)
2            FORMAT(1X,'VPCM3:',2(E10.3,2X)/1X,'FPURE:',2(E10.3,2X)/
     +       1X,'PVAP:',2(E10.3,2X)/1X,'VL(M3/KMOLE):',2(E10.3,2X))
             RETURN
             END
C****************************************************************
C                                                              *
C     Subroutine GIBPUR calculates the Gibbs free energy for all *
C     three numerical roots of the cubic EOS.                  *
C****************************************************************
             SUBROUTINE GIBPUR(Z,ICOMP,PVAP,ZCAP)
             DOUBLE PRECISION Z,GP,ZCAP,T1,T2,T3,T4,APUR,BPUR
     +       ,ACRS(2,2),BCRS(2,2),ALPHG,FPURE(2),ALF,BETA,T,
     +       P,R,ERROR,PVAP(2)
             COMMON /INPT/T,P,R,ERROR
             COMMON /MIX/APUR(2),BPUR(2),ACRS,BCRS,ALPHG,FPURE,ALF,BETA
             DIMENSION Z(3),GP(3)
             DO 20 IRT=1,3
               V=Z(IRT)*R*T/PVAP(ICOMP)
                 T1=Z(IRT)-1.0
                 T2=LOG(Z(IRT))
                 T3=LOG(V/(V-BPUR(ICOMP)))
                 T4=APUR(ICOMP)/(BPUR(ICOMP)*R*(T**1.5))
                 T4=T4*LOG((V+BPUR(ICOMP))/V)
                 GP(IRT)=T1-T2+T3-T4
20           CONTINUE
             ZCAP=Z(1)
             IF (GP(2) .LT. GP(1) .AND. GP(2) .LT. GP(3)) ZCAP=Z(2)
             IF (GP(3) .LT. GP(1) .AND. GP(3) .LT. GP(2)) ZCAP=Z(3)
             RETURN
           END
C****************************************************************
C                                                              *
C     Subroutine SUCESS drives the successive substitution     *
C     iteration.  Equilibrium ratios (K's) are defined.        *
C     Fugacities are calculated in FUGCOF.  The K's are varied  *
C     and the new values of mole fraction are calculated in     *
C     NEWKAY.  The successive substitution terminates when the  *
C     convergence criterion is satisfied or the number of       *
C     iterations exceeds the limit.                            *
C****************************************************************
             SUBROUTINE SUCESS(XMOL,ICOUNT,SUM)
             DOUBLE PRECISION TC,PC,OMEG,T,P,R,ERROR,APUR,BPUR,
     +       GIBN,GIBO,VOM,ALPHA,SUM,FUGA,VC,ALPHG,FPURE(2),
     +       ALF,BETA,VCM3,ACRS(2,2),XMOL,BCRS(2,2)

             COMMON /PURE/TC(2),PC(2),OMEG(2),VC(2)
```

```
          COMMON /INPT/T,P,R,ERROR
          COMMON /MIX/APUR(2),BPUR(2),ACRS,BCRS,ALPHG,FPURE,ALF,BETA
          COMMON /KAY/GIBN(2),GIBO(2),VOM(2),ALPHA
          COMMON /VOLUME/VCM3(2),FUGA(2,2)
          DIMENSION XMOL(2,2)
          ALPHA=1.0
          ICOUNT=1
          DO 10 KA=1,2
          GIBN(KA)=0.0
10        CONTINUE
          DO 20 ICOMP=1,2
          VOM(ICOMP)=XMOL(2,ICOMP)/XMOL(1,ICOMP)
20        CONTINUE
30        CONTINUE
          CALL FUGCOF(XMOL,FUGA,VCM3)
          CALL NEWKAY(FUGA,XMOL,SUM,ICOUNT)
          IF (SUM .LT. ERROR) GO TO 50
          IF (ICOUNT .GT. 500) GO TO 40
          ICOUNT=ICOUNT+1
          GO TO 30
40        CONTINUE
          WRITE(*,1000)
50        CONTINUE
          RETURN
1000      FORMAT(/,'****  ITERATIONS EXCEEDED LIMIT  ****')
          END
C****************************************************************
C                                                              *
C     Subroutine FUGCOF calculates fugacities for a given set of *
C     mole fractions.                                           *
C****************************************************************
          SUBROUTINE FUGCOF(XMOL,FUGA,VCM3)
          DOUBLE PRECISION T,P,R,ERROR,APUR,BPUR,ACRS(2,2)
     +    ,AMIX,BMIX,FUGA,VCM3,ACAP,BCAP,ZMAX,ZCAP,T1,T2,T3,T4,
     +    ALPHG,SUMA,SUMB,V,SUM3,SUM4,T5,T6,XMOL,Z,COEF,XGIB
     +    ,FPURE(2),ALF,BETA,G1,G2,G3,GAMA(2)
     +    ,BCRS(2,2)
          COMMON /INPT/T,P,R,ERROR
          COMMON /MIX/APUR(2),BPUR(2),ACRS,BCRS,ALPHG,FPURE,ALF,BETA
c         COMMON /VOLUME/VCM3(2)
          DIMENSION XMOL(2,2),FUGA(2,2),Z(3),COEF(3),XGIB(2),VCM3(2)

          DO 35 IPHAS=1,2
           G1=ALF/BETA
           G2=XMOL(IPHAS,1)/XMOL(IPHAS,2)
           G3=(1.0+G1*G2)**2
           GAMA(1)=EXP(ALF/G3)
             G1=BETA/ALF
             G2=XMOL(IPHAS,2)/XMOL(IPHAS,1)
             G3=(1.0+G1*G2)**2
             GAMA(2)=EXP(BETA/G3)
             DO 45 ICOMP=1,2
                 FUGA(IPHAS,ICOMP)=XMOL(IPHAS,ICOMP)*GAMA(ICOMP)*
     +           FPURE(ICOMP)
45           CONTINUE
35        CONTINUE
          RETURN
          END
```

```
C*******************************************************************
C                                                                  *
C     Subroutine NEWKAY adjusts the K's based on an accelerated    *
C     step size using the fugacities.  The mole fractions are      *
C     computed from these new K's.  If the mole fractions are      *
C     greater than 1.00 or less than 0.00, their values are reset  *
C     to 0.99 or 0.01 respectively.                                *
C                                                                  *
*                                                                  *
C*******************************************************************
      SUBROUTINE NEWKAY(FUGA,XMOL,SUM,ICOUNT)
      DOUBLE PRECISION T,P,R,ERROR,XMOL,GIBO,VOM,ALPHA
     +  ,FUGA,SUM,GIBN,DDEN,DNUM,GIBM,CHECK,VM21
      COMMON /KAY/GIBN(2),GIBO(2),VOM(2),ALPHA
      COMMON /INPT/T,P,R,ERROR
      DIMENSION FUGA(2,2),XMOL(2,2)
      DO 10 MA=1,2

      GIBO(MA)=GIBN(MA)
      GIBN(MA)=LOG(FUGA(2,MA)/FUGA(1,MA))
10    CONTINUE
      SUM=0.0
      DO 20 MG=1,2
      SUM=SUM+(GIBN(MG)*GIBN(MG))
20    CONTINUE
      IF (SUM .LT. ERROR) GO TO 90
      IF (ICOUNT .LE. 2) GO TO 40
      GIBM=ABS(GIBN(1))
      DDEN=0.0
      DNUM=0.0
      DO 30 MC=1,2
      IF (ABS(GIBN(MC)) .GT. GIBM) GIBM=ABS(GIBN(MC))
      DNUM=DNUM+(GIBO(MC)*GIBO(MC))
      DDEN=DDEN+(GIBO(MC)*(GIBN(MC)-GIBO(MC)))
30    CONTINUE
      ALPHA=ALPHA*ABS(DNUM/DDEN)
      CHECK=GIBM*ALPHA
      IF (CHECK .GT. 6.0) ALPHA=6.0/GIBM
40    CONTINUE
      DO 50 MD=1,2
      VOM(MD)=VOM(MD)*((FUGA(1,MD)/FUGA(2,MD))**ALPHA)
50    CONTINUE
      VM21=VOM(2)-VOM(1)
      XMOL(1,1)=(VOM(2)-1.0)/VM21
      XMOL(2,1)=XMOL(1,1)*VOM(1)
      XMOL(1,2)=1.0-XMOL(1,1)
      XMOL(2,2)=1.0-XMOL(2,1)

      DO 80 I57=1,2
      DO 70 I55=1,2
      IF (XMOL(I55,I57) .GE. 1.0) XMOL(I55,I57)=0.99
      IF (XMOL(I55,I57) .LE. 0.0) XMOL(I55,I57)=0.01
70    CONTINUE
80    CONTINUE
90    CONTINUE
      RETURN
      END
```

```
C***************************************************************
C                                                             *
C       Subroutine POWELL uses Powell's method to minimize the *
C       function "func".                                       *
C***************************************************************
        SUBROUTINE POWELL(p,xi,n,np,ftol,iter,fret)
        DOUBLE PRECISION p(np),xi(np,np),ftol,fret,pt(20),del,xit(20)
     +,fptt,ptt(20),fp,t

        INTEGER iter,n,np,NMAX,ITMAX
        EXTERNAL func
        PARAMETER (NMAX=20,ITMAX=200)
C   USES func,linmin
        INTEGER i,ibig,j
        fret=func(p)
        do 11 j=1,n
          pt(j)=p(j)
11      continue
        iter=0
1       iter=iter+1
        fp=fret
        ibig=0
        del=0.
        do 13 i=1,n
          do 12 j=1,n
            xit(j)=xi(j,i)
12        continue
          fptt=fret
          call linmin(p,xit,n,fret)
          if(abs(fptt-fret).gt.del)then
            del=abs(fptt-fret)
            ibig=i
          endif
13      continue
        if(2.*abs(fp-fret).le.ftol*(abs(fp)+abs(fret))) return
c        IF(fret.LE.0.1) RETURN
        if(iter.eq.ITMAX) then
        pause 'powell exceeding maximum iterations'
        print 16,fret
16      format(1x,'fret=func=',e10.3)
        end if
        do 14 j=1,n
          ptt(j)=2.*p(j)-pt(j)
          xit(j)=p(j)-pt(j)
          pt(j)=p(j)
14      continue
        fptt=func(ptt)
        if(fptt.ge.fp)goto 1
        t=2.*(fp-2.*fret+fptt)*(fp-fret-del)**2-del*(fp-fptt)**2
        if(t.ge.0.)goto 1
        call linmin(p,xit,n,fret)
        do 15 j=1,n
          xi(j,ibig)=xi(j,n)
          xi(j,n)=xit(j)
15      continue
        goto 1
        RETURN
        END
```

```
C*****************************************************************
C                                                               *
C     Subroutine linmin is used in subroutine powell.           *
C*****************************************************************
      SUBROUTINE linmin(p,xi,n,fret)
      DOUBLE PRECISION p(n),xi(n),TOL,f1dim,fret,ax,bx,fa,fb,fx,xmin,xx,
     +pcom(50),xicom(50),brent

      INTEGER n,NMAX
      PARAMETER (NMAX=50,TOL=1.e-4)
C     USES brent,f1dim,mnbrak
      INTEGER j,ncom
      COMMON /f1com/ pcom,xicom,ncom
      EXTERNAL f1dim
      ncom=n
      do 11 j=1,n
        pcom(j)=p(j)
        xicom(j)=xi(j)
11    continue
      ax=0.
c      xx=1.
       xx=0.05
      call mnbrak(ax,xx,bx,fa,fx,fb,f1dim)
      fret=brent(ax,xx,bx,f1dim,TOL,xmin)
      do 12 j=1,n
        xi(j)=xmin*xi(j)
        p(j)=p(j)+xi(j)
12    continue
      return
      END
C*****************************************************************
C                                                               *
C     Subroutine mnbrak is used in subroutine linmin.           *
C*****************************************************************
      SUBROUTINE mnbrak(ax,bx,cx,fa,fb,fc,func)
      DOUBLE PRECISION ax,bx,cx,fa,fb,fc,func,GOLD,GLIMIT,TINY,dum,fu,
     + q,r,u,ulim

      EXTERNAL func
      PARAMETER (GOLD=1.618034, GLIMIT=100., TINY=1.e-20)
      fa=func(ax)
      fb=func(bx)
      if(fb.gt.fa)then
        dum=ax
        ax=bx
        bx=dum
        dum=fb
        fb=fa
        fa=dum
      endif
      cx=bx+GOLD*(bx-ax)
      fc=func(cx)
1     if(fb.ge.fc)then
        r=(bx-ax)*(fb-fc)
        q=(bx-cx)*(fb-fa)
        u=bx-((bx-cx)*q-(bx-ax)*r)/(2.*sign(max(abs(q-r),TINY),q-r))
        ulim=bx+GLIMIT*(cx-bx)
        if((bx-u)*(u-cx).gt.0.)then
          fu=func(u)
          if(fu.lt.fc)then
```

```
          ax=bx
          fa=fb
          bx=u
          fb=fu
          return
        else if(fu.gt.fb)then
          cx=u
          fc=fu
          return
        endif
        u=cx+GOLD*(cx-bx)
        fu=func(u)
      else if((cx-u)*(u-ulim).gt.0.)then
        fu=func(u)
        if(fu.lt.fc)then
          bx=cx
          cx=u
          u=cx+GOLD*(cx-bx)
          fb=fc
          fc=fu
          fu=func(u)
        endif
      else if((u-ulim)*(ulim-cx).ge.0.)then
        u=ulim
        fu=func(u)
      else
        u=cx+GOLD*(cx-bx)
        fu=func(u)
      endif
      ax=bx
      bx=cx
      cx=u
      fa=fb
      fb=fc
      fc=fu
      goto 1
    endif
    return
    END
C****************************************************************
C                                                               *
C     Function brent is used in subroutine linmin.              *
C****************************************************************
      FUNCTION brent(ax,bx,cx,f,tol,xmin)
      DOUBLE PRECISION tol,f,ax,bx,xmin,cx,a,b,d,e,etemp,fu,fv,fw,fx,p
     +,q,r,tol1,tol2,u,v,w,x,xm,brent,CGOLD,ZEPS

      INTEGER ITMAX
      EXTERNAL f
      PARAMETER (ITMAX=100,CGOLD=.3819660,ZEPS=1.0e-10)
      INTEGER iter
      a=min(ax,cx)
      b=max(ax,cx)
      v=bx
      w=v
      x=v
      e=0.
      fx=f(x)
      fv=fx
      fw=fx
```

```
      do 11 iter=1,ITMAX
        xm=0.5*(a+b)
        tol1=tol*abs(x)+ZEPS
        tol2=2.*tol1
        if(abs(x-xm).le.(tol2-.5*(b-a))) goto 3
        if(abs(e).gt.tol1) then
          r=(x-w)*(fx-fv)
          q=(x-v)*(fx-fw)
          p=(x-v)*q-(x-w)*r
          q=2.*(q-r)
          if(q.gt.0.) p=-p
          q=abs(q)
          etemp=e
          e=d
          if(abs(p).ge.abs(.5*q*etemp).or.p.le.q*(a-x).or.p.ge.q*(b-x))
     *goto 1
          d=p/q
          u=x+d
          if(u-a.lt.tol2 .or. b-u.lt.tol2) d=sign(tol1,xm-x)
          goto 2
        endif
1       if(x.ge.xm) then
          e=a-x
        else
          e=b-x
        endif
        d=CGOLD*e
2       if(abs(d).ge.tol1) then
          u=x+d
        else
          u=x+sign(tol1,d)
        endif
        fu=f(u)
        if(fu.le.fx) then
          if(u.ge.x) then
            a=x
          else
            b=x
          endif
          v=w
          fv=fw
          w=x
          fw=fx
          x=u
          fx=fu
        else
          if(u.lt.x) then
            a=u
          else
            b=u
          endif
          if(fu.le.fw .or. w.eq.x) then
            v=w
            fv=fw
            w=u
            fw=fu
          else if(fu.le.fv .or. v.eq.x .or. v.eq.w) then
            v=u
            fv=fu
          endif
```

```
         endif
11       continue
         pause 'brent exceed maximum iterations'
3        xmin=x
         brent=fx
         return
         END
C********************************************************************
C                                                                  *
C       Function f1dim is used in subroutine linmin.               *
C********************************************************************
         FUNCTION f1dim(x)
         DOUBLE PRECISION x,f1dim,xt(50),pcom(50),xicom(50)

         INTEGER NMAX
         PARAMETER (NMAX=50)
C     USES func
         INTEGER j,ncom
         COMMON /f1com/ pcom,xicom,ncom
         do 11 j=1,ncom
           xt(j)=pcom(j)+x*xicom(j)
11       continue
         f1dim=func(xt)
         return
         END
C******************         END OF PROGRAM        *************
```

```
C********************************************************************
C                                                                  *
C                          PREOSVLL.FOR                            *
C_____ *
C                                                                  *
C     This program calculates phase compositions of three-phase    *
C     equilibrium in a ternary mixture at a specified temperature  *
C     and pressure.  Peng-Robinson equation of state is used and   *
C     the binary interaction parameters of the equation of state   *
C     are fitted to data.  Critical temperature of the third       *
C     component is also fitted.  The successive substitution       *
C     algorithm discussed by Heidemann is used to converge to a    *
C     solution representing a local minimum in the Gibbs free      *
C     energy.  An initial guess of mole fractions for the three    *
C     phases is required to initiate the calculations.             *
C                                                                  *
C                                                                  *
C     The elements of all 3x3 arrays except DELT are defined as:   *
C                                                                  *
C                                                                  *
C            G(CO2)          G(Acetone)          G(TCMTB)          *
C            L2(CO2)         L2(Acetone)         L2(TCMTB)         *
C            L1(CO2)         L1(Acetone)         L1(TCMTB)         *
C********************************************************************
        DOUBLE PRECISION FNAM,FDAT,FHOL,TC,PC,OMEG,T,P,R,ERROR,APUR(3)
     +  ,BPUR(3),ACRS(3,3),FSTX,CALX,SUM,SQRS,EXPX,DELT,XP,xi(7,7),TO,PO,
     +  DCA,DCW,DAW,FTOL,FRET,PS,VCM3,TC3,PC3,OMEG3,D12,D13,D23,D21,D31,
     +  D32
        COMMON /PURE/TC(3),PC(3),OMEG(3)
        COMMON / INPT/T,P,R,ERROR
        COMMON / MIX/APUR,BPUR,ACRS,DELT
C        COMMON / COMP/FSTX(3,9),CALX(3,9),ICOUNT,SUM,SQRS,K1,PS(3)
        COMMON / COMP/FSTX(3,3),CALX(3,3),ICOUNT,SUM,SQRS,K1,PS(3)
        COMMON /VOLUME/VCM3(3)
        DIMENSION EXPX(3,3),DELT(3,3),XP(7)
        INTEGER NDIM,K1,K2,ILOW,IUP,N
        PARAMETER(NDIM=7,FTOL=1.0E-6)
        INTEGER i,iter,np
        OPEN(UNIT=74,FILE='pr7gctam.out')
        N=3
        np=NDIM
        DO 33 I=1,NDIM
          DO 34 J=1,NDIM
            xi(I,J)=0.0
34        CONTINUE
33      CONTINUE
        DO 37 I=1,NDIM
          xi(I,I)=1.0
37      CONTINUE

        CALL DEFDAT
        K1=1
C        K1=3
C        OPEN(UNIT=24,FILE='fhol111')
        OPEN(UNIT=24,FILE='fholcta2')
C        OPEN(UNIT=24,FILE='fholc41')
C        OPEN(UNIT=24,FILE='fholc82')
        READ(24,*) TO,PS(1)
        DO 202 IPHAS=1,3
        READ(24,*) (FSTX(IPHAS,ICOMP),ICOMP=1,3)
```

```
202     CONTINUE
        CLOSE(UNIT=24,STATUS='KEEP')

c       OPEN(UNIT=34,FILE='fhol122b')
c       OPEN(UNIT=34,FILE='fholc43')
c       OPEN(UNIT=34,FILE='fholc83')
c       READ(34,*) TO,PS(2)
c       DO 302 IPHAS=1,3
c       READ(34,*) (FSTX(IPHAS,ICOMP),ICOMP=4,6)
c302     CONTINUE
c       CLOSE(UNIT=34,STATUS='KEEP')

c       OPEN(UNIT=44,FILE='fhol117')
C       OPEN(UNIT=44,FILE='fholc43')
c       OPEN(UNIT=44,FILE='fholc83')
c       READ(44,*) TO,PS(3)
c       DO 402 IPHAS=1,3
c       READ(44,*) (FSTX(IPHAS,ICOMP),ICOMP=7,9)
c402     CONTINUE
c       CLOSE(UNIT=44,STATUS='KEEP')

        WRITE(*,1000)
c1000    FORMAT(' INPUT D12, D13, AND D23: ')
1000    FORMAT(' INPUT D12, D13, D23, D21, D31, AND D32: ')
c       READ(*,*) D12,D13,D23
        READ(*,*) D12,D13,D23,D21,D31,D32
        XP(1)=D12
        XP(2)=D13
        XP(3)=D23
        XP(4)=D21
        XP(5)=D31
        XP(6)=D32

        WRITE(*,1004)
1004    FORMAT(' INPUT TC(3): ')
c1004    FORMAT(' INPUT OMEG(3): ')
C1004    FORMAT(' INPUT OMEG(3), TC(3), and PC(3): ')
        READ(*,*) TC3
C       XP(4)=OMEG3
        XP(7)=TC3
c       XP(8)=PC3
c       XP(9)=OMEG3

        PRINT 15,FUNC(XP),(xp(i),i=1,7)
 15     FORMAT(1X,'FUNCtry=SQRS=FOBJ=',E10.3,'deltas=',7(3x,f7.3))

        call POWELL(XP,xi,NDIM,np,FTOL,iter,fret)
        write(74,'(/1x,a,i3)') 'Iterations:',iter
        write(74,'(/1x,a/1x,7f12.6)') 'Minimum found at: ',
      1(XP(i),i=1,NDIM)
        write(74,'(/1x,a,f12.6)') 'Minimum function value =',fret

        DO 17 K2=1,K1
           ILOW=N*K2-N+1
           IUP=N*K2
           WRITE(74,1005) T,PS(K2)
           WRITE(74,1010)
           WRITE(74,1025)
           WRITE(74,1030) (FSTX(1,ICOMP),ICOMP=ILOW,IUP),(CALX(1,ICOMP),
      1    ICOMP=ILOW,IUP)
```

```
              WRITE(74,1040) (FSTX(2,ICOMP),ICOMP=ILOW,IUP),(CALX(2,ICOMP),
     1        ICOMP=ILOW,IUP)
              WRITE(74,1050) (FSTX(3,ICOMP),ICOMP=ILOW,IUP),(CALX(3,ICOMP),
     1        ICOMP=ILOW,IUP)
17       CONTINUE
         WRITE(74,1060) ICOUNT
         WRITE(74,1070) SUM
         WRITE(74,1080) SQRS
       WRITE(74,1090) (VCM3(IPHAS),IPHAS=1,3)
1005     FORMAT(/,15X,'  TEMPERATURE = ',F5.1,'  PRESSURE = ',F6.1)
c1010     FORMAT(/' PHASE IX(CO2) IX(TCMTB) IX(ALC)  FX(CO2) FX(TCMTB)
c    1 FX(ALC)')
1010  FORMAT(/' PHASE IX(CO2) IX(Acetone) IX(TCMTB)  FX(CO2) FX(Acetone)
     1 FX(TCMTB)')
1025     FORMAT(/,2('************************'))
1030     FORMAT(/,'  LIGHT   ',3(F6.3,3X),6X,3(F6.3,3X))
1040     FORMAT('  MIDDLE   ',3(F6.3,3X),6X,3(F6.3,3X))
1050     FORMAT('  HEAVY   ',3(F6.3,3X),6X,3(F6.3,3X))
1060     FORMAT(/,15X,'  THE NUMBER OF ITERATION WAS:    ',I3)
1070     FORMAT(15X,'  THE SUM OF THE SQUARES WAS:  ',E15.5)
1080     FORMAT(15X,'  THE SUM OF THE MOLE FRACTION SQUARES WAS: ',E15.5)
1090  FORMAT(5X,'MOLAR VOLUMES (CM3/MOLE)'/5X,' TOP(G)  MIDDLE(L2)
     1  LOW(L1)
     1  '/5X,3(F8.2,3X))
         STOP
         END
C**********************************************************************
         REAL FUNCTION FUNC(XP)
         DOUBLE PRECISION TC,PC,OMEG,T,P,R,ERROR,APUR(3),BPUR(3),ACRS(3,3)
     +  ,FSTX,CALX,SUM,SQRS,EXPX(3,3),DELT(3,3),XP(7),xi,TO,PO,DCA,DCW,
     +  DAW,FTOL,FRET,F(27),PS
         COMMON /PURE/TC(3),PC(3),OMEG(3)
         COMMON / INPT/T,P,R,ERROR
         COMMON / MIX/APUR,BPUR,ACRS,DELT
c         COMMON / COMP/FSTX(3,9),CALX(3,9),ICOUNT,SUM,SQRS,K1,PS(3)
         COMMON / COMP/FSTX(3,3),CALX(3,3),ICOUNT,SUM,SQRS,K1,PS(3)
         INTEGER N
         N=3
         DELT(1,2)=XP(1)
         DELT(1,3)=XP(2)
         DELT(2,3)=XP(3)
c         DELT(2,1)=DELT(1,2)
c         DELT(3,1)=DELT(1,3)
c         DELT(3,2)=DELT(2,3)
         DELT(2,1)=XP(4)
         DELT(3,1)=XP(5)
         DELT(3,2)=XP(6)
         DELT(1,1)=0.0
         DELT(2,2)=0.0
         DELT(3,3)=0.0
C         OMEG(3)=XP(4)
         TC(3)=XP(7)
c         PC(3)=XP(7)
c         OMEG(3)=XP(7)
         CALL PARAM
C         DO 30 JB=1,3
C            DO 20 JC=1,3
C                ACRS(JB,JC)=(1.0-DELT(JB,JC))*SQRT(APUR(JB)*APUR(JC))
C20          CONTINUE
C30       CONTINUE
```

```
            KK=0
            DO 301 K2=1,K1
               P=PS(K2)
               DO 201 IPHAS=1,3
                  JJ=0
                  DO 101 JCOMP=N*K2-N+1,N*K2
                     JJ=1+JJ
                     EXPX(IPHAS,JJ)=FSTX(IPHAS,JCOMP)
101               CONTINUE
201            CONTINUE
               CALL SUCESS(EXPX,ICOUNT,SUM)
               DO 211 IPHAS=1,3
                  JJ=0
                  DO 111 JCOMP=N*K2-N+1,N*K2
                     JJ=1+JJ
                     CALX(IPHAS,JCOMP)=EXPX(IPHAS,JJ)
111               CONTINUE
211            CONTINUE

               DO 24 J=1,N
                  DO 25 I=N*K2-N+1,N*K2
                     KK=KK+1
                     F(KK)=ABS((FSTX(J,I)-CALX(J,I))/(FSTX(J,I)+CALX(J,I)))
25                CONTINUE
24             CONTINUE
301         CONTINUE
            SQRS=0.0
            DO 35 L=1,9*K1
               SQRS=SQRS+(F(L)*F(L))
35          CONTINUE
            FUNC=SQRS
            RETURN
            END
C**********************************************************************
C                                                                    *
C     Subroutine DEFDAT asks for a datafile containing the           *
C     critical temperature, critical pressure, acentric factor,      *
C     and gas constant for the three pure components.  A             *
C     convergence criterion is also inputed.                         *
C**********************************************************************
            SUBROUTINE DEFDAT
            DOUBLE PRECISION FDAT,TC,PC,OMEG,VC(3),T,P,R,ERROR
            COMMON /PURE/TC(3),PC(3),OMEG(3)
            COMMON /INPT/T,P,R,ERROR
C           OPEN(UNIT=25,FILE='FDAT')
            OPEN(UNIT=25,FILE='FDATCTA')
C           OPEN(UNIT=25,FILE='FDATC4')
C           OPEN(UNIT=25,FILE='FDATC8')
            READ(25,*) R
            READ(25,*) TC(1),TC(2),TC(3)
            READ(25,*) PC(1),PC(2),PC(3)
            READ(25,*) OMEG(1),OMEG(2),OMEG(3)
            READ(25,*) VC(1),VC(2),VC(3)
            CLOSE(UNIT=25,STATUS='KEEP')
            WRITE(*,1020)
            READ*, ERROR
            RETURN
1020        FORMAT('  INPUT THE ERROR CRITERION:   '$)
            END
```

```
C******************************************************************
C                                                                *
C      Subroutine PARAM calculates the pure component and mixture *
C      parameters needed by the Peng-Robinson EOS.               *
C******************************************************************
       SUBROUTINE PARAM
       DOUBLE PRECISION TC,PC,OMEG,T,P,R,ERROR,APUR,BPUR,ACRS,XKAP
     + ,ALPH,APCT,APUR2,CT,DELT
       COMMON /PURE/TC(3),PC(3),OMEG(3)
       COMMON /INPT/T,P,R,ERROR
       COMMON /MIX/APUR(3),BPUR(3),ACRS(3,3),DELT
       DIMENSION ALPH(3),APCT(3),XKAP(3),DELT(3,3),APUR2(3)
       DO 10 JA=1,3
       XKAP(JA)= 0.37464+1.54226*OMEG(JA)-0.26992*OMEG(JA)*OMEG(JA)
       ALPH(JA)= 1.0+XKAP(JA)*(1.0-SQRT(T/TC(JA)))
       APCT(JA)=0.45724*R*R*TC(JA)*TC(JA)/PC(JA)
c      APUR2(JA)= APCT(JA)*ALPH(JA)*ALPH(JA)
       APUR(JA)= APCT(JA)*ALPH(JA)*ALPH(JA)
       BPUR(JA)=0.07780*R*TC(JA)/PC(JA)
10     CONTINUE
       CT=T-273.15
c      APUR(1)=((19.913*CT*CT)-(0.96975E+04*CT)+(4.2103E+06))*1E-6
c      APUR(2)=((70.999*CT*CT)-(7.72160E+04*CT)+(30.708E+06))*1E-6
C*EOH  APUR(2)=((35.925*CT*CT)-(5.29640E+04*CT)+(23.325E+06))*1E-6
c      APUR(3)=((7.5489*CT*CT)-(1.33520E+04*CT)+(9.8927E+06))*1E-6
       RETURN
       END
C******************************************************************
C                                                                *
C      Subroutine SUCESS drives the successive substitution      *
C      iteration.  Equilibrium ratios (K's) are defined.         *
C      Fugacities are calculated in FUGCOF.  The K's are varied  *
C      and the new values of mole fraction are calculated in     *
C      NEWKAY.  The successive substitution terminates when the  *
C      convergence criterion is satisfied or the number of       *
C      iterations exceeds the limit.                             *
C******************************************************************
       SUBROUTINE SUCESS(XMOL,ICOUNT,SUM)
       DOUBLE PRECISION TC,PC,OMEG,T,P,R,ERROR,APUR,BPUR,ACRS,XMOL,
     + GIBN,GIBO,VOL,VOM,ALPHA,SUM,FUGA,DELT
       COMMON /PURE/TC(3),PC(3),OMEG(3)
       COMMON /INPT/T,P,R,ERROR
       COMMON /MIX/APUR(3),BPUR(3),ACRS(3,3),DELT(3,3)
       COMMON /KAY/GIBN(6),GIBO(6),VOL(3),VOM(3),ALPHA
C      COMMON /VOLUME/VCM3(3)
       DIMENSION XMOL(3,3),FUGA(3,3)
       ALPHA=1.0
       ICOUNT=1
       DO 10 KA=1,3
       KB=KA+3
       GIBN(KA)=0.0
       GIBN(KB)=0.0
10     CONTINUE
       DO 20 ICOMP=1,3
       VOL(ICOMP)=XMOL(3,ICOMP)/XMOL(1,ICOMP)
       VOM(ICOMP)=XMOL(2,ICOMP)/XMOL(1,ICOMP)
20     CONTINUE
30     CONTINUE
       CALL FUGCOF(XMOL,FUGA)
       CALL NEWKAY(FUGA,XMOL,SUM,ICOUNT)
```

```
          IF (SUM .LT. ERROR) GO TO 50
c         IF (ICOUNT .GT. 500) GO TO 40
      IF (ICOUNT .GT. 1000) GO TO 40
          ICOUNT=ICOUNT+1
          GO TO 30
40        CONTINUE
          WRITE(*,1000)
50        CONTINUE
          RETURN
1000      FORMAT(/,'****  ITERATIONS EXCEEDED LIMIT  ****')
          END
C*******************************************************************
C                                                                 *
C     Subroutine FUGCOF calculates fugacities for a given set of  *
C     mole fractions.                                             *
C*******************************************************************
          SUBROUTINE FUGCOF(XMOL,FUGA)
          DOUBLE PRECISION T,P,R,ERROR,APUR,BPUR,ACRS,XMOL,Z,COEF,XGIB
     +    ,AMIX,BMIX,FUGA,VCM3,ACAP,BCAP,ZMAX,ZCAP,T1,T2,T3,T4,DELT
     +    ,T41,T42
          COMMON /INPT/T,P,R,ERROR
          COMMON /MIX/APUR(3),BPUR(3),ACRS(3,3),DELT(3,3)
          COMMON /VOLUME/VCM3(3)
          DIMENSION XMOL(3,3),FUGA(3,3),Z(3),COEF(3),XGIB(3)
          DO 80 IPHAS=1,3
          AMIX=0.0
          BMIX=0.0
          DO 20 ICOMP=1,3
          BMIX=BMIX+XMOL(IPHAS,ICOMP)*BPUR(ICOMP)
          DO 10 JCOMP=1,3
          ACRS(JCOMP,ICOMP)=(1.0-DELT(JCOMP,ICOMP)+(DELT(JCOMP,ICOMP)-
     +        DELT(ICOMP,JCOMP))*XMOL(IPHAS,JCOMP))*SQRT(APUR(JCOMP)
     +            *APUR(ICOMP))
c         ACRS(JCOMP,ICOMP)=(1.0-DELT(JCOMP,ICOMP))*SQRT(APUR(JCOMP)*
c     +        APUR(ICOMP))
          AMIX=AMIX+XMOL(IPHAS,JCOMP)*XMOL(IPHAS,ICOMP)*ACRS(JCOMP,ICOMP)
10        CONTINUE
20        CONTINUE
          ACAP=AMIX*P/(T*T*R*R)
          BCAP=BMIX*P/(R*T)
          COEF(1)=BCAP-1.0
          COEF(2)=(ACAP-3.0*BCAP*BCAP-2.0*BCAP)
          COEF(3)=(BCAP**3.0+BCAP*BCAP-ACAP*BCAP)
          CALL CUBIC(IROOT,Z,COEF)
          ZMAX=0.0
          DO 30 I=1,3
          IF (Z(I) .GT. ZMAX) ZMAX=Z(I)
30        CONTINUE
          DO 40 I=1,3
          IF (Z(I) .LE. 0.0) Z(I)=ZMAX
40        CONTINUE
          DO 50 III=1,3
          XGIB(III)=XMOL(IPHAS,III)
50        CONTINUE
          CALL GIBENG(Z,XGIB,AMIX,BMIX,ZCAP)
          DO 70 ICOMP=1,3
          T1=BPUR(ICOMP)*(ZCAP-1.0)/BMIX
          T2=LOG(ZCAP-BCAP)
          T3=LOG((ZCAP+2.414*BCAP)/(ZCAP-0.414*BCAP))
          T3=T3*ACAP/(2.0*SQRT(2.0)*BCAP)
```

```
            T4=0.0
            T41=0.0
            T42=0.0
   c         DO 60 LB=1,3
   c         T4=T4+XMOL(IPHAS,LB)*ACRS(LB,ICOMP)
   c60       CONTINUE
   c         T4=(T4*2.0/AMIX)-(BPUR(ICOMP)/BMIX)
            DO 60 J=1,3
            T4=T4+XMOL(IPHAS,J)*(ACRS(J,ICOMP)+ACRS(ICOMP,J))
            T42=T42+XMOL(IPHAS,J)*(DELT(ICOMP,J)-DELT(J,ICOMP))*SQRT(
        1         APUR(ICOMP)*APUR(J))
            DO 61 K=1,3
            T41=T41+XMOL(IPHAS,J)*XMOL(IPHAS,J)*XMOL(IPHAS,K)*(DELT(J,K)-
        1       DELT(K,J))*SQRT(APUR(J)*APUR(K))
   61       CONTINUE
   60       CONTINUE
            T4=((T4-T41+XMOL(IPHAS,ICOMP)*T42)/AMIX)-BPUR(ICOMP)/BMIX
            T3=T3*T4
            FUGA(IPHAS,ICOMP)=T1-T2-T3
            FUGA(IPHAS,ICOMP)=EXP(FUGA(IPHAS,ICOMP))
            FUGA(IPHAS,ICOMP)=XMOL(IPHAS,ICOMP)*FUGA(IPHAS,ICOMP)
   70       CONTINUE
            VCM3(IPHAS)=(ZCAP*R*T*1000)/P
   80       CONTINUE
            RETURN
            END
C*****************************************************************
C                                                               *
C     Subroutine GIBENG calculates the Gibbs free energy for all *
C     three numerical roots of the cubic EOS.                   *
C*****************************************************************
            SUBROUTINE GIBENG(Z,XMOL,AMIX,BMIX,ZCAP)
            DOUBLE PRECISION T,P,R,ERROR,XMOL,Z,G
        +   ,AMIX,BMIX,ZCAP,T1,T2,TSUM
            COMMON /INPT/T,P,R,ERROR
            DIMENSION Z(3),XMOL(3),G(3)
            DO 20 IRT=1,3
            T1=ABS((Z(IRT)-0.414214*BMIX)/(Z(IRT)+2.414214*BMIX))
            T1=(AMIX/(2.0*SQRT(2.0)*BMIX))*LOG(T1)
   C         T2=ABS((Z(IRT)-BMIX)/BMIX)
            T2=ABS(Z(IRT)-BMIX)
            T2=LOG(T2)
            TSUM=0.0
   C         DO 10 ICP=1,3
   C         TSUM=TSUM+(XMOL(ICP)*LOG(Z(IRT)/(XMOL(ICP)*P)))
   C10       CONTINUE
            G(IRT)=T1-T2-TSUM+Z(IRT)
   20       CONTINUE
            ZCAP=Z(1)
            IF (G(2) .LT. G(1) .AND. G(2) .LT. G(3)) ZCAP=Z(2)
            IF (G(3) .LT. G(1) .AND. G(3) .LT. G(2)) ZCAP=Z(3)
            RETURN
            END
```

```
C*****************************************************************
C                                                                *
C       Subroutine NEWKAY adjusts the K's based on an accelerated *
C       step size using the fugacities.  The mole fractions are   *
C       computed from these new K's.  If the mole fractions are   *
C       greater than 1.00 or less than 0.00, their values are reset *
C       to 0.99 or 0.01 respectively.                             *
C*****************************************************************
        SUBROUTINE NEWKAY(FUGA,XMOL,SUM,ICOUNT)
        DOUBLE PRECISION T,P,R,ERROR,XMOL,Z,GIBO,VOL,VOM,ALPHA
     +  ,FUGA,SUM,GIBN,DDEN,DNUM,GIBM,CHECK,VL21,VL31,VM21,VM31
        COMMON /KAY/GIBN(6),GIBO(6),VOL(3),VOM(3),ALPHA
        COMMON /INPT/T,P,R,ERROR
        DIMENSION FUGA(3,3),XMOL(3,3)
        DO 10 MA=1,3
        MB=MA+3
        GIBO(MA)=GIBN(MA)
        GIBO(MB)=GIBN(MB)
        GIBN(MA)=LOG(FUGA(3,MA)/FUGA(1,MA))
        GIBN(MB)=LOG(FUGA(2,MA)/FUGA(1,MA))
10      CONTINUE
        SUM=0.0
        DO 20 MG=1,6
        SUM=SUM+(GIBN(MG)*GIBN(MG))
20      CONTINUE
        IF (SUM .LT. ERROR) GO TO 90
        IF (ICOUNT .LE. 2) GO TO 40
        GIBM=ABS(GIBN(1))
        DDEN=0.0
        DNUM=0.0
        DO 30 MC=1,6
        IF (ABS(GIBN(MC)) .GT. GIBM) GIBM=ABS(GIBN(MC))
        DNUM=DNUM+(GIBO(MC)*GIBO(MC))
        DDEN=DDEN+(GIBO(MC)*(GIBN(MC)-GIBO(MC)))
30      CONTINUE
        ALPHA=ALPHA*ABS(DNUM/DDEN)
        CHECK=GIBM*ALPHA
        IF (CHECK .GT. 6.0) ALPHA=6.0/GIBM
40      CONTINUE
        DO 50 MD=1,3
        VOL(MD)=VOL(MD)*((FUGA(1,MD)/FUGA(3,MD))**ALPHA)
        VOM(MD)=VOM(MD)*((FUGA(1,MD)/FUGA(2,MD))**ALPHA)
50      CONTINUE
        VL21=VOL(2)-VOL(1)
        VL31=VOL(3)-VOL(1)
        VM21=VOM(2)-VOM(1)
        VM31=VOM(3)-VOM(1)
        XMOL(1,3)=(VM21*(1.0-VOL(1)))-(VL21*(1.0-VOM(1)))
        XMOL(1,3)=XMOL(1,3)/((VL31*VM21)-(VL21*VM31))
        XMOL(1,2)=((1.0-VOM(1))/VM21)-(XMOL(1,3)*VM31/VM21)
        XMOL(1,1)=1.0-XMOL(1,3)-XMOL(1,2)
        DO 60 ICOMP=1,3
        XMOL(2,ICOMP)=XMOL(1,ICOMP)*VOM(ICOMP)
        XMOL(3,ICOMP)=XMOL(1,ICOMP)*VOL(ICOMP)
60      CONTINUE
        DO 80 I57=1,3
        DO 70 I55=1,3
        IF (XMOL(I55,I57) .GE. 1.0) XMOL(I55,I57)=0.99
        IF (XMOL(I55,I57) .LE. 0.0) XMOL(I55,I57)=0.01
70      CONTINUE
```

```
80         CONTINUE
90         CONTINUE
           RETURN
           END
C*********************************************************************
C                                                                    *
C     Subroutine CUBIC determines the roots of a cubic equation      *
C     using a trigonometric algorithm.                               *
C*********************************************************************
           SUBROUTINE CUBIC(IROOT,Z,AA)
           DOUBLE PRECISION Z,AA,PI,TRD,Q,R,SUM,S1,S2,Y1,Y2,Y3,XA,XB,T11,
     +     PHI,ZZ
           DIMENSION Z(3),AA(3)
           PI=3.1415926540
           TRD=1.0/3.0
           Q=(3.0*AA(2)-AA(1)**2)/3.0
           R=(27.0*AA(3)-9.0*AA(1)*AA(2)+2.0*(AA(1)**3))/27.0
           SUM=(Q/3.0)**3+(R/2.0)**2
           IF (SUM) 90,10,20
10         IROOT=0
           S1=(-R/2.0)**TRD
           S2=S1
           Y1=S1+S2
           Y2=-Y1/2.0
           Y3=Y2
           Z(1)=Y1-AA(1)/3.0
           Z(2)=Y2-AA(1)/3.0
           Z(3)=Z(2)
           RETURN
20         IROOT=1
           XA=-R/2.0+SQRT(SUM)
           IF (XA) 30, 40, 40
30         XA=-XA
           S1=-(XA**TRD)
           GO TO 50
40         S1=XA**TRD
50         XB=-R/2.0-SQRT(SUM)
           IF (XB) 60,70,70
60         XB=-XB
           S2=-(XB**TRD)
           GO TO 80
70         S2=XB**TRD
80         CONTINUE
           Y1=S1+S2
           Z(1)=Y1-AA(1)/3.0
           Z(2)=Z(1)
           Z(3)=Z(1)
           RETURN
90         IROOT=-1
           T11=2.0*SQRT(-Q/3.0)
           PHI=((R/2.0)**2)/((Q/3.0)**3)
           ZZ=SQRT(-PHI)
           ZZ=SQRT(1.0-ZZ*ZZ)/ZZ
           IF (R) 110,100,100
100        T11=-T11
110        CONTINUE
           PHI=ATAN(ZZ)
           Z(1)=T11*COS(PHI/3.0)
           Z(2)=T11*COS((PHI+2.0*PI)/3.0)
           Z(3)=T11*COS((PHI+4.0*PI)/3.0)
```

```
          DO 120 I=1,3
120       Z(I)=Z(I)-AA(1)/3.0
130       RETURN
          END
C****************************************************************
C                                                              *
C     Subroutine POWELL uses Powell's method to minimize the   *
C     function "func".                                         *
C****************************************************************
          SUBROUTINE POWELL(p,xi,n,np,ftol,iter,fret)
          DOUBLE PRECISION p(np),xi(np,np),ftol,fret,pt(20),del,xit(20)
         +,fptt,ptt(20),fp,t

          INTEGER iter,n,np,NMAX,ITMAX
          EXTERNAL func
          PARAMETER (NMAX=20,ITMAX=200)
C     USES func,linmin
          INTEGER i,ibig,j
          fret=func(p)
          do 11 j=1,n
            pt(j)=p(j)
11        continue
          iter=0
1         iter=iter+1
          fp=fret
          ibig=0
          del=0.
          do 13 i=1,n
            do 12 j=1,n
              xit(j)=xi(j,i)
12          continue
            fptt=fret
            call linmin(p,xit,n,fret)
            if(abs(fptt-fret).gt.del)then
              del=abs(fptt-fret)
              ibig=i
            endif
13        continue
          if(2.*abs(fp-fret).le.ftol*(abs(fp)+abs(fret)))return
          if(iter.eq.ITMAX) pause 'powell exceeding maximum iterations'
          do 14 j=1,n
            ptt(j)=2.*p(j)-pt(j)
            xit(j)=p(j)-pt(j)
            pt(j)=p(j)
14        continue
          fptt=func(ptt)
          if(fptt.ge.fp)goto 1
          t=2.*(fp-2.*fret+fptt)*(fp-fret-del)**2-del*(fp-fptt)**2
          if(t.ge.0.)goto 1
          call linmin(p,xit,n,fret)
          do 15 j=1,n
            xi(j,ibig)=xi(j,n)
            xi(j,n)=xit(j)
15        continue
          goto 1
          RETURN
          END
```

```
C*********************************************************************
C                                                                    *
C      Subroutine linmin is used in subroutine powell.               *
C*********************************************************************
       SUBROUTINE linmin(p,xi,n,fret)
       DOUBLE PRECISION p(n),xi(n),TOL,f1dim,fret,ax,bx,fa,fb,fx,xmin,xx,
      +pcom(50),xicom(50),brent

       INTEGER n,NMAX
       PARAMETER (NMAX=50,TOL=1.e-4)
C      USES brent,f1dim,mnbrak
       INTEGER j,ncom
       COMMON /f1com/ pcom,xicom,ncom
       EXTERNAL f1dim
       ncom=n
       do 11 j=1,n
         pcom(j)=p(j)
         xicom(j)=xi(j)
11     continue
       ax=0.
c       xx=1.
cgood      xx=0.05
         xx=0.01
       call mnbrak(ax,xx,bx,fa,fx,fb,f1dim)
       fret=brent(ax,xx,bx,f1dim,TOL,xmin)
       do 12 j=1,n
         xi(j)=xmin*xi(j)
         p(j)=p(j)+xi(j)
12     continue
       return
       END
C*********************************************************************
C                                                                    *
C      Subroutine mnbrak is used in subroutine linmin.               *
C*********************************************************************
       SUBROUTINE mnbrak(ax,bx,cx,fa,fb,fc,func)
       DOUBLE PRECISION ax,bx,cx,fa,fb,fc,func,GOLD,DLIMIT,TINY,dum,fu,
      + q,r,u,ulim

       EXTERNAL func
       PARAMETER (GOLD=1.618034, GLIMIT=100., TINY=1.e-20)
       fa=func(ax)
       fb=func(bx)
       if(fb.gt.fa)then
         dum=ax
         ax=bx
         bx=dum
         dum=fb
         fb=fa
         fa=dum
       endif
       cx=bx+GOLD*(bx-ax)
       fc=func(cx)
1      if(fb.ge.fc)then
         r=(bx-ax)*(fb-fc)
         q=(bx-cx)*(fb-fa)
         u=bx-((bx-cx)*q-(bx-ax)*r)/(2.*sign(max(abs(q-r),TINY),q-r))
         ulim=bx+GLIMIT*(cx-bx)
         if((bx-u)*(u-cx).gt.0.)then
           fu=func(u)
```

```
         if(fu.lt.fc)then
            ax=bx
            fa=fb
            bx=u
            fb=fu
            return
         else if(fu.gt.fb)then
            cx=u
            fc=fu
            return
         endif
         u=cx+GOLD*(cx-bx)
         fu=func(u)
       else if((cx-u)*(u-ulim).gt.0.)then
         fu=func(u)
         if(fu.lt.fc)then
            bx=cx
            cx=u
            u=cx+GOLD*(cx-bx)
            fb=fc
            fc=fu
            fu=func(u)
         endif
       else if((u-ulim)*(ulim-cx).ge.0.)then
         u=ulim
         fu=func(u)
       else
         u=cx+GOLD*(cx-bx)
         fu=func(u)
       endif
       ax=bx
       bx=cx
       cx=u
       fa=fb
       fb=fc
       fc=fu
       goto 1
     endif
     return
     END
C****************************************************************
C                                                              *
C     Function brent is used in subroutine linmin.            *
C****************************************************************
       FUNCTION brent(ax,bx,cx,f,tol,xmin)
       DOUBLE PRECISION tol,f,ax,bx,xmin,cx,a,b,d,e,etemp,fu,fv,fw,fx,p
      +,q,r,tol1,tol2,u,v,w,x,xm,brent,CGOLD,ZEPS

       INTEGER ITMAX
       EXTERNAL f
       PARAMETER (ITMAX=100,CGOLD=.3819660,ZEPS=1.0e-10)
       INTEGER iter
       a=min(ax,cx)
       b=max(ax,cx)
       v=bx
       w=v
       x=v
       e=0.
       fx=f(x)
       fv=fx
```

```
      fw=fx
      do 11 iter=1,ITMAX
        xm=0.5*(a+b)
        tol1=tol*abs(x)+ZEPS
        tol2=2.*tol1
        if(abs(x-xm).le.(tol2-.5*(b-a))) goto 3
        if(abs(e).gt.tol1) then
          r=(x-w)*(fx-fv)
          q=(x-v)*(fx-fw)
          p=(x-v)*q-(x-w)*r
          q=2.*(q-r)
          if(q.gt.0.) p=-p
          q=abs(q)
          etemp=e
          e=d
          if(abs(p).ge.abs(.5*q*etemp).or.p.le.q*(a-x).or.p.ge.q*(b-x))
     *goto 1
          d=p/q
          u=x+d
          if(u-a.lt.tol2 .or. b-u.lt.tol2) d=sign(tol1,xm-x)
          goto 2
        endif
1       if(x.ge.xm) then
          e=a-x
        else
          e=b-x
        endif
        d=CGOLD*e
2       if(abs(d).ge.tol1) then
          u=x+d
        else
          u=x+sign(tol1,d)
        endif
        fu=f(u)
        if(fu.le.fx) then
          if(u.ge.x) then
            a=x
          else
            b=x
          endif
          v=w
          fv=fw
          w=x
          fw=fx
          x=u
          fx=fu
        else
          if(u.lt.x) then
            a=u
          else
            b=u
          endif
          if(fu.le.fw .or. w.eq.x) then
            v=w
            fv=fw
            w=u
            fw=fu
          else if(fu.le.fv .or. v.eq.x .or. v.eq.w) then
            v=u
            fv=fu
```

```
              endif
            endif
11        continue
          pause 'brent exceed maximum iterations'
3         xmin=x
          brent=fx
          return
          END
C*****************************************************************
C                                                               *
C       Function f1dim is used in subroutine linmin.            *
C*****************************************************************
          FUNCTION f1dim(x)
          DOUBLE PRECISION x,f1dim,xt(50),pcom(50),xicom(50)

          INTEGER NMAX
          PARAMETER (NMAX=50)
C     USES func
          INTEGER j,ncom
          COMMON /f1com/ pcom,xicom,ncom
          do 11 j=1,ncom
            xt(j)=pcom(j)+x*xicom(j)
11        continue
          f1dim=func(xt)
          return
          END
C******************       END OF PROGRAM      *****************
```